Three Dimensional Telomeric Profiles in Circulating Tumour Cells as a Method of Monitoring Treatment Response in High-Risk Prostate Cancer Patients

By

Landon Wark

University of Manitoba

A Thesis submitted to the Faculty of Graduate Studies of The University of Manitoba in partial fulfilment of the requirements of the degree of:

Master of Science

Department of Human Anatomy & Cell Science,

University of Manitoba

1.) Abstract

Prostate cancer is the second most commonly diagnosed cancer in men throughout the world. Because prognosis can vary depending on the stage of the tumour, precise diagnosis is vital.

Circulating tumour cells (CTC) detach from primary and secondary tumour sites into the bloodstream.

Changes in three-dimensional (3D) nuclear organization are associated with different types of cancer and were examined in this study in CTCs of high-risk prostate cancer patients.

We isolated CTCs from blood samples of 20 high-risk prostate cancer patients before any treatment; after beginning neoadjuvant androgen deprivation therapy (ADT), before radiotherapy (RT), and 2 months after completing RT. CTCs were isolated by processing 3mL of blood through a filtration device. Telomere-specific fluorescence *in situ* hybridization was performed on filters containing cells, and 3D images of 30 CTCs per filter were analysed.

Differential changes in 3D nuclear telomere organization were observed post ADT and RT; patients in this study fell into three groups depending on the change in CTC telomeric profiles in response to ADT. These groups then displayed responses characteristic to each group upon delivery of RT.

In conclusion, 3D nuclear telomere profiles in circulating tumour cells post-ADT may be indicative of both ADT response and predictive of RT response in high-risk prostate cancer.

2.) Table of Contents

3.) List of Figures

4.) List of Tables

5.) List of Abbreviations

°C	degrees Celsius
3D	three dimensional
3D-CRT	three dimensional conformational radiotherapy
53PB1	p53 binding protein 1
aCGH	array comparative genomic hybridization
ADT	androgen deprivation therapy
AFM	atomic force microscopy
ALT	alternative lengthening of telomeres
AR	androgen receptor
ARE	androgen response elements
ATM	ataxia telangiectasia mutated
BFB	breakage-fusion-bridge
BSA	bovine serum albumin
CARM1	coactivator-associated arginine methyltransferase 1
CBP	CREB-binding protein
CHIP	chromatin immunoprecipitation
CHiP	chromatin immunoprecipitation
CREB	cAMP response element binding
CRPC	castrate-resistant prostate cancer
CTC	circulating tumor cell
ctDNA	circulating tumor DNA
Cy3	cyanine 3
DAPI	4',6-diamidino-2-phenylindole
DHT	dihydrotestosterone
D-loop	displacement loop
DNA	deoxyribonucleic acid
DNA-PKcs	DNA protein kinase catalytic subunit
DRE	digital rectal exam
DSB	double-strand breaks
DTC	disseminated tumour cell
EBRT	external beam radiotherapy
EDTA	ethylenediaminetetraacetic acid
EMT	epithelial-mesenchymal transition
EMT	epithelial to mesenchymal transition
EpCAM	epithelial cell adhesion molecule
ERG	ETS-related gene
ETS	erythroblast transformation- specific

FACS	fluorescent activated cell sorting
GI	genomic instability
GnRH	gonadotropin-releasing hormone
HRR	homologous recombination repair
IMRT	intensity modulation radiotherapy
LH	luteinizing hormone
LHRH	luteinizing hormone releasing hormone
m	month
MACS	magnetically activated cell sorting
MB	megabases
$MgCl_2$	magnesium chloride
mL	millilitres
mm	millimeters
mM	millimolar
MRI	magnetic resonance imaging
NHEJ	non-homologous end joining
nm	nanometers
PBS	phosphate buffered saline
PCa	prostate cancer
PCR	polymerase chain reaction
PGA	percentage of genomic alterations
PIN	prostatic intraepithelial neoplasia
POT1	protection of telomeres 1
PRMT1	protein arginine N-methyltransferase 1
PSA	prostate specific antigen
pTEN	phosphatase and tensin homolog
PTEN	phosphatase and tensin homolog
QFISH	quantitative fluorescent *in-situ* hybridization
Rap1	repressor / activator protein 1
RBCs	red blood cells
RNA	ribonucleic acid
RP	radical prostatectomy
RT	radiation therapy
SRC-1	steroid receptor coactivator 1
SSC	solution of saline citrate
tif	tagged image file format
TIN2	TRF1- and TRF2-Interacting Nuclear Protein 2
TMPRSS2	Transmembrane protease, serine 2
TOP2B	topoisomerase IIB
TPP1	TINT1, PTOP, PIP1
TRF	telomere retention factor

Tris	Tris(hydroxymethyl)aminomethane
TRUS	trans-rectal, ultrasound-guided
YFP	yellow fluorescent protein
μL	microlitres

6.) Acknowledgments

I'd like to thank Dr. Sabine Mai for her guidance and support over the years of gathering data and writing this thesis, as well as the members of her lab, especially Cheryl Lynn-Dawn Taylor-Kashton Esq. and Amanda Righolt-Guffei Esq. for their knowledge of techniques and grant navigation and Dr. Ludger Klewes and Daniel Lichtenstejn the Genomic Centre for Cancer Research and Diagnosis for their help.

Thanks to my committee members Drs. Sabine Holmbach-Klonisch, Kirk McManus and Harvey Quon for their help and guidance/occasional kick in the pants.

Several others contributed their efforts to this work including: Cecile LeClerc and Brandon Dyck with their work in the automated CTC enumeration, Mary Cheung who performed the statistical analysis, and Julius Awe who did the preliminary work on the CTC filters.

Funding of this work was provided by the Cancer Care Manitoba Foundation.

Finally, thanks to my parents, Diane and Larry, and my sister, Morghan for their love and support.

7.) Introduction & Literature Review

7.1.) Prostate Cancer

Prostate cancer is an umbrella term for the development of malignant tumours in the prostate gland of the male urogenital tract. Prostate cancer is a complex disease with many forms, possible patient outcomes, and consequences for the patient and for society as a whole.

7.1.1.) Epidemiology

7.1.1.1.) Distribution among total cancer cases

Prostate cancer (PCa) is the second most common cancer diagnosed in men throughout the world (Baade, Youlden, and Krnjacki 2009; Schoenborn, Nelson, and Fang 2013) and, amongst men diagnosed with any type of cancer, prostate cancer accounts for 1 in 6 mortalities (Baade, Youlden, and Krnjacki 2009). Within Canada prostate cancer accounted for 23.9% (69.06/100,000 individuals) of all new cancer case in men with an estimated 24,000 new cases diagnosed in 2015 (Canadian Cancer Society's Advisory Committee on Cancer Statistics 2015). The proportion of new cases in the United States is similar with 241,740 in 2012 (American Cancer Society 2012) in a population approximately nine times as large (76.96/100,000).

7.1.1.2.) Distribution among age groups

Prostate cancer is often described as a disease of the elderly, with the majority of cases occurring between the ages of 60 and 65 (Canadian Cancer Society's Advisory Committee on Cancer Statistics 2015). A diagnosis of prostate cancer is not unheard of in males under the age of fifty (Kinnear et al. 2016; American Cancer Society 2012)), but these occurrences generally have lower average Gleason scores, lower median PSA levels and a greater percentage of T stage <2 primary tumours (see section 0 for information of staging).

The majority of prostate cancer cases are slow to develop (Carozzi et al. 2015) and – because they are not often seen in individuals younger than 50 years of age – may remain indolent until mortality occurs due to complications of old age. This indolent group of cases is often marked for active surveillance only (Trock 2014), as treatment may severely decrease a patient's quality of life (Nguyen et al. 2014) without providing any measurable decrease in tumour advancement. However there exists an aggressive subset of PCa cases (stage IV) that develop much more quickly and pose a serious, immediate threat to the life of the patient (Mathers et al. 2011).

7.1.1.3.) Mortality in prostate cancer

Despite being the number one type of newly diagnosed cancer among men in Canada, prostate cancer is the third most common fatal type of cancer behind lung and colorectal with 10.1% (4,100) of male cancer related fatalities (Canadian Cancer Society's Advisory Committee on Cancer Statistics 2015). In the United States, it is the second most common cause of cancer related death, causing 9% (28,170) of these fatalities (American Cancer Society 2012).

According to an epidemiological study of the Regensburg regional tumour registry patients diagnosed with PCa stages I, II or III had a five-year survival rate of 90% and a minimum ten-year survival rate of 75% (Mathers et al. 2011). In comparison, those diagnosed with stage IV PCa had a five-year survival rate of 45% and a ten-year survival rate of 28% (Mathers et al. 2011). Specifics of staging are discussed in section 7.1.1.8.) TNM Tumour staging.Diagnosis & Staging of prostate cancer

Diagnosis methods of PCa ranges from conceptually simple yet invasive (biopsy and tissue analysis), to complex titrations of proteins found in the serum of the blood, to combinations of sophisticated imaging techniques. Recent controversy over certain methods such

as PSA measurements has brought to the front the possibility of over-diagnosis (Rönnau et al. 2014), highlighting the need for exact methods of diagnosis and staging, leading to demand for more powerful methods, which in turn leads to cost/benefit analyses (Sharova et al. 2016). As such it is important to identify the strengths and weaknesses of each approach.

7.1.1.4.) Prostate Specific Antigen (PSA) as a diagnostic tool in prostate cancer

Prostate Specific Antigen (PSA) is a protein secreted by the normal prostate into the prostatic ducts and the urethra to liquefy the ejaculate and allow the free motion of sperm (Balk, Ko, and Bubley 2003). An important study in 1987 showed a strong correlation between PSA levels in the blood serum and advanced clinical tumour stage, showing also that PSA dropped to undetectable levels after radical prostatectomy (Stamey et al. 1987). While serum PSA level is correlated to PCa it is also related to prostatitis, irritation, benign prostatic hyperplasia (non-cancerous enlargement of the prostate), recent ejaculation and even a recent digital rectal exam (Chybowski, Bergstralh, and Oesterling 1992; Baade, Youlden, and Krnjacki 2009; Frankel et al. 2003). As such PSA cannot be used for a definitive diagnosis, rather it is used to identify patients for further diagnostics.

Changes in PSA levels before treatment are used to evaluate prognosis. An increase of 2.0 ng/mL in the year prior to radical prostatectomy is associated with a decreased time to death (D'Amico et al. 2004).

7.1.1.5.) Digital Rectal Exam as a diagnostic tool in prostate cancer

A digit rectal exam (DRE) is simply a palpation of the prostate through the rectum, checking for any abnormal mass within the organ. As is to be expected from non-visual diagnostics, digital rectal exams are inexact. In fact biases in detection rates have been discovered based on the handedness of examiner (Ploussard and Nicolaiew 2014). DRE will also

miss smaller early stage tumours and is most frequently used to reduce false positive levels of PSA tests.

7.1.1.6.) Application of trans-rectal Ultrasonography Guided biopsy in prostate cancer

When PSA testing reveals elevated serum levels the next step in diagnosis is biopsy (Pokorny et al. 2014). As of 2008 the most commonly performed type of biopsy was trans-rectal ultrasonography (TRUS) guided biopsy (Shariat and Roehrborn 2008). The method of TRUS-guided biopsy involves inserting an ultrasonic probe into the rectum and using the resulting imaging to guide placement of a biopsy needle through the rectal wall and the fascia between the rectum and the prostate, taking between 10 and 14 biopsy cores (Shariat and Roehrborn 2008).

While it is a commonly used technique there are concerns regarding the incidence of infection and erectile dysfunction with use of TRUS biopsies (Trock 2014).

An additional weakness in the TRUS workflow is low resolution which can find only larger tumour foci with problems in determining tumour grade (Washington et al. 2012; Hwang and Lee 2014). A recent increased interest in personalized medicine has brought with it an interest in focal therapy to supplant the use of active surveillance in early stage prostate cancer (Washington et al. 2012). This inability of TRUS to identify smaller, early stage foci is leading it to be combined with or replaced with more advanced magnetic resonance imaging (MRI) technology with the medical community working toward broad based adoption (Dickinson et al. 2011).

7.1.1.7.) Magnetic Resonance Image-guided biopsies

Two types of MRI-guided biopsies are available. One is conducted in real time inside the MRI chamber itself while the second, MRI combined with TRUS used saved MRI images in

combination with active ultrasonography to guide the urologist to the identified foci (Hwang and Lee 2014).

When correlated to the results of tissue excised during surgery MRI has been shown to increase the detection of intermediate and high-risk PCa by 17.7%, decrease the misdiagnosis of low-risk PCa by 89.4% and even decreased the need for a physical biopsy by 51% (Pokorny et al. 2014). MRI-guided biopsy also has the advantage of being able to image the entire prostate, making the relocating of identified tumour foci more accurate when the time comes for surgery or the targeting of radiation therapies (Hwang and Lee 2014).

7.1.1.8.) TNM Tumour staging

TNM staging is a collection of three descriptions of the spread of a solid tumour within the body. T described the extent of the original tumour inside the observed organ. N describes the extent of tumour spread to the nearby lymph nodes. M describes the extent of distant metastases.

7.1.1.8.1) T stage

The T parameter is a measure of the spread of the primary tumour within the prostate organ as well as the nearby tissues. Tx indicates that a solid tumour cannot be evaluated while T_0 indicates there is no evidence of a tumour. T1 indicates that the cancer cannot be felt or seen by the naked eye. T2 indicates that cancer can be seen via imaging or felt with DRE but is confined to the prostate gland. T3a indicates that the cancer has spread past the prostate gland and T3b into the seminal vesicles. T4 indicates that the primary tumour has grown into organs surrounding the prostate other than the seminal vesicles (Jager et al. 1996).

7.1.1.8.2) N stage

The N parameter of TNM staging indicates the spread of the tumour into the lymph nodes: NX indicates that lymph nodes were not assessed. N0 indicates no spread into the nearby lymph nodes. N1 indicates that tumour cells have been observed in nearby lymph nodes. (Jager et al. 1996)

7.1.1.8.3) M stage

The M parameter indicates the metastatic status of the tumour. M0 indicates no spread of tumour beyond the lymph nodes of the pelvis. M1a: metastatic sites have been found in lymph nodes outside the pelvic area. M1b: metastatic sites have been found in the bones. M1c: metastatic sites have been found outside the lymph nodes or the bones (i.e., in the lungs). (Jager et al. 1996)

7.1.1.9.) Gleason Score

Gleason scoring is a system for evaluating prostate biopsy tissue developed by pathologist Donald Gleason and others at the Veterans Administration Cooperative Urological Research Group in the 1960's and modified by the International Society of Urological Pathology in 2005 (Leze, Maciel-Osorio, and Mandarim-de-Lacerda 2014). Currently the Gleason system is the most widely used system for evaluating prostate cancer worldwide.

The scoring system is based on the predominant patterns of tissue differentiation seen by a pathologist in the hematoxylin and eosin stained biopsy sample. Well differentiated tissue with normally formed prostate glands is given a value of 1 with poorly differentiated, nearly glandless tissue given a value of 5. Values in between are a gradient of tissue differentiation (See **Figure 1** for examples).

Figure 1: Examples of tissue differentiation in the five patterns of the Gleason scoring system. (From National Cancer Institute (NIH) - http://training.seer.cancer.gov/prostate/abstract-code-stage/morphology.html. Image is in the public domain.)

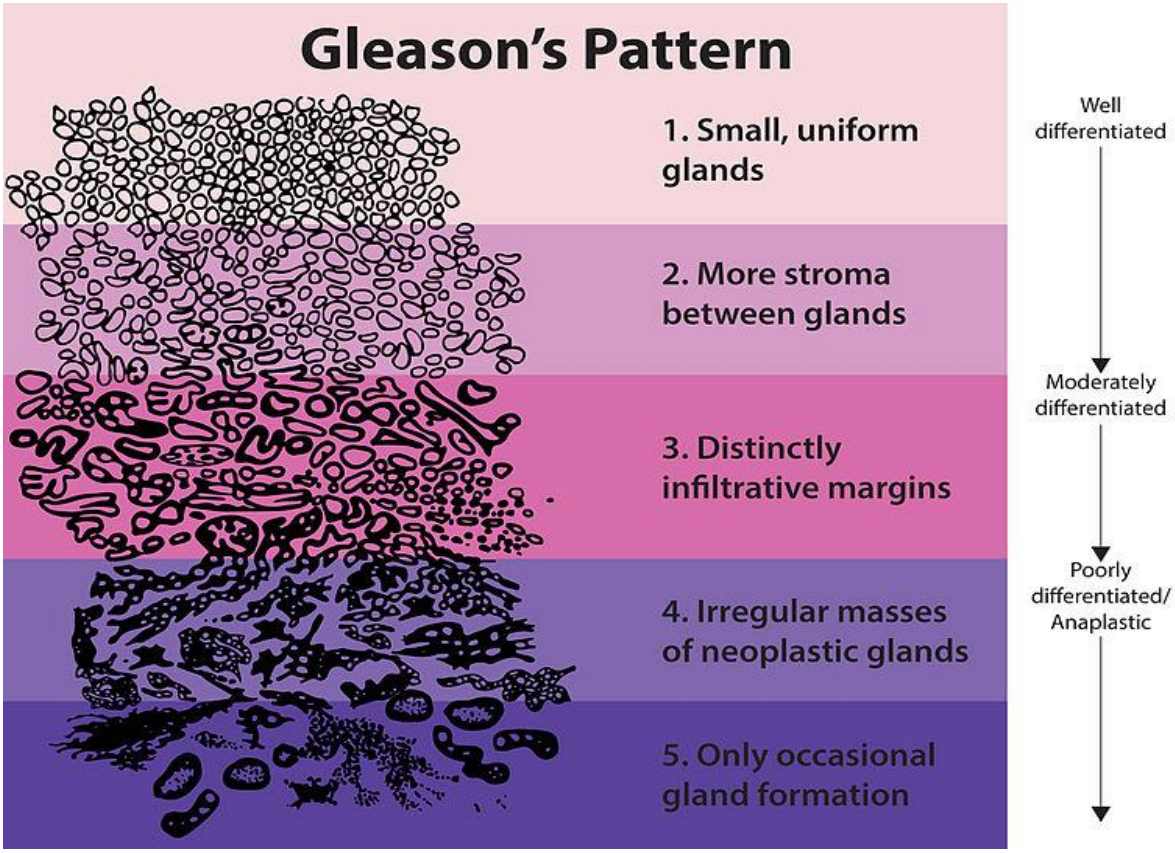

The overall Gleason score is determined by the addition of the most prominent tissue pattern value with that of the second most prominent (if it comprises more than 3% of the tumour). While this has the benefit of being a simple, single value it does introduce some ambiguity with a Gleason score of 7 possibly representing a 3 + 4 which has a slightly better prognosis than a 4 + 3 (Humphrey 2004).

In 2014 efforts were made to refine the Gleason grading system into a 5 point scale while adoption has been slow; the system is used by the World Health Organization for the 2016

edition of its manual “Pathology and Genetics of Tumours of the Urinary System and Male Genital Organs (World Health Organization 2016)”.

7.1.1.10.) D’Amico Criteria

The D’Amico criteria consolidates the circulating PSA level, Gleason Score and TNM score of a patient into a simple description of PCa which indicates how likely a patient is to experience relapse following localized treatment. The criteria divides PCa into three categories: low (PSA ≤ 10ng/mL, Gleason score ≤ 6, or clinical stage T1-2a), intermediate (PSA 10 <> 20ng/mL, Gleason score 7, or clinical stage T2b) and high (PSA > 20ng/mL, Gleason score ≥ 8, or clinical stage T2c-3a) risk (D’Amico et al. 1998). It should be noted that patients are assigned to a higher category based on any one variable (for example: a PSA level of 25ng/mL is sufficient to categorize a patient as high risk regardless of Gleason score or tumour grade).

7.1.2.) Tumour Heterogeneity and its complications in biopsies

Currently there is some controversy over the exact source of the majority of PCa tumour cells. It is generally agreed that the epithelial cells of the glands are involved, but whether they are basal or luminal cells is debated and studies have been produced supporting both (Z. A. Wang et al. 2014; R. A. Taylor et al. 2012). (Z. A. Wang et al. 2014) suggests that basal cells may be involved in PCa development but only after they have differentiated into luminal cells. Coupled with their more convincing experimental approach of tracking the progression of PCa in two groups of mice with yellow fluorescent protein (YFP) labelled luminal and basal epithelial cells respectively and charting YFP expression in resulting tumours (Z. A. Wang et al. 2014), the luminal epithelial cell hypothesis has considerably more supporting evidence. Despite these inquiries in the field, the question has not yet been settled conclusively.

One of the defining features of prostate cancer is the number of multiple tumour foci which can develop in a single prostate over time (Lindberg et al. 2013). Each of these foci can display different genetic aberrations with few of them in common with other tumours in the same prostate (Lindberg et al. 2013; Lindberg et al. 2014; Schoenborn, Nelson, and Fang 2013; Lalonde et al. 2014). This variety in the tumour population gives PCa a potentially large pool of genetic diversity to draw from, with one clone flourishing when another is destroyed by treatment. One study linked the amount of genomic alterations amongst prostate tumours foci with a decrease in five-year survival rates (Lalonde et al. 2014).

High tumour heterogeneity also means that the biopsy process comes with increased complexity in prostate cancer; with the potential of selecting a less consequential tumour focus rising with an increased number of tumour foci. A prostate cancer biopsy will not always be able to provide a picture of the state of the prostate as a whole, possibly missing segments that might threaten the survival of the patient (Taneja et al. 2013).

7.1.3.) Treatment & Management of prostate cancer

As the prognoses of PCa are diverse, from indolent to aggressive and that treatment involving possible sexual dysfunction and hormonal imbalances are potentially emotional issues, recommending an effective treatment free of side effects for the patient is a vital matter. Since almost all PCa require either testosterone or dihydrotestosterone for growth, when treatment is necessary hormone related therapy is usually the first recommendation.

7.1.3.1.) Androgen Deprivation & Hormone Therapy

In its normal state the prostate responds to androgens produced by the gonads with an increase in size and weight, growing to approximately 20g post-puberty from 4g pre-puberty (Wilson 2011). A reduced form of testosterone, dihydrotestosterone (DHT) is implicated as the

primary activator of the androgen receptor (AR) (with testosterone as a secondary but still relevant activator) which crosses into the nucleus, dimerizes and functions as a transcription factor whose downstream targets include Insulin-like Growth Factor-I Receptor (Pandini et al. 2005) (The AR's implication in PCa is discussed more fully in section 7.1.4.) page 15).

The observation made in the late nineteenth century that surgical castration reduced the size of a hyperplastic prostate (i.e. an enlarged but non-malignant prostate) (Cabot 1896) led to the finding that luteinizing hormone releasing hormone (LHRH) analogs decreased the level of serum testosterone as well as the size of prostatic hyperplasia (Peters and Walsh 1987). In 1966 Charles Huggins won the Nobel Prize in physiology for discovering that androgen ablation therapy caused regression of both primary and metastatic androgen-dependent prostate cancer. This has led to the modern practice of androgen deprivation therapy (ADT).

ADT is prescribed as a front-line treatment in multiple forms of prostate cancer (Lu-Yao et al. 2014). The goal of ADT is to either decrease the levels of androgens available to activate the androgen receptor with LHRH (ant)agonists (leuprolide acetate, goserelin acetate, triptorelin pamoate) or to interfere with the functioning of the androgen receptor in the prostate itself through use of an AR antagonist (Bicalutamide, Enzalutamide).

A LHRH antagonist's method of action is to compete with the receptor of natural LHRH compounds secreted by the hypothalamus, thereby blocking the production of luteinizing hormone (LH) in the pituitary gland which in turn will down regulate the production of testosterone in the Leydig cells of the testes (Schally 1999). While they have been shown to be an effective method of ADT, faster to produce a response (Schally 1999; Moul 2014) and do not produce an initial hormone surge (Kimura et al. 2015), LHRH antagonists usually give deference to agonists as these have a longer duration of action. LHRH agonists are derivatives of natural

LHRH that are less sensitive to enzymatic degradation and have an increased affinity for the receptor in the pituitary (Gomella 2009). Constant activation of the LHRH receptor induces a downregulation of its expression which leads to a decrease in the LH and subsequent decrease in levels of testosterone (Schally 1999).

Because the adrenal glands and even the prostate stroma may also produce small amounts of testosterone an anti-androgen is added to LHRH agonists. Bicalutamide is generally considered the standard, and is the anti-androgen used for this study. It binds directly to the androgen receptor, preventing ligand binding and activation. Since the more advanced Enzalutamide received FDA approval in 2012 it has been replacing Bicalutamide as the choice for treatment (Rodriguez-Vida et al. 2015).Through this it is hoped the proliferative factors targeted by the AR will be down regulated, halting the abnormal growth of the prostate.

It has been shown that the addition of radiation therapy to ADT results in a 10% increase in 10-year survival rate (Mohiuddin, Baker, and Chen 2015). The continuation of ADT for 24 months post-RT can further increase the 10-year survival rate by 9% over radiation alone (Mohiuddin, Baker, and Chen 2015).

In some cases of metastatic PCa the action of orchiectomy (removal of the testes) may be undertaken in an attempt to further reduce the amount of testosterone available to activate the androgen receptor. This has been found to be an effective method of reducing androgens with less adverse effects than chemical androgen deprivation (M. Sun et al. 2016), but has the drawback of being a permanent and may be unattractive to patients for this reason (Prostate Cancer Foundation 2016; Gomella 2009).

Though it is effective, side effects with ADT are almost a certainty and can include: physical fatigue, severe depression, gynecomastia, sexual dysfunction, decreased bone density with possible osteoporosis, metabolic dysfunction and even hot flashes (Nguyen et al. 2014).

While androgen deprivation is a common therapy for aggressive and advanced PCa (Nguyen et al. 2014) its effects are almost always temporary as most patients receiving ADT will progress to castrate-resistant prostate cancer (CRPC) within 18-24 months (Hotte and Saad 2010). This stage of PCa is discussed in sections7.1.5.2.) Castrate Resistant Prostate Cancer and 7.1.4.) Androgen Receptor

7.1.3.2.) Radiation Therapy

The goal of radiation therapy is simply to introduce breakages into the DNA of tumour cells, disrupting the cellular machinery to the point where the cell is no longer capable of survival. In order to prevent the same damage from happening in surrounding healthy cells targeting must be extremely accurate, making diagnosing and locating tumour foci of paramount importance (see section 7.1.1.7.) .

Two major types of radiation therapy are possible, brachytherapy and the more familiar external beam radiotherapy (EBRT) (Amin, Sher, and Konski 2014).

7.1.3.2.1) Brachytherapy

Brachytherapy, preferred for early stage, localized tumours involves the placement of radioactive isotope pellets (typically: iodine 125 (half-life 59.4 days) or palladium 103 (half-life 17 days) within the prostate (Morton and Hoskin 2013). The standard procedure for this utilizes a technique almost identical to TRUS-guided biopsy: an ultrasound probe is inserted into the rectum and used to guide the placement of fine needles into the prostate, only rather than removal of material from foci within the organ, material is inserted throughout the prostate

(Morton and Hoskin 2013). Brachytherapy has been shown to produce rates of biochemical failure (a rise of 2ng/mL above the lowest PSA level achieved (Roach et al. 2006)) for low-risk prostate cancer similar to radical prostatectomy or external beam radiation (Kupelian et al. 2004) but with lower risk of urinary incontinence than surgery and lower risk of sexual dysfunction than surgery or EBRT (Kupelian et al. 2004).

7.1.3.2.2) External Beam Radiotherapy

The procedure of EBRT involves bombarding an area of the patient's body (in the case of this study, the pelvic area and specifically the prostate) with a beam of ionizing radiation derived from a linear accelerator (Amin, Sher, and Konski 2014). Because such a beam would, by its linear nature interact with normal tissue surrounding the tumour early radiotherapy was limited to lower dosage (60-70 Grays (GY) (Fenoglietto et al. 2008)) to remain below toxic levels of radiation. Modern radiotherapy uses two main methods to focus many smaller, less intense beams and conform them to the three-dimensional (3D) structure of the tumour. In the mid-1990's three-dimensional conformational radiotherapy (3D-CRT) was developed using CT images to create a "cross fire" of less intense beams having the same (or larger) cumulative intensity as the older single beam (Fenoglietto et al. 2008). This was an improvement over the existing method but remnants of toxic side effects still limited dosage (Fenoglietto et al. 2008).

Research has shown that high dosage radiation (78–80 GY) produces a more favourable outcome (both clinical and biochemical) than lower dosages in high-risk patients (Qi and Moul 2015; Fenoglietto et al. 2008). 3D intensity modulation radiotherapy (or more simply intensity modulation radiotherapy (IMRT)) is a more advanced derivative of 3D-CRT uses a non-uniform beam whose segments can be modified in intensity to further narrow areas of higher intensity and avoid unintended exposure (Fenoglietto et al. 2008).

Numerous reports have shown the superiority of IMRT over 3D-CRT (Fenoglietto et al. 2008; Amin, Sher, and Konski 2014) and its rate of usage has risen, however economic issues have hindered its widespread adoption (E. H. Wang et al. 2015).

7.1.3.3.) Other treatments

Other treatments used in combating prostate cancer, but not part of our study include: radical prostatectomy, chemotherapy and cryoablation.

7.1.3.3.1) Prostatectomy

Partial prostatectomy is used only in the cases of benign disease, with malignant tumours total removal of the prostate (radical prostatectomy) is recommended in some cases of intermediate or high risk prostate cancer.

Whether radical prostatectomy (RP) is preferable to RT in high-risk prostate cancer is still under debate. Studies have shown a lower rate of PCa specific mortality (Qi & Moul, 2015) and it has a better rate of biochemical failure-free survival than does radiotherapy, however a few studies have shown no significant difference in outcome (Kupelian et al. 2004). RP also has a higher rate of side effects, especially of urinary incontinence (Potosky et al. 2004), and long term sexual dysfunction (Clavell-Hernandez and Wang 2015). Damage to the nerves drastically increases the odds of these side effects and in recent years nerve sparing techniques have been developed to help prevent this from occurring.

7.1.3.3.2) Cryoablation

Cryoablation is a minimally invasive, effective surgical technique that is currently used primarily when the patient has already failed a primary treatment (Kovac et al. 2016) Metal rods are inserted through the skin into the prostate and chilled to -186°C using argon gas while the

urethra is protected by a catheter full of warm liquid (Drachenberg 2000). Impotence is almost certain with this procedure, incidence being 94.9% (Bahn et al. 2002).

7.1.3.3.3) Chemotherapy

Within the realm of prostate cancer chemotherapy is relegated to a palliative technique used to slow the advancement of the disease. The currently most common treatment is with anti-mitotic taxanes Docetaxel and Cabazitaxel (Crawford et al. 2015) paired with a corticosteroid to relieve inflammation.

7.1.4.) Androgen Receptor

The gene coding for the androgen receptor is located on the q11-q12 region of the X chromosome (Schweizer and Yu 2015). The androgen receptor is a nuclear hormone binding receptor crucial for the development of both the primary and secondary sex characteristics in males. Upon binding either testosterone or the more potent dihydrotestosterone - produced by 5α-reductase action on testosterone - AR sheds heatshock proteins and relocates to the nucleus where it homodimerizes and binds to androgen response elements (ARE). AR is also phosphorylated in the nucleus which can occur both before and after it binds to the ARE.

7.1.4.1.) AR coactivators

After AR binds it recruits steroid receptor coactivator 1 (SRC-1) which greatly increases its transcription factor activity. SRC-1 recruitment is facilitated by GATA2-binding protein, itself a promoter of AR transcription that may be upregulated in PCa (He et al. 2014). Often called nuclear receptor coactivator 1 (NCOA1) SRC-1 interacts with many hormone receptors (including estrogen receptor alpha and thyroid receptor beta) through a nuclear receptor interaction domain. SRC-1 potentiates activity of the bound androgen receptor, increasing its activity even at low levels. Decreased expression of SRC-1 has been shown to reduce

proliferation in the hormone sensitive LNCaP cell line, but not in the insensitive DU-145 or PC3 lines (Agoulnik et al. 2005). SRC-1 has also been shown to play a role in the activation of AR by interleukin-6 in castrate resistant prostate cancer cell lines (Ueda et al. 2002) (see section 7.1.5.2.) Castrate Resistant Prostate Cancer). (B. S. Taylor et al. 2010) found increased expression of SRC-1 in 37% of all metastatic PCa analyzed.

Once SRC-1 has been recruited to AR on the ARE it recruits additional proteins to active domains on its C-terminus. The cAMP response element binding protein (CREB)-binding protein (CBP), p300 and p/CAF a chromatin remodelling and two histone acetyltransferases respectively interact with AD1 and acetylate histones in the enhancer and promoter regions of the target genes (Walsh et al. 2012; Powell et al. 2004). AD1 has also shown to interact with RNA helicase when CBP is present which in turn mediates the AR/coactivator interaction with RNA polymerase II (Nakajima et al. 1997).

AD2 recruits the methyltransferases coactivator-associated arginine methyltransferase 1 (CARM1) and protein arginine N-methyltransferase 1 (PRMT1) which further modify chromatin of the target genes (Walsh et al. 2012).

7.1.4.2.) Androgen receptor mediated gene transcription

In a ChIP study on the androgen receptor's effect on PSA transcription it was revealed that AR did not bind to the promoter of PSA, but rather an upstream enhancer region (Q. Wang, Carroll, and Brown 2005). Genome wide analysis of prostate cell lines has shown that about 86-95% of binding sites for androgen receptor are located upstream (≥50kb) of the target promoter (Bolton et al. 2007). Because of this a conformational change in the quaternary structure of the chromosome is necessary to bring transcriptional machinery interacting with CBP to the promoter of the target gene. The association of distal ARE enhancer regions with the proximal

promoter of the target gene was shown using chromosome conformation capture technology in both PSA (Q. Wang, Carroll, and Brown 2005) and more importantly the *TMPRSS2* gene (Q. Wang et al. 2007) whose fusion with *ERG* is reported as occurring in 30% - 70% of all treatment naïve prostate cancers (Attard et al. 2009).

This distant enhancer action of the AR has been proposed as a model for how *TMPRSS2* and *ERG* (located 3MB upstream on chromosome 21) come into close enough proximity to become fused in such a high proportion of PCa (Wu et al. 2011; Katsogiannou et al. 2015). An alternative explanation is that dysregulation of the nuclear architecture (see section 7.2.7.) brings together elements of the genome that would not normally occupy the same location in the nucleus.

Further this model may be able to account for the high incidence of genomic instability (GI) in high-risk prostate cancer through the creation of dicentric chromosomes via fusion of chromosome segments which might not otherwise be in close enough proximity if not for the distal enhancer method of AR gene regulation.

7.1.4.3.) DNA repair

The androgen receptor's activity within DNA damage response is diverse. Many of its downstream targets as a transcription factor are components of the cell's DNA repair machinery. Goodwin et al. (2013) showed that AR levels are increased in response to DNA damage which led to an increase in two homologous recombination repair (HRR) proteins (namely XRCC2 and XRCC3) as well as the DNA protein kinase catalytic subunit which plays a vital role in non-homologous end-joining (NHEJ) repair. The AR target gene has been shown to bind to the N terminal domain of ATM, a key cell cycle checkpoint protein in DNA damage response and accelerates its activation (Bowen et al. 2013). Polkinghorn et al. (2013) found an increased

expression of 144 DNA repair related genes with increased expression associated with an increase in AR in human primary tumour tissue.

Numerous DNA repair proteins have been shown to interact with AR and increase its transcriptional activity. Co-immunoprecipitation has found interactions between AR and hRad9 (checkpoint protein), MAGE11 (CHK1 phosphorylation target), BRCA 1&2, DNA-PK and PARP1 (Ta and Gioeli 2014). Interestingly topoisomerase IIB (TOP2B) has been shown to be necessary for AR-mediated gene transcription (Ju et al. 2006). TOP2B has been a target of anti-cancer drug Mitoxantrone in acute lymphoblastic leukemia and mutations in the TOP2B gene and its recruitment to AR target gene sites by AR, along with its function of creating transient DNA breaks has been implicated in chromosome translocations and the *TMPRSS2:ERG* gene fusion (Haffner et al. 2010).

Of particular interest to this project is the finding by Zhou et al. (2013) and Kim et al. (2010). They reported AR bound chromatin in the LNCaP castrate-sensitive PCa cell line contained telomeric repeats and proteins and that telomeric DNA was associated with AR. Immunofluorescence revealed the co-localization of AR with the shelterin protein TIN2. The addition of the anti-androgen Bicalutamide initiated the disruption of the telomere chromatin in LNCaP, but not in the castrate-resistant PC3 line and initiated the recruited of p53 binding protein 1 (53BP1) to the telomeres along with the phosphorylation of γH2AX. Use of siRNA against AR produced similar results. Use of transcriptional inhibitors showed that disruption of the transcription factor activity of AR was not the cause of this telomere disruption.

The findings that decreases in AR activation following administration of bicalutamide cause telomere disruption (Zhou et al. 2013; Kim et al. 2010) indicate that even a transient decrease in testosterone levels can cause genomic instability by inducing telomere dysfunction in

the prostate. This dysfunction includes fragile telomeres and sister chromatid fusions. This could provide an explanation why telomere shortening is an early event in PCa (Meeker et al. 2002) if chromosome breakage were to occur at the telomeres. It may also explain why PCa is predominantly found in the elderly men (see section 7.1.1.2.) who may have decreased levels of testosterone (Snyder et al. 2016). A transient decrease in levels of testosterone may lead to a decrease in active AR available to maintain stability of the telomeres. This in turn could lead to the formation of sister chromatid telomere fusions as is seen in (Zhou et al. 2013). Returning to normal or elevated testosterone levels could then trigger cell division, inducing chromosome damaging events such as anaphase bridges. A second possibility is that there is competition between the transcription factor function of AR and the telomere maintenance function of AR whereby an increase in AR-related transcription decreases the active AR available for telomere maintenance. However, since AR-related telomere stability is a relatively new discovery no evidence exists to support this hypothesis.

7.1.5.) Progression

Progression of PCa to a more aggressive form in the literature falls into two categories, castration resistant prostate cancer and metastatic prostate cancer. These can occur separately or together and each presents new challenges in management.

7.1.5.1.) EMT transition & Metastasis

Epithelial to mesenchymal transition is an important process in natural embryogenesis by which epithelial cells lose polarity and adhesion, migrating into a new mesenchymal layer (Y. Sun et al. 2012). It is also an enabler of metastasis in cancer with cell illegitimately gaining the ability of intravasion into the bloodstream after losing important e-cadherins responsible for cell-cell adhesion (Hanahan and Weinberg 2011).

EMT is an important step in the generation of CTCs and has been shown to be increased by ADT (Y. Sun et al. 2012; C.-L. Chen et al. 2013) in prostate cancer. Since androgens are responsible for the differentiation of prostate tissue, this is to be expected. While a search of the literature shows no evidence of decreased differentiation in prostate CTCs, CTCs from colorectal cancer patients have shown stem cell-like properties in *ex vivo* culture (Grillet et al. 2016). CTCs having undergone EMT also express less epithelial genes (C.-L. Chen et al. 2013), making them less likely to be picked up by detection methods based on epithelial cell markers (see section 7.3.2.1.) EpCAM).

After making its way into the peripheral blood as a CTC (see section 7.3.) cells sloughed off from the main tumour are subjected to stresses which include mechanical shearing, active immune response and an environment which may not meet its needs for survival. The CTC may also become trapped within a distant part of the body. At this point it has become a disseminated tumour cell (DTC). If the CTC manages to integrate into this environment, grow and divide it has become a metastatic tumour. Despite the estimation that only 0.01% of all CTCs can go on to become metastases (Zhe, Cher, and Bonfil 2011) over 90% of all cancer related fatalities are from metastatic progression (Mehlen and Puisieux 2006).

The most common site of metastasis in PCa is the bone with the lungs and brain also as high frequency sites. It has been suggested the reason bones are the most common sites of metastasis is because certain bone cells produce interleukin-6 which can be an alternative activator of AR as mediated by SRC-1 (Ueda et al. 2002) (see section 7.1.4.1.)

Because metastasis is frequently coupled to castrate resistance in PCa the treatment options are narrowed and systemic approaches must be taken. Following transition to metastasis the 5 year survival rate drops to less than 30%.

7.1.5.2.) Castrate Resistant Prostate Cancer

The development of PCa from androgen dependant to androgen independent occurs in nearly every case of advanced prostate cancer. At this point PCa cells have acquired the ability to proliferate without the binding of the ligand to AR. Maintenance of the AR pathway has been found in a majority of CRPC (Schweizer and Yu 2015), indicating that prostate cells retain their reliance on AR even when depletion of endocrine AR has failed to stop their proliferation. The molecular mechanism of this phenomenon are diverse, however there are three main pathways that may lead to this outcome.

7.1.5.2.1) Localized production of androgens

The reliance of PCa cells on endocrine signalling is the reason for the initial success of ADT in PCa treatment. However, the prostate stroma possesses the ability to make small amounts of androgens on its own. The removal of endocrine androgens by ADT selects for any subpopulation of prostate cells which have acquired mutations increasing their output of autocrine androgens. Termed endocrine/paracrine transition this increase in levels of androgen has been found in castrate resistant PCa and can be caused by the conversion of non-testosterone hormones to DHT within the prostate (K.-H. Chang et al. 2011) or the production of testosterone from cholesterol in prostate cancer cells (Dillard, Lin, and Khan 2008). Levels of AR can be increased as a result of increased production in the Leydig cells of the testes, within the adrenal glands or through de novo synthesis in the prostate itself. Testosterone levels have been found to be increased in bone metastases of CRPC in a castrate environment (Kobayashi et al. 2013). Levels of steroidogenic enzymes were also found in CRPC (Kobayashi et al. 2013).

7.1.5.2.2) Changes in AR concentration

As with any gene the AR gene can increase in copy number, transcription frequency, mRNA stability, protein stability leading to an increase in the AR levels within prostate cells. Research has shown that androgen dependent cells lines that progress to castrate resistance show increased levels of AR (Kobayashi et al. 2013). C. D. Chen et al. 2004 showed that even a small increase in the levels of full length AR mRNA was sufficient to progress mouse xenografts of prostate cancer cell lines to castrate resistance. Although increased levels of AR may be present in certain prostate cancers, it must still be converted to its active form in order to have any effect on tumourigenesis.

7.1.5.2.3) Changes in AR action

Anti-androgens such as Bicalutamide bind to specific regions of the androgen receptor (in the case of Bicalutimide the binding site is adjacent to the androgen binding site (Osguthorpe and Hagler 2011)) and disrupt the function of AR as a transcription factor. Mutations in the protein sequence of AR change the shape of these binding domains, preventing action of androgen antagonists or in some cases converting them to strong agonists (Culig et al. 1999).

Changes in the androgen binding site of AR or even in AR coactivators can also alter its affinity for androgens (C. Chang 2002) and/or broaden the number of ligands which can activate it (Veldscholte et al. 1990; Matias et al. 2002).

Splice variants lacking a ligand binding domain such as AR^{v567es} which is upregulated in metastatic CRPC (S. Sun et al. 2010) resulted in the AR constitutively active and localizing exclusively in the nucleus (Dehm et al. 2008) and increased the expression of full length AR (Dehm et al. 2008; S. Sun et al. 2010). Androgen receptor variant 7 (AR-V7) is currently a major focus of study. Similar to AR^{v567es} it lacks the ligand binding domain which has caused it to

become constitutively active (Guo et al. 2009). Unlike AR^{v567es} AR-V7 regulates the canonical AR target genes as well as a unique group of its own targets (Shafi, Yen, and Weigel 2013; Hu et al. 2009).

7.1.6.) Common genetic changes in Prostate Cancer

7.1.6.1.) PTEN loss

PTEN loss is an early genetic change in PCa. 70% of primary PCa tumours show loss of at least one allele of phosphatase and tensin homolog (*PTEN*) (Z. Chen et al. 2005; Karantanos et al. 2014) and the PCa cell lines LNCaP and PC-3 are known to harbour mutations in *PTEN*. *PTEN*'s function as a tumour suppressor has been widely documented (Hlobilkova et al. 2000; Lotan et al. 2014; Attard et al. 2009; Saal et al. 2007) with its primary function in this regard being arrest of the cell cycle by dephosphorylating PI3K lipid intermediates (Bostrom et al. 2015) and interrupting the Akt signalling pathway. Mice that are heterozygous for *PTEN* have shown an increased development of systemic tumours with phosphorylated Akt kinase (Suzuki et al. 1998) and an increase in prostatic intraepithelial neoplasia (PIN) with a long latency of about 10 months (Freeman et al. 2003). Prostate cancer cell lines homozygous for *PTEN* deletion have shown an increase in cell proliferation over those heterozygous for *PTEN* deletion *in vitro* as well as an increase in tumourigenic potential in mouse xenografts (Jiao et al. 2007). Interestingly tumourigenic potential of the xenografted homozygous cell lines was the same in males, castrated males and even females, indicating that *PTEN* deletion is one possible pathway toward development of castration resistant PCa (Jiao et al. 2007).

In human tumours loss of *PTEN* has been shown to correlate with an upgrade from active surveillance to radical prostatectomy (Lotan et al. 2014) and recent single cell FISH analysis of

banked surgical specimens showed that *PTEN* loss was one of the most frequent genomic changes involved in PCa disease progression (Heselmeyer-Haddad et al. 2014).

PTEN loss has also been linked to genomic instability (Z. Sun et al. 2014; Hubbard et al. 2015), pointing out the role its high frequency of deletion in prostate cancer might play in the high level of genomic instability in high-risk prostate cancer (see section 7.2.9.1.) Prostate Cancer and Genomic Instability).

7.1.6.2.) TMPRSS2:ERG

Transmembrane protease, serine 2 (*TMPRSS2*) is a transmembrane serine protease whose exact biological activity has not been yet described, however it has been demonstrated that *TMPRSS2* expression is regulated by androgen (Lin et al. 1999). Fusions of *TMPRSS2* and the transcription factor erythroblast transformation- specific (ETS)-related gene (*ERG*) are reported in 30-70% of prostate cancers (Attard et al. 2009). *ERG* binds to purine rich regions of DNA and oddly has been shown by chromatin immunoprecipitation (ChIP)-seq and ChIiP-PCR to bind the promoter of the androgen receptor and decreased the levels of AR (Yu et al. 2010) as well as its downstream targets. It is suggested that this phenomenon may induce a dedifferentiation in prostate cells toward a more stem-like phenotype in which genomic instability is more common. However, since they increased expression of *ERG* alone and not the fusion protein whose levels would be decreased following a decrease in AR, it has not been determined if this would occur *in vivo*. Still, this might account for the epithelial to mesenchymal transition (EMT) that is commonly seen in PCa (Yu et al. 2010).

7.1.6.3.) MYC

An increase in nuclear *cMYC* is an early event in some PCa cases, with positive immune-staining in 72.5% of of hormone-naïve and radical prostatectomy patients (Zeng et al. 2015).

MYC has been identified as an oncogene since its discovery in Burkitt's lymphoma patients in 1972 (Manolov and Manolova 1972). *MYC* is upregulated in a wide variety of cancers (Louis et al. 2005) especially in Burkitt's lymphoma where its position on chromosome 8 is frequently translocated (Zech et al. 1976). The effects of *cMYC* upregulation are varied (Mai and Garini 2005) and include across the board increases in transcription, chromosomal rearrangements, and importantly the creation of telomeric aggregates (Mai and Garini 2005; Caporali et al. 2007; Louis et al. 2005) (see section 7.2.6.) . *cMYC* has also been shown to disrupt the nuclear architecture (Gadji et al. 2011) (see section 7.2.7.) as well as suppressing double strand break repair (Ramalingam and Doetsch 2012)

cMYC has been shown to be sufficient (when coupled with *PTEN* deletion (see section 7.1.6.1.) to initiate genomic instability and progression to a lethal metastatic cancer in a mouse model (Hubbard et al. 2015) and has been associated with a poor prognosis in prostate cancer patients when found with the *TMPRSS*:*ERG*-fusion gene (Rye et al. 2014).

7.2.) Telomeres and Genomic Instability

In 2009 Elizabeth Blackburn, Carol Greider, and Jack Szostak shared the Nobel Prize in physiology for their shared discovery of the physical structure of telomeres. Over the years intense attention has been paid to these unassuming segments of DNA for their role in aging and disease.

7.2.1.) Telomere Structure

Telomeres are the specialized chromatin structures of $(TTAGGG)_n$ repeats located at the end of linear eukaryotic chromosomes. Due to the way DNA is replicated all telomeres possess a 3' overhang, which if left exposed can be identified by the cells DNA repair machinery as a double strand break. Because of this, telomeres are typically bound by a group of proteins called

Shelterin. Human shelterin contains six distinct proteins: telomere retention factors 1 & 2 (TRF1 & TRF2) which bind double stranded telomeric repeats and provide a scaffold for the binding of other proteins via their large homology domains; TIN2 binds and stabilizes TRF1 & 2 as well as recruiting TPP1 which in turn binds POT1. POT1 binds to the single stranded 3' overhang. The sixth protein Rap1 interacts exclusively with TRF2. The telomere-shelterin complex forms a structure called a T-loop, a key function of which is to sequester the 3' overhang in a displacement loop (D-loop), inaccessible to the cell's repair machinery (Doksani and de Lange 2014).

7.2.2.) End replication problem & shortened telomeres

When a cell's DNA is replicated, because DNA polymerase II can only replicate from a 5' to 3' direction, a small segment of the lagging strand of the chromosome end is lost (Marcomini and Gasser 2015). This is called the end replication problem. Telomeres provide repetitive segments of DNA which are easier to replace (having a dedicated enzyme, telomerase) and the loss of which will be less compromising to the standard functioning of the cell than the loss of gene-rich segments. The attrition of telomeres increases with each round of DNA replication until the telomeres have reached a critical limit called the Hayflick limit. Below the minimum threshold of 12.8 repeats (Capper et al. 2007) telomeres become “critically” short. At this point conformational stress on the telomere makes it impossible to maintain the T-loop structure. Without the T-loop structure the 3’ end of the telomeres cannot be segregated and will be identified by the cell as a double strand break.

7.2.3.) Uncapped telomeres

Within a normal cell a “naked” telomere being recognized as a double strand break, whether by critical shortening or by a dysfunction of the shelterin capping proteins, will cause

the recruitment of the Mre11-Rad50-Nbs1 (MRN) complex and activate the ataxia telangiectasia mutated (ATM) pathway halt the cell cycle as the cell attempts to repair the damaged chromosome (Doksani and de Lange 2014).

7.2.4.) Lengthening of telomeres

Tumour cells, having bypassed many growth inhibition signals; grow, divide and replicate their DNA frequently reach the Hayflick limit quickly. If they are to continue dividing they either need to maintain the length of their telomeres and/or bypass any checkpoints within the cell cycle which would cause the cells to enter replicative senescence. The primary method of maintaining telomere length is through the enzyme telomerase which is active in 90% of human cancers (Shay and Wright 2011). The telomerase enzyme uses a reverse transcriptase function and an ribonucleic acid (RNA) template to add TTAGGG repeats to the end of the telomeres. A less frequent method of telomere elongation is alternative lengthening of telomeres (ALT)(Mirjolet et al. 2015). ALT is a recombination based method of elongation and was shown early on to rely on a homologous recombination protein RAD52 in telomerase null yeast (Cesare and Reddel 2010). High levels of ALT have been shown to generate higher levels of sister chromatid exchanges (Nabetani and Ishikawa 2011) which requires efficient resolution of the Holliday junctions generated by homologous recombination (Nabetani and Ishikawa 2011). Interestingly, XRCC3 - which interacts with RAD51 to form the CX3 complex, a key mediator of this resolution (Chun, Buechelmaier, and Powell 2013; Nabetani and Ishikawa 2011) - has been shown to be regulated by the androgen receptor (Karanika et al. 2014) and is necessary for the generation of small circularized extrachromosomal DNA fragments called t-circles characteristic of ALT (Compton et al. 2007).

7.2.5.) Illegitimate repair

DNA double strand breaks are handled by one of two main pathways depending on which phase of the cell cycle the cell is arrested in. At the S/G2checkpoint the less error prone HRR is preferred, while at the G1/early S checkpoint the less accurate non-homologous end joining is necessary (Mladenov et al. 2016) as no homologous copy is present.

7.2.5.1.) Non-homologous end joining

Upon the detection of a DSB by the MRN complex the Ku70/80 heterodimer (Ku complex) binds to each end of the break and recruits the DNA protein kinase catalytic subunit (DNA-PKcs) which phosphorylates Artemis (Lieber et al. 2010). Artemis:DNA-PKcs, activated by phosphorylation removes any single strand overhangs (Lieber et al. 2010). A DNA-ligase 4 complex then rejoins the ends of the break, completing repair. Although homologous sequences are not required for NHEJ, small segments of homology can form transient bonds during this process.

Within the field of prostate cancer it has been shown that ERG is a frequent interactor with the key NHEJ component DNA-PKcs, which is necessary for ERG's transcription factor activity (Brenner et al. 2011). Increases in DNA damage in cells with this fusion protein result in an increase in ETS transcription or interference with the DNA repair function of DNA-PKcs.

7.2.5.2.) Homologous Recombination Repair

Homologous recombination repair begins, similar to NHEJ, with the MRN complex being recruited to the DSB. The nuclease Exo1 trims back DNA surrounding the break, leaving 3' overhangs on both ends (X. Li and Heyer 2008; Mladenov et al. 2016). The helicase complex Dna2/BLM unzips the DNA helix on either end of the break (Mladenov et al. 2016). RAD51 catalyzes recognition of a homologous region for the damaged section (X. Li and Heyer 2008).

The broken strand invades the homologous strand, forming a displacement loop (D-loop) similar to that seen in normal telomeres. A DNA polymerase (research indicates polymerase δ is preferentially used (Maloisel, Fabre, and Gangloff 2008)), using the homologous strand as a template extends the 3' end of the broken strand until there is sufficient overlap for the broken strand to be "captured" by the 3' end of the other broken strand. Polymerization of DNA displaces the homologous strand, forming a displacement loop (D-loop). In eukaryotes the classic model for the completion of the repair is the Double Strand Break Repair (DSBR) pathway (X. Li and Heyer 2008). In DSRB the 5' strand invades the displaced strand (termed second strand capture) and is completed by DNA polymerase. This leads to the formation of a structure called a double Holliday junction which must be resolved by the endonucleases EXO1, SGS1 and the MLH1-MLH3 heterodimer cleaving the displaced strands and ligases rejoining them with their complimentary strands (see Figure 2, page 30 for a schematic). Depending on the resolution of the Holliday junctions cross-over events may occur between the homologous strands.

Figure 2: Schematic of DSBR pathway. From (Sung and Klein 2006). Image has been placed in the public domain by the authors.

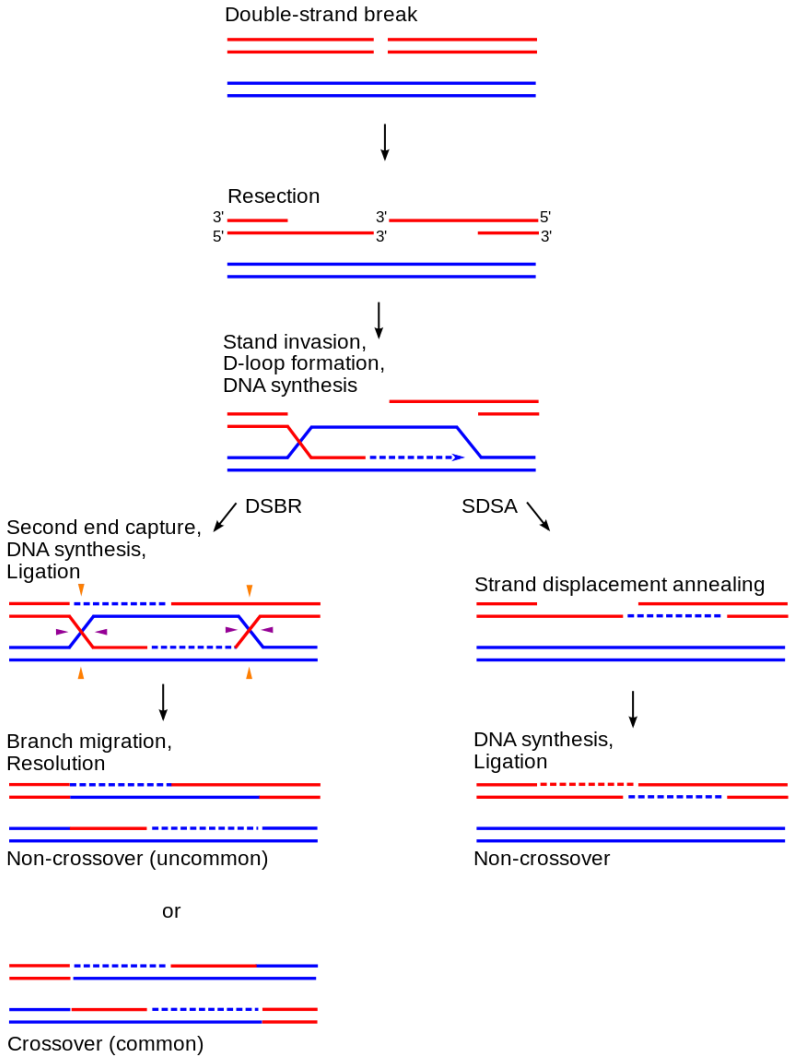

Telomeres lend themselves well to homologous repair. ALT is a homologous recombination mechanism that already functions on telomeres and in their uncapped state telomeres possess a ready-made 3’ overhang as well as numerous homologous regions throughout the nucleus. In addition, many of the proteins seen in HRR are seen in relation to uncapped telomeres in mice as well, such as Mre11, Rad50, Xrs2, Mec1, Cdc13, Est1, Est2,

yKu70/80 (Marcomini and Gasser 2015). If cross-over events were to occur in the illegitimate HRR repair of telomeres it may lead to the formation of telomere fusions and dicentric chromosomes.

7.2.6.) Breakage-Fusion-Bridge cycle and consequences

Illegitimate repair can lead to chromosome ends being fused together creating dicentric chromosomes or Robertsonian chromosomes. Fused telomeres are identified as telomere aggregates which show an increase in signal intensity during QFISH analysis (Vermolen et al. 2005). Spindle fibres then attach to each of the centromeres of dicentric chromosomes which may result in either the entire fused chromosome migrating into a single daughter cell or being pulled towards both forming cells, becoming an anaphase bridge (see **Figure 9**, page 54). If the dicentric chromosome splits in two during this process, one daughter cell inherits a terminal deletion and the other one an unbalanced translocation. During the next cell cycle, if the chromosome bearing this terminal deletion is still unable to form a t-loop another anaphase bridge may form and breakage of chromosomes will be repeated. Called the Breakage-Fusion-Bridge (BFB) cycle, over many successive cell cycles this phenomenon can lead to gain and loss of large segments of chromosomes or even whole chromosomes (Genesca et al. 2011). Throughout this process it is possible for daughter cells to gain (or lose) large amounts of genetic information as well as showing an increased number of telomeres as interstitial signals (Mai 2010).

7.2.7.) Three-dimensional nuclear organization of telomeres and the nuclear architecture

There is extensive evidence in the literature that the position of chromosomes in the nucleus is not random, but rather that chromosomes take up evolutionarily conserved "chromosome territories" which are cell type specific (Cremer and Cremer 2010; Weierich et al.

2003; Gadji et al. 2011; De Vos et al. 2009; Solovei et al. 2009). Changes in these territories has been shown to initiate tumourigenesis as far back as 1914 (Boveri 2008, translation). Recent research has shown alteration in the position of chromosomes lead to tumourigenesis in Hodgkin's lymphoma (Guffei et al. 2010), hereditary breast cancer (Wark et al. 2013) and ovarian cancer (Capo-chichi et al. 2011).

Lamin A, which is a key scaffold protein in the maintenance of nuclear architecture (Gonzalez-Suarez et al. 2009) has been identified as interacting with telomeres (Gonzalez-Suarez et al. 2009). Alterations that affect lamin A have been shown to result in shortened telomeres, aneuploidy and increased genomic instability (Gonzalez-Suarez et al. 2009) as well as changes in nuclear morphology and localization of telomeres (Taimen et al. 2009).

This change in position of the chromosomes allows for segments within certain chromosomes that would never usually interact become translocated during the repair of DNA damage (Gadji et al. 2011).

The Mai lab has been very active in the field of using quantitative telomere length (as measured by the intensity of a fluorescent probe bound to telomere repeats) and 3D nuclear position to make inquiries about nuclear architecture as it relates to tumour states (Vermolen et al. 2005; Gadji et al. 2012; Klewes et al. 2011; Wark et al. 2014; Adebayo Awe et al. 2013; Chuang et al. 2004; Kuzyk and Mai 2012; Mai and Garini 2006) and has created proprietary software for this analysis (Vermolen et al. 2005), as well as the positioning and number of centromeres (Silva et al. 2008).

7.2.8.) Relation of telomere length to disease states

Telomere shortening has been identified as an early event in many cancers (Meeker et al. 2002; Wark et al. 2014; Meeker, Hicks, Gabrielson, et al. 2004; Meeker, Hicks, Iacobuzio-

Donahue, et al. 2004), and has been identified, specifically in prostate cancer (Heaphy et al. 2015; Vukovic et al. 2007; Joshua et al. 2011) as an early indication of genomic instability. Previous work performed in our lab has utilized differences in telomere length to identify subpopulations within myelodysplastic syndromes and acute myeloid leukemia (Gadji et al. 2012), glioblastoma (Gadji et al., 2010), Hodgkin's lymphoma (Knecht et al. 2012) thyroid carcinoma (Wark et al. 2014), and CTCs of colon & breast cancer, melanoma, moderate-risk prostate cancer and a lung cancer cell line (Adebayo Awe et al. 2013). In these works telomere length (see section 10.2.) 44 for specifics on telomere length measurements) and increased telomere number has correlated to a more aggressive form of the disease through genomic instability.

7.2.9.) Genomic Instability

In 2011 an updated version of (Hanahan and Weinberg 2000) identified genomic instability as an enabling characteristic of cancer (Hanahan and Weinberg 2011).

Genomic instability comprises various large-scale alterations in the genomic content of a cell (Tapia-Laliena et al. 2014). At the sequence level these alterations include deletions, duplications and inversions, translocations, chromosome fusions and aneuploidy, all of which can lead to increased numbers of tumour promoter genes, decreases in tumour suppressor genes or changes in sequence leading to the expression of oncogenes (Hanahan and Weinberg 2011; Tapia-Laliena et al. 2014).

Any of these sequence alterations can lead to tumourigenesis by failure of apoptosis, bypassing of critical cell cycle checkpoints, an increase in angiogenesis or any combination of the above (Hanahan and Weinberg 2011; Tapia-Laliena et al. 2014).

7.2.9.1.) Prostate Cancer and Genomic Instability

Prostate cancer – especially high-risk prostate cancer - is often identified as having a high degree of genomic instability compared with other forms of cancer (Beheshti et al. 2001; Tapia-Laliena et al. 2014). This includes everything from deletions and copy number alterations to multiple whole chromosome gains and losses (aneuploidy). Because multiple tumour foci are often present in the prostate (Boyd et al. 2012) a potentially very large pool of clones may develop with various resistances to treatment due to the gain of tumour promoter and loss of tumour suppressor genes. In addition to being an early event in PCa development, GI has also been associated with progression to CRPC in a mouse xenograft model (Legrier et al. 2009). Work with *pTEN* and *p53* deficient mouse models with inducible telomerase (Ding et al. 2012) has shown that aggressive prostate tumours capable of forming bone metastases display large scale genomic alterations. In fact, high risk patients have primary tumours showing a median of 90 structural rearrangements (Schoenborn, Nelson, and Fang 2013). Lalonde et al. 2014 has indicated that a percentage of genomic alterations (PGA) ≥7.49 corresponded to a decreased relapse period for patients undergoing image-guided radiotherapy with a hazard ratio of 4.5x.

Taken together these observations indicate that our method of analyzing genomic instability in CTCs should yield important information about the outcome of the patient's therapy.

7.3.) Circulating Tumour Cells (CTCs)

Human blood contains millions of cells per millilitre. While levels of normal white blood cells may be indicative of systemic disease, CTCs offer the unique opportunity to obtain information about localized solid tumours based on the cells they shed into the peripheral blood.

7.3.1.) History of Study

Circulating tumour cells (CTCs) were first observed in 1869 by Thomas Ashworth in the blood of a man with metastatic cancer (Ashworth 1869). Along with this discovery Ashworth surmised that “cells identical with those of the cancer itself being seen in the blood may tend to throw some light upon the mode of origin of multiple tumours existing in the same person” (Ashworth 1869). Only occasional reports of CTCs were published for the next eighty years. In 1955 H.C. Engell reported finding CTCs in half of 140 cancer patients. Subsequent studies in the 1960’s were shown to have very low specificity and interest in CTCs waned until sensitive immunohistochemistry antibodies were used to find neuroblastoma CTCs in patient blood in the late 1980’s (Moss and Sanders 1990). CTCs enrichment began in 1998 when the first method for isolating them from was developed by attaching ferromagnetic particles to the antibodies (Racila et al. 1998). Today, CTCs are seen as being a potential indicator of disease severity as the number of CTCs in a patient’s blood before treatment has been linked to patient survival (see section 7.3.3.) page 38).

7.3.2.) Methods of isolation

As CTC enrichment is a relatively new field there are currently many novel methods being developed using multiple properties of CTCs and are discussed below.

7.3.2.1.) EpCAM

The most well established method currently is the use of CTC specific surface antigens (such as Epithelial cell adhesion molecule (EpCAM)) (“https://www.cellsearchctc.com/”) to bind antibodies conjugated with magnetic or fluorescently labelled markers. Cells are then sorted out using either magnetically activated cell sorting (MACS) (Schmitz et al. 1994) or fluorescent activated cell sorting (FACS) (Bonner 1972). The current most commonly used method for

isolating CTCs using this antigen based approach is CellSearch (Janssen Diagnostics, Raritan, New Jersey, United States). While it has been cleared by the FDA for use in prognosis and monitoring of metastatic breast, colorectal, and prostate cancer this method has limitations, most notably that it can fail to isolate CTCs which have <2000 EpCAM molecules on their cell surface (Coumans et al. 2010). In the epithelial-mesenchymal transition (EMT) undergone by more invasive tumour cells, critical for metastasis, the expression of EpCAM may be lost (Dolfus et al. 2015). Additional EMT genes have been found to be expressed in castration-resistant PCa (C.-L. Chen et al. 2013) which indicates that EpCAM based isolation may be less effective in more advanced tumours. In fact, a recent project (Loh et al. 2014) attempted to isolate CTCs from the blood of patients diagnosed with high-risk non-metastatic prostate cancer using CellSearch and was only able to get results from 14% of patients and even then at a maximum rate of 3 cells per 7.5mL of blood.

A second study has shown that CellSearch may capture only 60% of the CTCs that are captured by filtration methods (Adams et al. 2015).

7.3.2.2.) Microfluidics

A large area of focus in this field is the use of microfluidics, which applies selective forces to separate cells as they pass through small diameter channels. Studies have included the use of nano-mechanical phenotypes (elasticity, deformation, and adhesion) (Osmulski et al. 2014), electroactivity (Kobayashi et al. 2015), and even acoustical techniques (P. Li et al. 2015). This area of the CTC isolation field is very dynamic with techniques being constantly refined.

7.3.2.3.) Filtration

A smaller area of study (including this work) has concentrated on filtration using the size of CTCs (see section 1.3.1) to trap them for analysis (Desitter et al. 2011; Vona et al. 2000). Due

to their larger size when compared to lymphocytes (a CTC:lymphocyte area ratio of 4:1 for the prostate cancer cells line LNCaP as reported by (Vona et al. 2000)) and an average size of cells from the LNCaP cell line has been reported as 17 + 1.5μm (Zheng et al. 2007) it is possible to separate CTCs from whole blood with over 90% efficiency using a filtration method based on size as described in (Desitter et al. 2011). The average nuclear diameter reported for CTCs isolated from PCa patients using this method is between 9.1 and 15.7 (Awe et al. 2016. In comparison theaverage size of the average peripheral blood lymphocyte is 7-10μm.

CTC counts in prostate cancer using filtration methods have been shown to isolate between 2.8 and 15.3 CTCs/mL in T >3 prostate cancer patients, superior to the ≥5 CTCs in 7.5mL of blood that are considered prognostic using ScreenCell (Dolfus et al. 2015).

All filtration methods are based on a common concept: Patient blood samples are incubated in a buffer containing hemolytic agents and para-formaldehyde for cell pre-fixation. A polycarbonate filter with pores of uniform size (with size depending on the filtration method) is used to capture CTCs larger than the pore size while allowing the smaller red blood cells (RBC) and lymphocytes to pass through along with the blood/buffer melange (Dolfus et al. 2015). CTC filtration methods in general allows for simple, efficient separation of larger cells from the general population as well as providing a structure that is suitable for the various procedures required for molecular analysis and has been shown to retain 85%-100% of epithelial cells while allowing the passage of 99.9% of blood cells (Zabaglo et al. 2003).

ScreenCell^{tm} is further elucidated in the Materials and Methods section.

7.3.2.4.) Miscellaneous Isolation Methods

An early technique utilizing cellular properties of CTCs was to use Ficoll to isolate the cells based on their lower buoyant density when compared to normal blood cells (Rosenberg et

al. 2002), however because of its low specificity this technique is seldom used today (Zhe, Cher, and Bonfil 2011).

7.3.3.) Enumeration in cancer studies

Racila et al. 1998 reported a "good" correlation between the number of CTCs found in patient blood during treatment for breast cancer and patient response to chemotherapy (i.e. CTC levels decreased during patient remission and increased during patient relapse). More recent studies have displayed some conflicting results with (de Bono et al. 2008) reporting that metastatic CRPC displayed a worse overall survival and that an increase in CTCs post-treatment was associated with a worse overall survival than a decrease. Conversely, studies, also performed on metastatic CRPC have shown no relation between CTC counts and clinical evaluators such as Gleason score or T-staging (Kolostova et al. 2014; Loh et al. 2014). (Meyer et al. 2016), performed enumeration on locally advanced CRPC and also found no correlation between tissue staging as well as no statistically significant correlation with biochemical failure relapse. (Thalgott et al. 2013) showed a negative correlation between CTC counts in metastatic prostate cancer and PSA doubling time (i.e. as doubling time increased, CTC counts decreased), which is the opposite result one would expect, however (Goodman et al. 2011) have shown no correlation between PSA levels and CTC counts.

7.3.4.) Genetic similarity to source tumours

Array Comparative Genomic Hybridization (aCGH) (Møller et al. 2013; Paris et al. 2009) has shown that CTCs are genetically similar to their primary tumours, containing 80-90% of the same genomic copy number variations (Paris et al. 2009). One group (Helzer et al. 2009) found that CTCs from a mouse xenograft model of prostate cancer were transcriptionally similar to primary tumours. FISH experiments on CTCs and patient tissue samples showed concordant

PTEN gene status in 84% and 62% of fresh and archived tissue respectively (Punnoose et al. 2015).

7.3.5.) Other telomere studies on CTCs

Few studies have looked at telomeres in CTCs. Another study by our lab showed that measurement of telomere lengths can define subpopulations within the circulating tumour cell populations from prostate, colon, breast, melanoma tumours and a lung cell line (Adebayo Awe et al. 2013). This indicates that not all CTCs come from the same source with the same genetic background with the same levels of genomic instability. Another study, looking at telomerase activity in CTCs of metastatic CRPC in a Phase III Study of Docetaxel and Atrasentan found telomerase activity level had a Cox hazard ratio of 1.14 (Goldkorn, Ely, and Tangen 2014). This indicates that those patients displaying active telomere length maintenance via telomerase are 1.14 times more likely to incur mortality than those without and that CTC telomere status may be relevant to patient outcome.

7.3.6.) Circulating tumour DNA

A field of study related to circulating tumour cells is the study of circulating tumour DNA (ctDNA) (van de Stolpe and den Toonder 2014). This method isolates free DNA from patient blood, amplifies it using PCR (Bettegowda et al. 2014). While this technique has been able to identify circulating DNA in >75% of patients with certain types of cancer (Bettegowda et al. 2014), a circulating tumour DNA test has only been able to find ctDNA in <50% of prostate cancer patients (Bettegowda et al. 2014).

While it has produced results that relate changes in the genome to various types of cancer (Aarthy et al. 2015) there is a problem with identifying the source of the ctDNA. Research

indicates that ctDNA comes from apoptotic cells within the tumour (Stroun et al. 2001), which means that any cells shedding ctDNA will not be need to be targeted for treatment.

8.) Rationale

Studies going back over twenty years have used cells distant from the primary tumour to inform on the possible status of a primary prostate tumour. Bazinet et al. (1992) commented on Gleason score, ploidy and antigenic heterogeneity in metastases removed from lymph nodes. Hofer et al. 2006 correlated patient outcome with the size of lymph node metastases. Gao et al. (2014) established prostate organoid cultures from the lymph nodes advanced patients and compared copy number variations to known aggressive disease profiles. Other studies (Danila, Fleisher, and Scher 2011; de Bono et al. 2008; Lowes et al. 2015) have used CTCs in an attempt to predict the outcome of a primary tumour, however none of these have used ScreenCell filters which can capture all CTCs of a certain size rather than relying on surface markers that may be unreliable in a heterogeneous CTC sample.

Our lab has a long history of using telomeric data to describe possible genomic instability (Gadji et al. 2012; Kuzyk and Mai 2012; Wark et al. 2014; Adebayo Awe et al. 2013; Knecht et al. 2012) and has embarked on a prostate cancer study using CTCs isolated with the ScreenCell device since 2011.

9.) Hypothesis

This project is meant to determine whether measurement of a sample of circulating tumour cells in locally advanced, high-risk prostate cancer patients can determine differences in response to treatment over an observation period of six months. Based upon previous work done in this areas of CTCs, telomere analysis and PCa the following are expected:

1. The telomeric profiles of circulating tumour cells will vary between patients both before and after radiation and androgen deprivation therapy.
2. Patients whose CTCs show both fewer and/or smaller telomeres will also show increases in established markers for aggressiveness, such as Gleason score and PSA levels.
3. Patients whose CTCs show both fewer and/or smaller telomeres will also have a shorter period of disease free survival.

10.) Materials and Methods

This project was carried out in accordance with University of Manitoba Ethic Protocol (Ethics Reference No. H2011:336). Patient samples were transferred in a blinded manner with only a patient identifying number and date as distinguishing characteristics.

10.1.) Patient Blood Sampling & CTC Isolation

20 patients receiving ADT with the anti-androgen Bicalutimide and either leuprolide or goserelin as gonadotropin-releasing hormone (GnRH) agonist and 7800 centi-Grays of radiation over 39 fractions for RT were selected for this study. Patients had to meet the D'Amico criteria for locally advanced high risk prostate cancer to be considered for inclusion in this study. Absence of bone metastases was confirmed using a technetium bone scan, ensuring that any CTCs found were from the primary tumour.

Table 1: Summary of patient clinical information (Gleason and TNM staging was performed at baseline only)

			PSA (ng/mL)		
PatientID	Gleason Score (+0m)	TNM Staging (+0m)	+0 months	+2 months	+6 months
MB0389PR	9	T2bNXMX	11.24	1.28	0.03
MB0393PR	9	T2b	29.48	17.99	0.5
MB0394PR	9	T2a	13.27	7.44	0.01
MB0405PR	8	T2b	2.87	0.26	0.01
MB0408PR	8	T2a	7.44	0.34	0.02
MB0410PR	9	T2a	0.78	0.02	0.01
MB0413PR	9	T2c	25.22	4.97	0.03

MB0418PR	9	T2c	14.42	1.54	0.38
MB0421PR	9	T1c	8.68	0.2	0.16
MB0426PR	8	T1c	6.93	0.11	0.05
MB0438PR	8	T2b	23.19	5.22	0.16
MB0441PR	7	T3NxM0	7.41	4.71	1.52
MB0444PR	9	T2a	11.91	2.71	0.09
MB0445PR	7	T2b	26.55	0.51	0.03
MB0446PR	9	T2c	23.8	1.87	1.32
MB0452PR	8	T1cN0MX	9.27	0.19	0.01
MB0461PR	9	T2a	11.26	1.23	0.09
MB0466PR	8	T2a	11.25	0.01	1.64
MB0475PR	7	T2a	26.11	0.82	0.01
MB0500PR	9	T1c	14.28	1.47	0.02

9mL of blood from each patient was collected in Vacutainer^{R} blood collection tubes (with Ethylenediaminetetraacetic acid (EDTA) as anti-coagulant) was drawn at each time point and processed within two hours.

Figure 3: Timeline of treatment time and duration (coloured bars) and sampling points (blue circles) throughout course of patient monitoring.

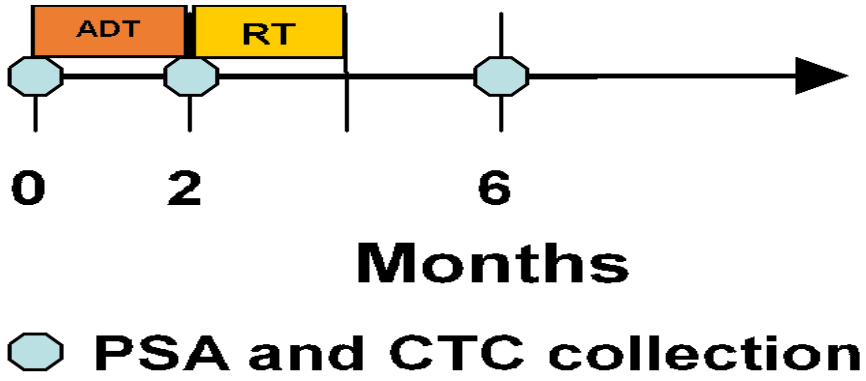

6mL was used to obtained serum samples which were frozen at -20°C. The remainder (3mL)was incubated and fixed in 4mL ScreenCell® FC2 buffer at room temperature for 8 minutes, inverting throughout and then drained via vacuum tube through a ScreenCell Cyto-filter (Desitter et al. 2011) containing 1×10^5 pores/cm^2 pores that are 7.5 ± 0.36µm in diameter to separate out CTCs and lymphocytes deposited on the filter by fluid dynamics, though it should be noted that lymphocytes will not be cleared completely, merely depleted). Filters were stored at 4°C for a maximum of three months before further processing.

10.2.) Quantitative Fluorescent *in situ* Hybridization (QFISH)

Filters containing sample were incubated in 1x PBS for 5 minutes followed by a 10 minute fixation in 3.7% formaldehyde/1x PBS. 3 washes of 5 minutes each in 1x PBS was used to clear any remaining formaldehyde from the filters. Deproteinization was performed via protein degradation with a 10-minute incubation at 37°C in 0.01M HCl/50µg/mL Pepsin. Then 1 wash of 5 minutes in 1x PBS followed by a post-fixation for 10 minutes in 3.7% formaldehyde/1x PBS. 3 washes of 5 minutes each in 1x PBS. The filters were then dehydrated in a series of 3 ethanol washes (70%, 90%, 100%) followed by air drying until completely dry.

The filters were placed on a standard microscopy slide and 4μL of a cyanine 3 (Cy3) fluorescently conjugated, telomere specific protein/nucleic acid (PNA) probe (Dako, 1100 Burloak Dr, Burlington, Ontario, Canada L7L 6B2) was placed in the centre. A 24x24mm coverslip was placed over the filter and sealed with 1% agar. Slides were denatured on a Hybrite (Abbott Molecular, 1300 E Touhy Ave, Des Plaines, IL, USA, 60018) at 80°C for 3 minutes followed by hybridization for 120 minutes at 37°C. After hybridization the filters were removed from the slides and washed twice in 70% formamide/10mM Tris(hydroxymethyl)aminomethane (Tris) (pH 7.4) for 15 minutes each to remove excess probe, followed by a 1 minute wash in 1x PBS. Filters were then washed at 55°C for 5 minutes in 0.1x SSC and then at room temperature twice for five minutes each in 2x SSC/0.05% Polysorbate 20 to permeabilize the cell membrane for 4',6-diamidino-2-phenylindole (DAPI) counterstaining. The filters were again dehydrated in a series of ethanol washes (70%, 90%, 100%) followed by air drying until completely dry. They were attached to new microscopy slides with clear nail polish. Anti-bleach with DAPI (Vector labs, Burlington, Ontario, Canada) was added and a custom coverslip placed on the filter.

Binding of the PNA probe to the telomere repeats produces a cumulative fluorescence with an intensity proportional to the number of telomere repeats. This intensity is used as a surrogate for telomere length in the analysis.

10.3.) Three Dimensional QFISH Imaging

CTCs were isolated based on size and to a lesser extent pleomorphism of their DAPI stained nuclei. Slides were imaged on a Zeiss AxioImager Z2 microscope with a Zeiss Axio Cam model MRmm Rev 3 digital camera using AxioVision Release 4.8.2 (Carl Zeiss MicroImaging GmbH). A Cy3 filter was used to detect the Cy3 probe hybridized to the telomeric repeats (initial exposure time of 500ms, reduced to 20ms with replacement of the microscope light source,

calibration was performed by measuring exposure time of tri-coloured beads (Molecular Probes, Eugene, Oregon, USA) and confirmed by reimaging a recent filter with the new exposure time and comparing results). DAPI filter exposure times differed between slides. 80 focal planes spaced 200nm apart were imaged in order to create a three-dimensional representation of the circulating tumour cells and lymphocytes on the filter. Images were deconvolved using a constrained iterative algorithm (Schaefer, Schuster, and Herz 2001).

Figure 4: Example of a circulating tumor cell captured on top of a filter pore (red arrow). A) Two-dimensional image. Nuclear DNA stained with DAPI (blue), telomeres labelled with telomere specific Cy3-labelled probe (red); B) The same cell as in A) illustrated in three-dimensional representation, view from top. Red spots represent telomere FISH signals; C) The same cell as in A) with three-dimensional representation of telomere FISH signals, view from the side.

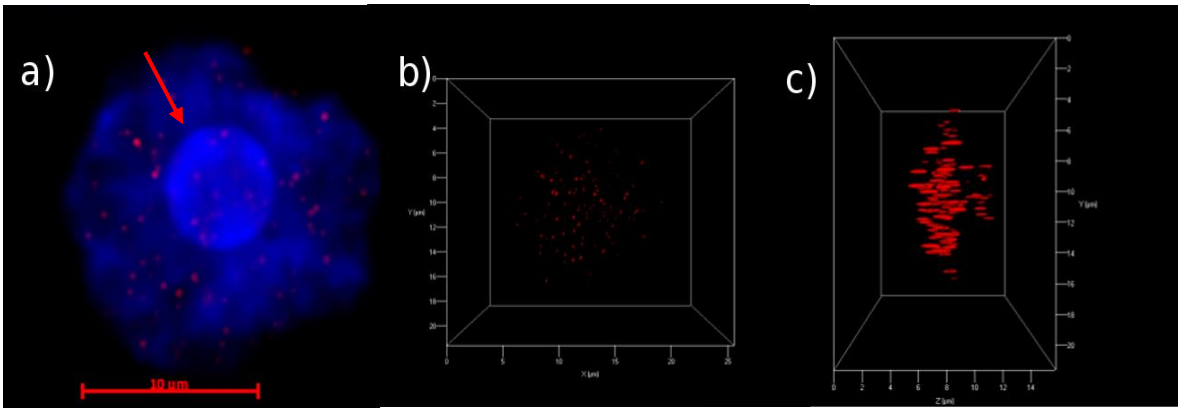

10.4.) QFISH Analysis

For each patient sample 30 CTCs and 30 lymphocytes (used as internal controls) nuclei from the same filter were distinguished based on size and analyzed using our TeloView software (Vermolen et al. 2005). This software creates orthogonal views of the cell nucleus along the xy, yz and xz axes and identifies signals in the Cy3 channel. Intensity in Arbitrary Units (AU) is

calculated using the average intensity per pixel of a signal multiplied by the number of pixels making up that signal. Positional data is extracted using the 3D position of signals in relation to each other and to the overlapping DAPI channel. Nuclear volume in μm^3 is calculated based on multiplying the number of pixels making up the nucleus by the height and width of each pixel (scale axial = 102nm) along with the depth of each slice (scale lateral = 200nm).

Data was obtained on the intensity of each signal, whether that signal could be considered an aggregate (two or more signals that cannot be resolved due to proximity and the optical resolution limit of conventional microscopy (200nm), defined as a signal with intensity above the standard deviation of signal intensity for that cell), the number of signals as well as the nuclear volume per cell. Each of these measurements were used to distinguish the CTCs at time points from the same patient.

a) b) c)

The decision was made to disregard clusters of CTC from the telomere analysis as it can be difficult to distinguish between cells lying in close proximity on the filter and signals from a second cell may end up being included in the first, artificially inflating the number of signals.

10.4.1.) Non-subjective ranking of changes in number of short telomeres

Rather than rely on a strictly subjective visual method of qualifying which patient fell into which group I developed a way to compare the histograms using the difference between the peaks of each curve and continuing to plot the difference of the counts in each 1000 AU bin until both curves reached a consistent count of 0 signals (see, **Figure 5**, , page 48). A line of best fit was fitted to the plot of differences and its first degree coefficient was used as a summary for the size of the difference between the peaks of the two curves. The leading coefficient was ignored as it was only relevant as the differences became vanishingly small.

Figure 5: Example of slope formula creation between time points using code given in Appendix 9.1. a) The classical comparison of telomere size and count. b) Calculated differences between the bins from peak to difference = 0. c) Black dots in B represent the calculated difference between bin counts at the intensity indicated on the x-axis, blue line indicates line of best fit.

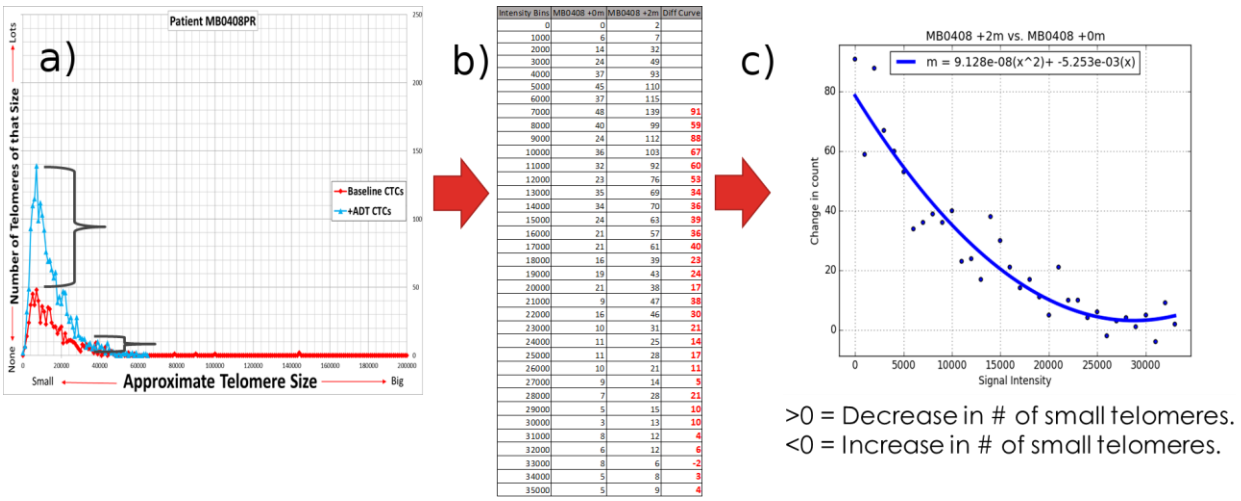

Intensity Bins	MB0408 +0m	MB0408 +2m	Diff Curve
0	0	2	
1000	6	7	
2000	14	32	
3000	24	49	
4000	37	93	
5000	45	110	
6000	37	115	
7000	48	139	91
8000	40	99	59
9000	24	112	88
10000	36	103	67
11000	32	92	60
12000	23	76	53
13000	35	69	34
14000	34	70	36
15000	24	63	39
16000	21	57	36
17000	21	61	40
18000	16	39	23
19000	19	43	24
20000	21	38	17
21000	9	47	38
22000	16	46	30
23000	10	31	21
24000	11	25	14
25000	11	28	17
26000	10	21	11
27000	9	14	5
28000	7	28	21
29000	5	15	10
30000	3	13	10
31000	8	12	4
32000	6	12	6
33000	8	6	-2
34000	5	8	3
35000	5	9	4

10.5.) Immunocytochemistry

In order to confirm the prostatic origin of captured CTCs a check for the presence of androgen receptor (AR) was made on CTC filters using directly fluorescently labelled AR-441 mouse monoclonal antibody (Santa Cruz) raised against amino acids 299-315 of the human androgen receptor. This segment of the AR is found within the NH_2 terminal trans-activation domain (NTD) and is present in all splice variants common in PCa (van der Steen, Tindall, and Huang 2013).In order to confirm the prostatic origin of captured CTCs a check for the presence of androgen receptor (AR) was made on CTC filters using an AR-441 mouse monoclonal antibody (Santa Cruz) raised against amino acids 299-315 of the human androgen receptor. This segment of the AR is found within the NH_2 terminal trans-activation domain (NTD) and is present in all splice variants common in PCa (van der Steen, Tindall, and Huang 2013). The antibody was

directly labelled with a fluorescein (FITC) fluorophore.

Filters containing sample were incubated in 1x PBS/50mM $MgCl_2$ for 5 minutes followed by a 20 minute fixation in 3.7% formaldehyde/1x PBS. Then 3 washes of 5 minutes each in 1x PBS/50mM $MgCl_2$. This was followed by blocking in 4x SSC/4% BSA at 37°C for 30 minutes. The antibody was applied in a concentration of 1:50 (20ng/µL) and allowed to incubate at 37°C for 30 minutes. Excess antibody was washed off in 3 1x PBS/50mM $MgCl_2$ washes of 5 minutes each. The filters were dehydrated in a series of ethanol washes (70%, 90%, 100%) followed by air drying until completely dry. They were attached to new microscopy slides with clear nail polish. Anti-bleach with DAPI (Vector labs) was added and a custom coverslip placed on the filter.

The choice was made not to perform immunocytochemistry on the same filters as QFISH as any overlap between the FITC and Cy3 emission spectra would lead to a shift in the intensity in the telomere signals as the Cy3 image may include FITC background (see **Figure 6**, page 50, overlap of green and yellow).

Figure 6: Comparison of the FITC and Cy3 excitation and emission spectra. (From**:** https://www.thermofisher.com/ca/en/home/life-science/cell-analysis/labeling-chemistry/fluorescence-spectraviewer.html**)**

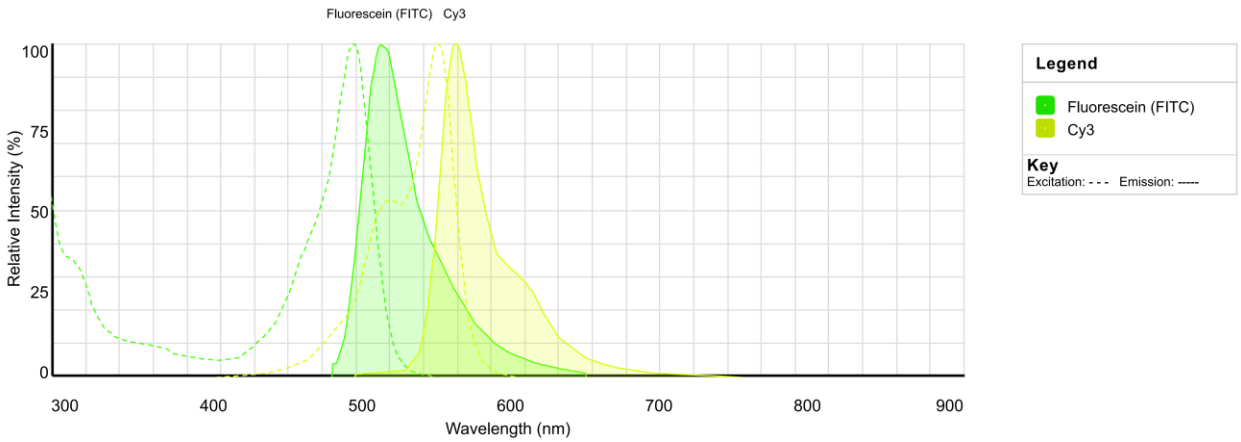

10.6.) CTC Enumeration

In order to expedite automated focusing filters that were previously processed using the QFISH procedure were removed from their metal ring using an 8mm biopsy punch and remounted on a new slide using Vectashield with DAPI and a fresh 18mmx18mm coverslip. This method offered superior focussing ability when compared to leaving the filter attached to its ring.

Filters were imaged on a Zeiss Axio Imager Z2 microscope with a Plan-APOCHROMAT 40x (numerical aperture 0.98) objective (Zeiss, Oberkochen, Germany). Images were acquired using GenASIs software (ASI, Vista California, USA) and then exported using the Tagged Image File (tif) Format. Images were reviewed using ImageJ where CTCs were identified manually and their common features (area $\geq$ 2500, solidity (the proportion of pixels in a convex hull around the region of interest that are also with the region of interest), $\geq$ 0.90, circularity (the ratio between two circles large enough to enclose the region of interest and small enough to fit into the region of interest respectively) $\geq$ 0.60, standard deviation of DAPI intensity < 11) were extracted.

Using a python 3.4 algorithm, the tif images were converted into binary images and segmented with a watershed algorithm (See appendix 9.2). Criteria for inclusion in the set of CTCs were cell size (Minimum area: 2000 pixels Maximum: ∞ pixels), circularity (Minimum:0.60 Maximum:0.9) and solidity (Minimum:0.90).

Figure 7: a) Example of numerical values extracted from scanned tif images using ImageJ. b) Example of a scanned tif before application of cell identification algorithm. c) The same scanned tif as in b) with identified cells covered red and green mask.

a)

	Label	Area	Mean	StdDev	Mode	Min	Max	Perim.	Width	Height	Major	Minor	Angle	Circ.
53	107_0-DAPI 2.tif:0007-0134	384.363	15163.68	1950.236	15952	10041	20825	76.44	22.95	22.44	22.886	21.384	135.365	0.827
54	107_0-DAPI 2.tif:0011-0266	272.39	16046.75	2906.038	17525	9302	24592	65.147	19.635	18.36	19.726	17.582	155.839	0.807
55	107_0-DAPI 2.tif:0010-0217	674.894	21805.13	6488.9	17541	10828	36929	105.717	30.09	30.6	31.815	27.009	56.621	0.759
56	107_0-DAPI 2.tif:0013-0384	782.641	24773.9	6165.13	25312	10982	38467	124.026	35.955	35.445	32.164	30.982	169.054	0.639

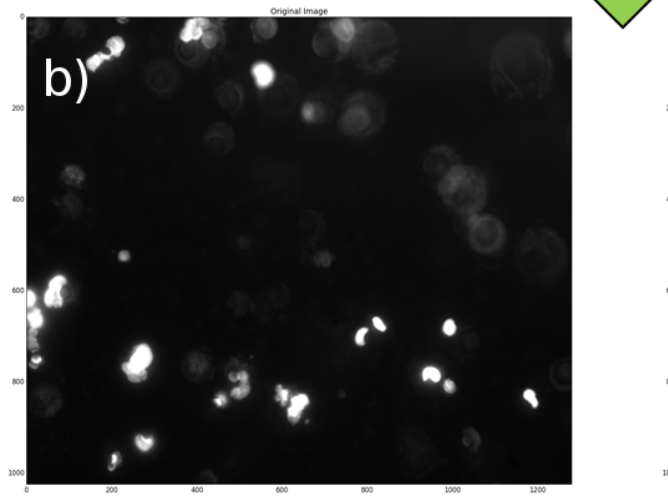

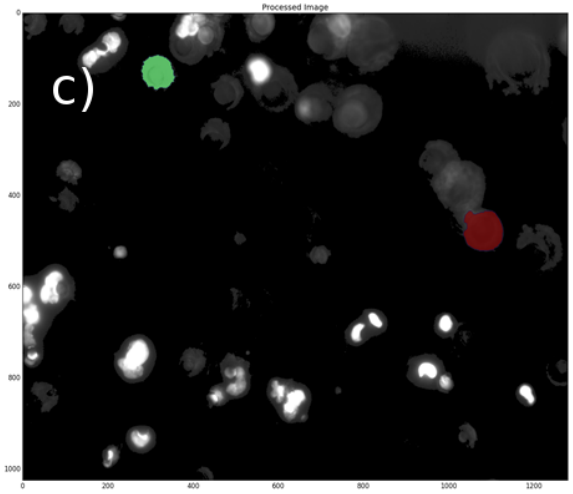

The decision was made to disregard clusters of CTC from the enumeration analysis as it is uncertain whether the suction action of the filter would pull CTCs which may not be associated in the patient's blood into the same pore, creating artificial clusters.

10.7.) Statistics

Samples were clustered into groups based on a principal component analysis of three dimensional nuclear profiles as well as CTC enumeration counts using a centroid clustering procedure. Correlations of parameters (e.g. CTC counts with PSA levels) were done using the Spearman's rank correlation coefficient, which compares the ranks (highest to lowest) of two features. Statistical analysis was performed by Statistician Mary Cheung using Statistical Analysis System (SAS) version 9.3.

11.) Results

11.1.) Cell Morphology

Cursory visual analysis of the CTCs on the filter membranes revealed a wide diversity of cell sizes and shapes. While the majority of patient samples displayed cell nuclei stained with DAPI with a maximum diameter of roughly 10-25µm some patients displayed extraordinarily large cells/clusters over 40µm in diameter (see section 14.4.) page 108). Others displayed strands of DAPI stained chromatin reaching between nuclei (see **Figure 9**, page 54) indicating there was a problem segregating chromosomes during anaphase. Still other samples showed what appeared to be cells with degraded DNA, displaying invaginations within the cell nuclei. Typically, these invaginated nuclei were seen in post-radiation (+6m) samples (see **Figure 8**, page 53), although 2 of the post-ADT (+2m) samples had few of these invaginated nuclei as well.

Figure 8: Example of increased nuclear dysmorphy within nuclei of CTCs from patient MB0394 after the introduction of ionizing radiation. a) nucleus of a CTC from patient at +0m. Bright region indicates autofluorescenceauto-fluorescence of a filter pore. b) nucleus of a CTC from patient at +2m. c) nucleus of a CTC from patient at +6m. Extreme changes in morphology were seen in patients post-RT (i.e. +6m)

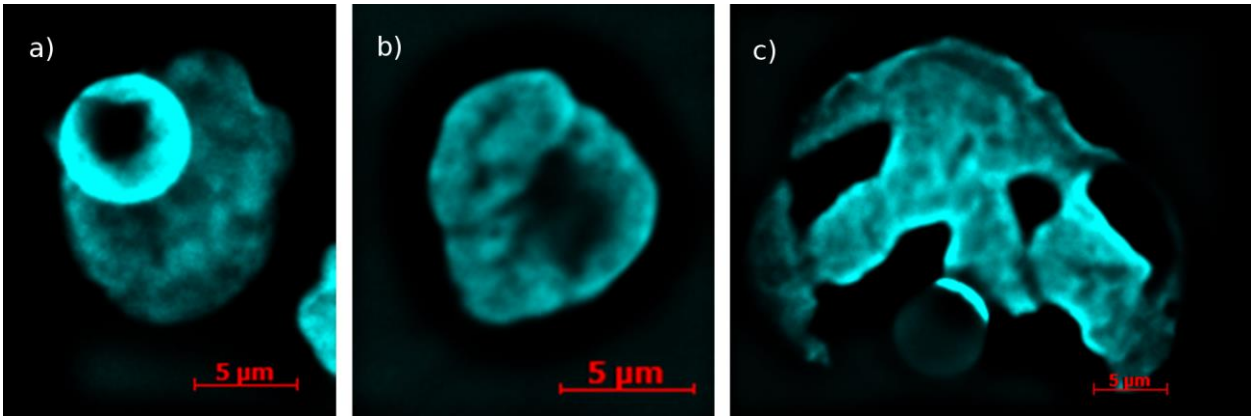

In conclusion, a large heterogeneity of nuclear shapes was noted among circulating tumour cells both before and after treatment with ADT and RT.

Figure 9: Example of chromatin bridge occurrence in untreated high-risk prostate cancer cells with DAPI stain. An example of auto-fluorescence in a filter pore is marked with a red arrow.

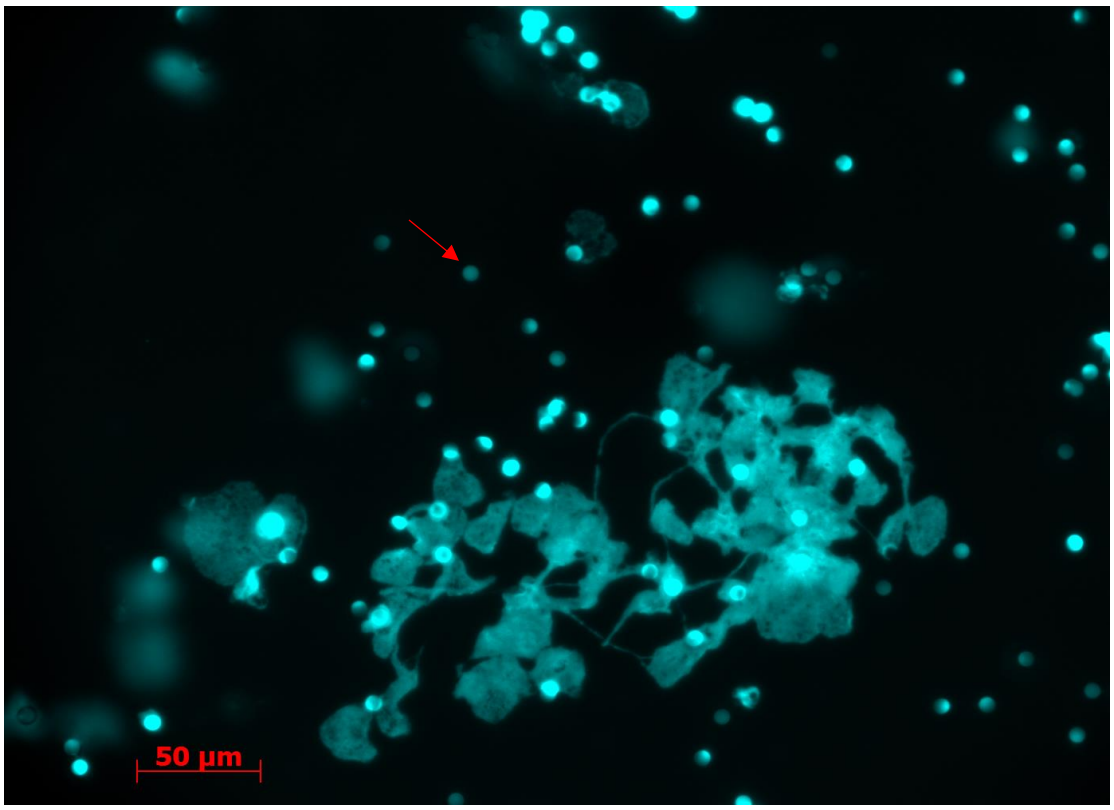

11.2.) Immunocytochemisty

Three filters that were created from duplicate patient samples for androgen receptor staining showed fluorescent staining on a majority of cells that were larger in diameter than 10µm and an absence of staining on cell that were smaller in diameter than 8µm. This is expected due to the heterogeneous expression of the AR as described in (P. Li et al. 2002). Androgen staining was seen throughout the cell as both the active and inactive form of AR was stained.

Figure 10: Example of immunocytochemistry using androgen receptor antibody (FITC) with nuclear counterstain (DAPI) on patient blood captured on ScreenCell filters. a) shows a larger captured CTC (marked with yellow asterisk) b) shows smaller captured lymphocytes on the same filter (marked with white arrows). Staining to confirm lymphocytic origin of cells in b) was performed in a related publication (Awe, 2016, under review)

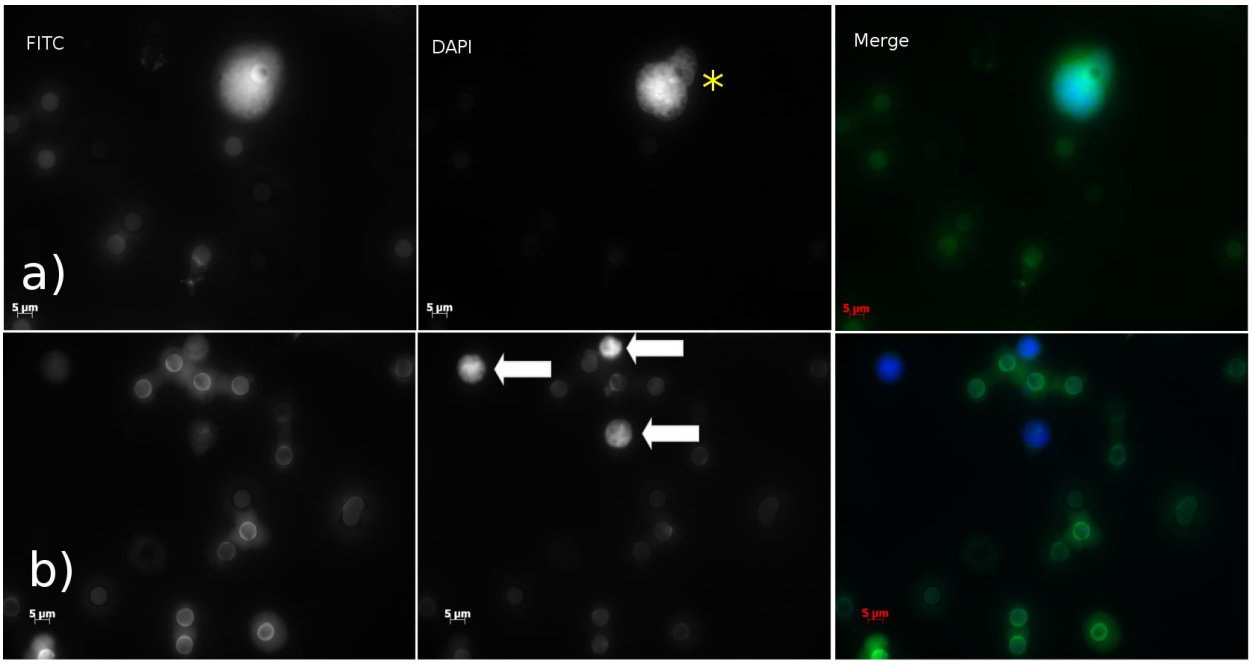

11.3.) Telomere Analysis

11.3.1.) Changes in CTC telomere profiles from 0-2 months

Using a comparison of the +0m (pre-treatment) and +2m (2 months into ADT) prostate CTC samples (**Figure 5**, page 48) we were able to divide patients into three distinct groups: 1) Patients who showed a decrease in the number of short telomeres within the thirty cells analyzed between the two time points. 2) Patients who showed virtually no change in the number of short telomeres within the thirty cells analyzed between the two time points. 3) Patients who showed an increase in the number of short telomeres within the thirty cells analyzed between the two time points.

Upon applying the ranking algorithm (see Materials and Methods 2.4.1) the difference in number of short telomeres yielded a single unit-less number, which allowed for a non-subjective way to place each sample into one of the three groups, which, for the initial 20 samples, faithfully reproduced the results of the subjective visual analysis and allowed for quantification of the groups. Patients scoring over $1x10^{-3}$ (high number of short telomeres at +0m, smaller number at +2m) were placed in group 1. Those between $1x10^{-3}$ and $-1x10^{-3}$ were placed in group 2 (low number of short telomeres at +0m, little difference +2m). Those less than $-1x10^{-3}$ (low number of short telomeres at +0m, higher number +2m) were placed in group 3 (See **Figure 11**, page 57; , **Figure 12**, page 58; , **Figure 13**, page 59). These values were chosen as they were approximately the values of patient samples that were frequently placed in different groups during iterations of visual analysis. All together 9 of our 20 patients were placed in group 1 (see **Figure 11**, page 57 as an example), 5/20 were placed in group 2 (**Figure 12**, page 58 as example), and 6/20 were placed in group 3 (**Figure 13**, page 59 as example).

Table 2, page 61 provides a summary of the degree of change in the number of short telomeres in a numerical format.

Figure 11: Example of telomere length profile of a patient (MB0426) assigned to group 1. Baseline profile in red, post-androgen deprivation therapy in blue, post-radiotherapy in green. In this group large numbers of small telomeres were reduced after ADT and little change was seen post-RT. Inlay A) calculated curve summarizing the degree of change in number of short telomeres between +0m and +2m. Inlay B) calculated curve summarizing the degree of change in number of short telomeres between +2m and +6m.

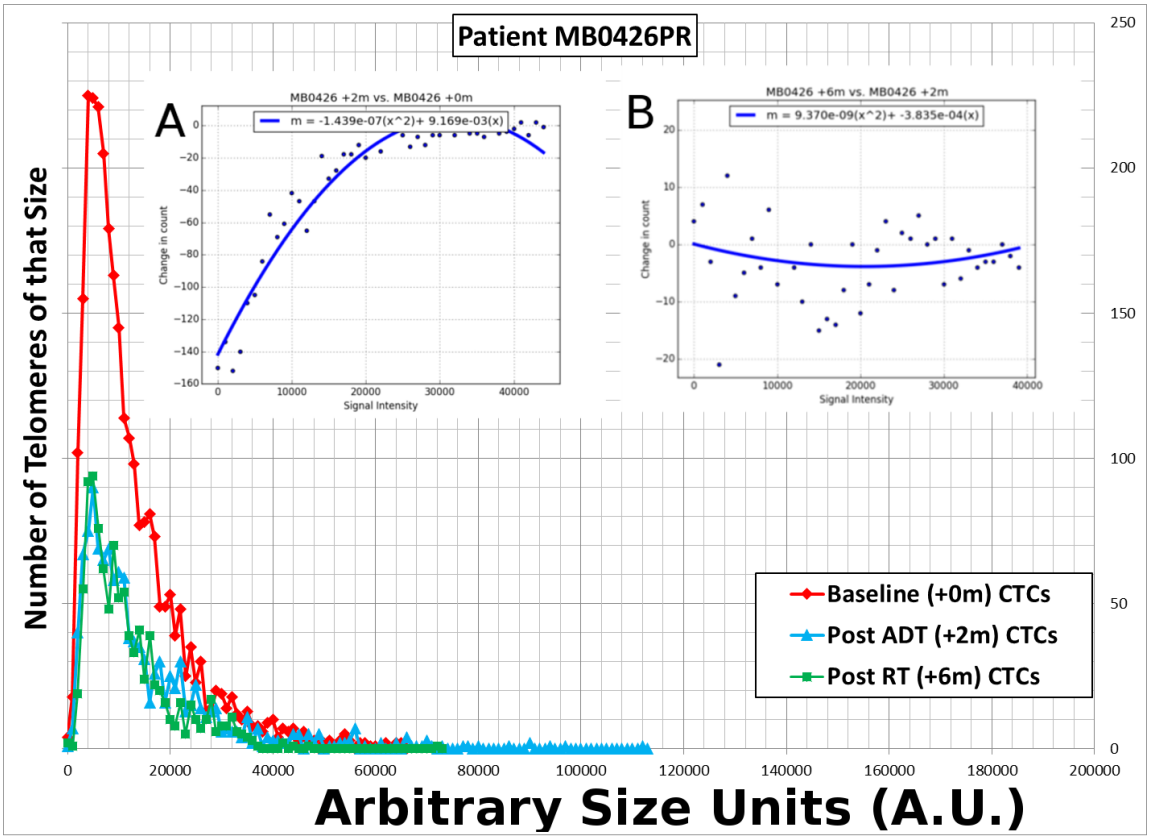

Figure 12: Example of telomere length profile of a patient (MB0405) assigned to group 2. Baseline profile in red, post-androgen deprivation therapy in blue, post-radiotherapy in green. In this group little change was seen in short telomere numbers post-ADT or post-RT. Inlay A) calculated curve summarizing the degree of change in number of short telomeres between +0m and +2m. Inlay B) calculated curve summarizing the degree of change in number of short telomeres between +2m and +6m.

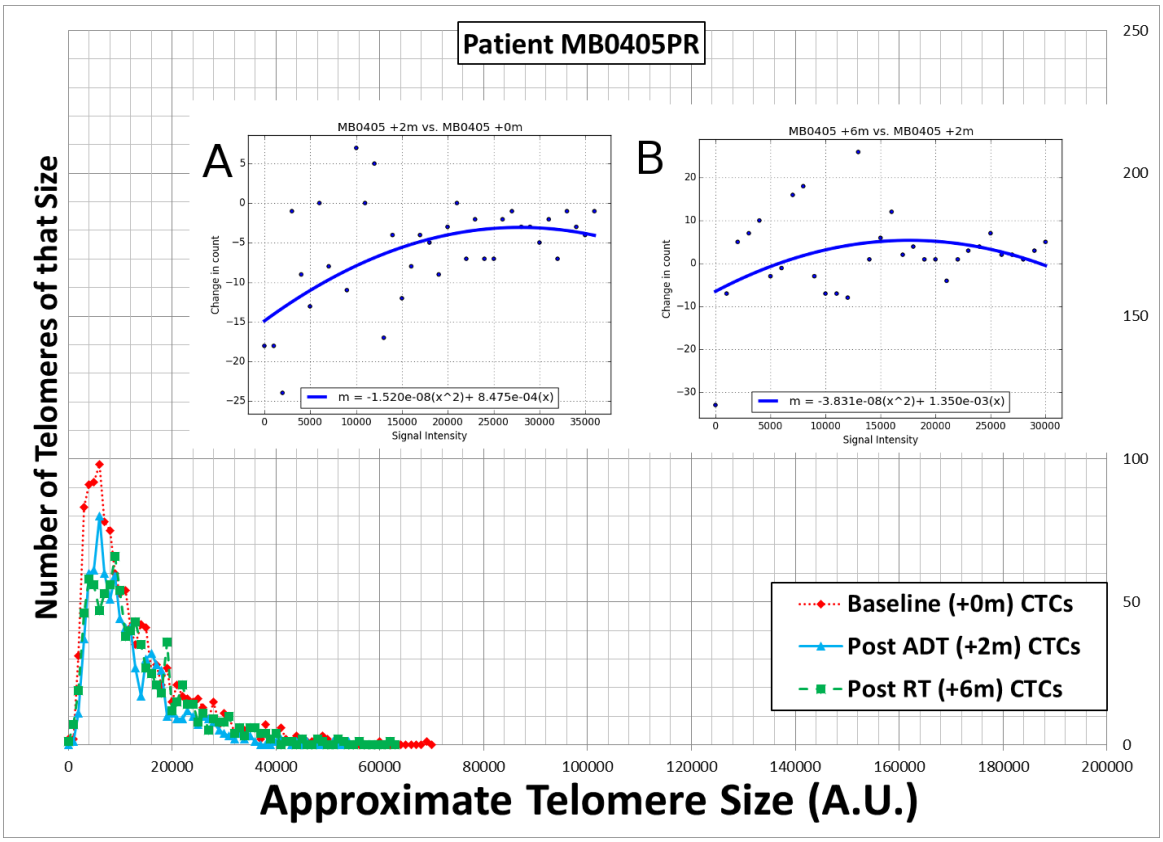

Figure 13: Example of telomere length profile of a patient (MB0408) assigned to group 3. Baseline profile in red, post-androgen deprivation therapy in blue, post-radiotherapy in green. This In this group numbers of short telomeres increased post-ADT before returning to baseline levels post-RT. Inlay A) calculated curve summarizing the degree of change in number of short telomeres between +0m and +2m. Inlay B) calculated curve summarizing the degree of change in number of short telomeres between +2m and +6m.

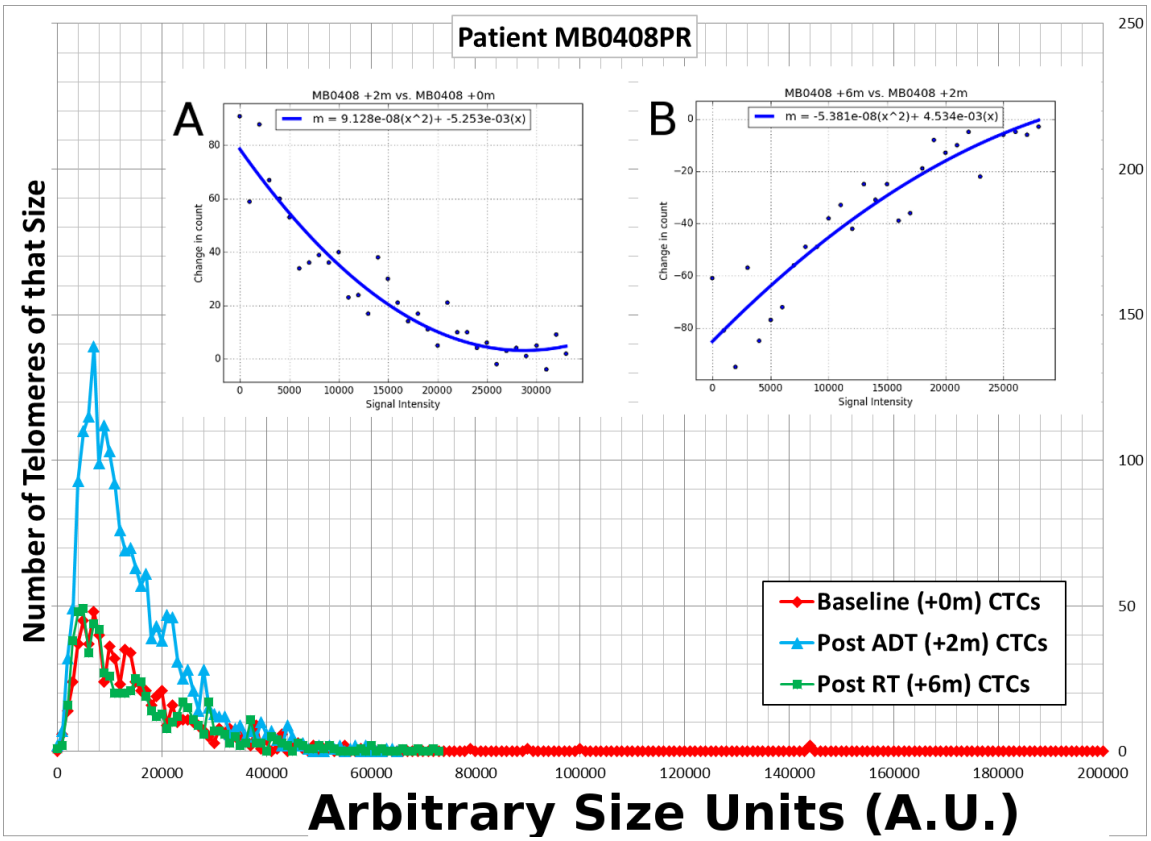

11.3.2.) Changes in CTC telomere profiles from 2-6 months

Patients showed a predictable response to initial radiation treatment (at +6m) based upon which group they fell into during the 0-2 month time points. Group 2 showed very little or no change in

Figure 14: Summary of degree in change in the number of short telomeres in each of the twenty 0-2 (grey) and 2-6 month (white) patients. Sorted based on degree of change at 0-2 months. Numerical values are given in **Table 2**, page 61.

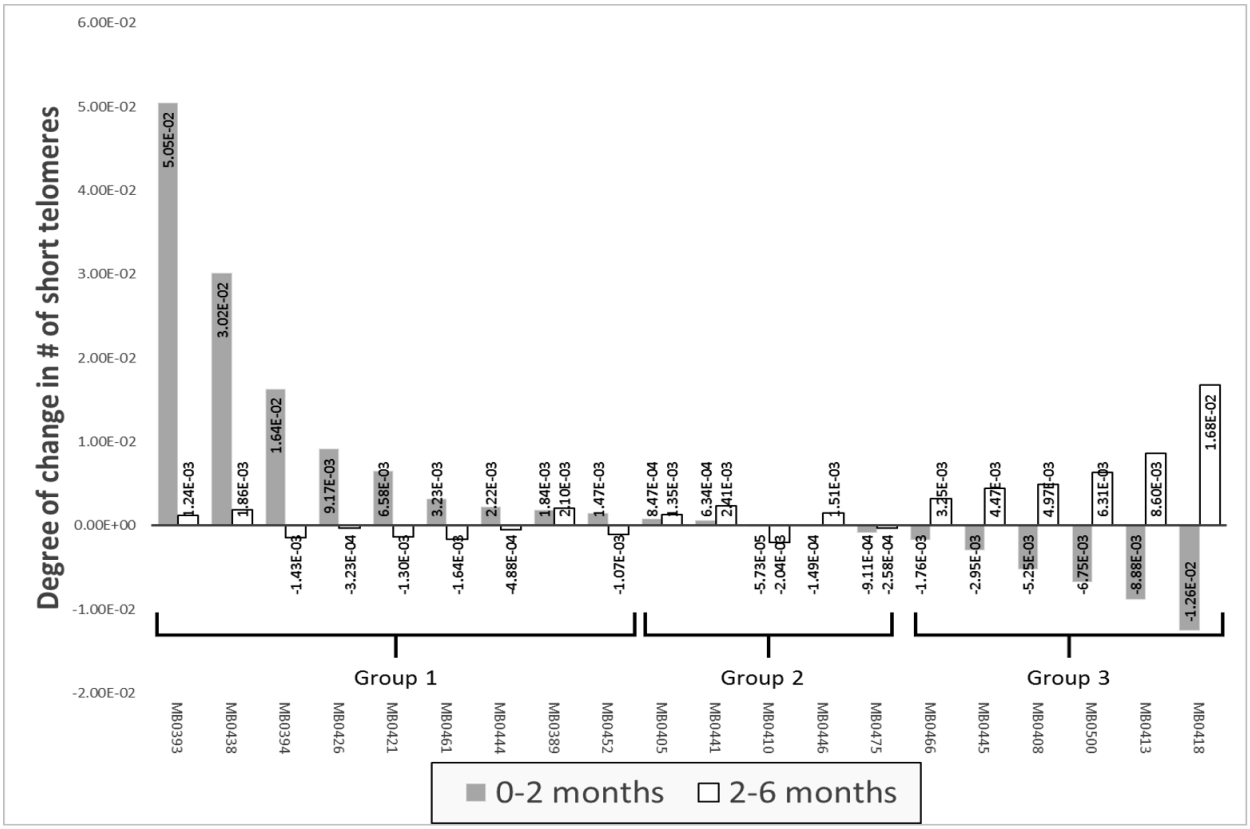

the number of short telomeres from +2 months to +6 months as did Group 1 in contrast to the large changes seen from +0 to +2 months in that group. A surprising result was that Group 3 had an almost mirror image decrease in the number of short telomeres compared to the increases seen in the 0-2 month comparison (**Figure 14**, page 59 as an example).

Table 2: Summary of line slope as a measure of degree of change in the number of short telomeres and the groupings of each patient.

	Group	Slope +0 to +2 months	Slope +2 to +6 months
MB0393	Group 1	5.05E-02	1.24E-03
MB0438	Group 1	3.02E-02	1.86E-03
MB0394	Group 1	1.64E-02	-1.43E-03
MB0426	Group 1	9.17E-03	-3.23E-04
MB0421	Group 1	6.58E-03	-1.30E-03
MB0461	Group 1	3.23E-03	-1.64E-03
MB0444	Group 1	2.22E-03	-4.88E-04
MB0389	Group 1	1.84E-03	2.10E-03
MB0452	Group 1	1.47E-03	-1.07E-03
MB0405	Group 2	8.47E-04	1.35E-03
MB0441	Group 2	6.34E-04	2.41E-03
MB0410	Group 2	-5.73E-05	-2.04E-03
MB0446	Group 2	-1.49E-04	1.51E-03
MB0475	Group 2	-9.11E-04	-2.58E-04
MB0466	Group 3	-1.76E-03	3.25E-03
MB0445	Group 3	-2.95E-03	4.47E-03
MB0408	Group 3	-5.25E-03	4.97E-03
MB0500	Group 3	-6.75E-03	6.31E-03
MB0413	Group 3	-8.88E-03	8.60E-03
MB0418	Group 3	-1.26E-02	1.68E-02

11.4.) CTC Enumeration

In contrast to circulating tumour cell enumeration done on samples using the established CellSearch method which was able to find only single digit counts of CTCs in 7.5mL of blood; the size based ScreenCell approach gave a minimum concentration of 13.0 CTCs in a single millilitre of high-risk patient blood and a maximum of over 268.7 CTCs in a single millilitre (**Table 3**, page 63).

11.4.1.) CTC enumeration at +0 months

The minimum concentration of CTCs found per millilitre of patient blood at the +0m baseline was 28.0 with the median and the maximum being 95.5 and 259.7 respectively. The mean concentration of CTCs/mL at +0m was 109.19.

For statistical analysis we compared the automated count of CTCs found per millilitre of patient blood to the metrics that were analyzed during three-dimensional imaging including: the average number of telomere signals per cell, the average percentage of signals classified as aggregates per cell, the average intensity of all signals in a sample, the average nuclear volume per cell and the average number of signals per unit of volume. Testing for correlation of CTC concentration with all of these variables (see appendix 14.3.) yielded a high R-squared value of 0.708 with the average telomere signal intensity for each sample. This means that before any treatment is given, as the average telomere length in each patient decreases the number of CTCs tends to increase.

Patients that were classified in group 1 by the telomere analysis showed a tendency toward having a higher number of CTCs at +0m, with 6/9 being in the top 50% and 4/9 being in the fourth quartile with regards to CTC concentration. Those classified in group 2 showed a high variability with 2/5 in the first quartile, 1/5 in the second quartile and 2/5 in the third quartile.

Group 3 also showed high variability out of the groups with regards to CTC concentration with 3/6 falling in ranks 8, 10 & 11; 1/6 falling in the top 25% and 1/6 falling in the bottom 10% (see **Table 3**, page 63).

Table 3: Clinical grading at baseline as well as CTC counts and PSA levels between sampling time points based on group number.

		+0m				+2m		+6m	
Patient	Telomere Group	Gleason Score	Tumour Grade	CTCs/ mL	PSA ng/mL	CTCs/ mL	PSA ng/mL	CTCs/ mL	PSA ng/mL
MB0389	Group 1	9	T2bNXMX	30.0	0.03	27.7	11.24	16.0	0.03
MB0393	Group 1	9	T2b	259.7	17.99	33.7	29.48	78.3	0.1
MB0394	Group 1	7	T2a	209.7	13.27	220.0	0.01	113.0	0.01
MB0421	Group 1	9	T1c	123.7	8.68	72.0	5.41	43.3	0.01
MB0426	Group 1	8	T1c	162.0	6.93	93.3	7.44	44.7	0.02
MB0438	Group 1	8	T2b	220.7	23.19	154.0	0.02	73.3	0.01
MB0441	Group 1	7	T3NxM0	52.3	1.5	141.7	25.22	15.7	0.04
MB0446	Group 1	9	T2c	117.3	23.8	77.7	14.42	15.3	0.38
MB0452	Group 1	7	T1cN0MX	45.0	9.27	28.7	0.20	30.7	0.16
MB0405	Group 2	7	T2b	157.3	5.83	107.3	0.11	86.0	0.05
MB0410	Group 2	9	T2a	38.7	0.78	32.3	5.22	218.7	0.16
MB0444	Group 2	6	T2a	139.0	11.91	77.3	2.35	22.3	1.71
MB0445	Group 2	7	T2b	86.7	40.02	41.7	2.62	22.7	2.71
MB0475	Group 2	7	T2a	28.0	9.52	109.0	26.66	33.7	0.03
MB0408	Group 3	7	T2a	29.7	7.4	68.0	1.87	35.3	1.32
MB0413	Group 3	9	T2c	75.0	26.68	145.3	0.19	268.7	0.01
MB0418	Group 3	9	T2c	170.0	10.79	26.3	1.23	71.0	0.09
MB0461	Group 3	6	T2a	96.3	11.26	106.7	5.57	50.7	1.64
MB0466	Group 3	8	T2a	48.0	11.25	69.7	7.77	69.7	0.82
MB0500	Group 3	9	N/A	94.7	14.25	14.7	1.47	13.0	0.02

11.4.2.) CTC enumeration at +2 months

From the baseline time point to post androgen deprivation therapy +2m time point 65% (13/20) patients showed a decrease in the concentration of CTCs/mL (see **Table 3**, page 63). All but 1/9 of group 1 showed such a decrease. Groups 2 & 3 had 1/5 and 4/6 respectively with

increases in the concentrations of CTCs. The minimum concentration of CTCs/mL fell to 14.7 with the median and maximum falling to 74.7 and 220.0 respectively.

Interestingly upon directing multivariate analysis toward the telomeric intensity which had the highest correlation to CTC concentrations at the baseline time point there was a drop in the R-squared value to 0.010 indicating that less than 1% of any variability in the number of CTCs may be explained by any variability in the telomeric profiles (specifically in the mean telomere intensity as seen at +0m) (see 14.3.) page 107).

11.4.3.) CTC enumeration at +6 months

By six months the minimum concentration of CTCs increased to 13.0 with a median of 44.0 and a maximum of 268.7.

After radiotherapy 70% (14/20) of patients showed a decrease in the concentration of CTCs. An additional 2 samples showed an increase of less than 3 CTCs per mL.

The multivariate analysis at +6m showed an increased R-squared value of the average telomere intensity to 0.056 which could still account for only about 3% of the variability in the concentration of CTCs. These results could indicate that genomic instability drives the evolution of tumour foci in the prostate (and thus the number of CTCs) at baseline, before selective pressures such as scarcity of androgen and radiation are introduced into the tumour environment.

12.) Discussion

The results of this project have shown that there is heterogeneity at baseline in the telomere profiles and CTC counts between patients who have the same TNM staging and/or Gleason score. These parameters for measuring how a disease might progress are not necessarily related, and according to the literature CTC counts are superior to PSA levels for predicting the progression of prostate cancer (Kolostova et al. 2014; Goodman et al. 2011).

There are also differences in the way 3D telomere profiles change in response to treatments. We have used these differences to place patients into Group 1 (degree of change in number of short telomeres $\geq 1x10^{-3}$), Group 2 (degree of change in number of short telomeres $> 1x10^{-3}$, $< -1x10^{-3}$) or Group 3 (degree of change in number of short telomeres $\leq -1x10^{-3}$) and showed that the group into which a patient is placed in response to hormone therapy is predictive of the way the telomere profiles will change in response to radiation therapy. How this relates to the patient outcome is discussed in section 12.5.3.) page 75.

12.1.) Methods of Treatment Evaluation in Multifocal Prostate Tumours

Treatment of any form of cancer has always been a balancing act between damaging malignant cells and sparing healthy cells. Within the discipline of radiation therapy this involves proper targeting of the tumour area, however the multi-focal nature of prostate cancer makes this inherently difficult. Methods of precisely tracking the progress of the patient during treatment are needed, especially in the case of aggressive cancers with a small window of treatment efficacy.

Currently the method of short-term evaluation for prostate cancer treatment is through measurement of PSA levels following treatment. What is known as biochemical failure of treatment is an increase of 2ng/mL above the lowest PSA level achieved (Roach et al. 2006). The use of this biomarker does not offer any way to differentiate between any increase in the size of

the tumour itself and any co-morbid prostatic hyperplasia or less aggressive tumour growth. Nor does this method offer any insight into the molecular condition of the tumour, information which may help in fine-tuning of treatment.

Much effort is being directed towards enumeration of CTCs as a method of patient prognosis references. Our method of CTC analysis offers enumeration as well as possible molecular analysis of captured CTCs.

12.2.) Changes in Morphology

The development of cells with invaginated nuclei seen at +6m points to the development of apoptotic cells whose nuclei have begun to take on a horseshoe-like appearance. The development of these cells points to large scale disruption of the cells most likely from ionizing radiation used for RT. That some of these invaginated nuclei were seen in the samples of +2m patients may be an indication that deprivation of androgens causes similar large scale disruptions in PCa cells, possibly through the disruption of telomere stability (see Section 7.1.4.3.)

12.3.) Enumeration of Circulating Tumour Cells

12.3.1.) Changes in CTC counts

Unfortunately, the follow-up period of this study was too short to provide any insight into the correlation between CTC enumeration and the end treatment result. Goodman et al. (2011) and de Bono et al. (2008) have reported that initial CTC enumeration had predictive value of progression to CRPC independent of other diagnostic parameters, but that this predictive value was not present when monitored beyond the baseline.

There is a paucity of convincing studies that provide a link between enumeration of PCa CTCs during treatment and the treatment outcome. And because enumeration cannot provide any information on the molecular nature of the tumour cells (Rodriguez-Lee, Kuhn, and Webb 2014)

posits that “Simple enumeration of CTCs will not contribute significantly to the development of improved or more personalized cancer treatments.” Because of this I think it is fair to infer that our CTC counts taking place after the beginning of ADT will show no correlation with the eventual treatment outcome of the patients in this study as to be determined at a future time.

The literature does, however, show a link between the initial levels of CTCs and the progression to castrate resistant prostate cancer for patients with hormone sensitive PCa (Goodman et al. 2011). This indicates that what is important in the end treatment outcome of PCa is not the sheer number of cells that survive the initial treatment, but the amount of genetic diversity available for the generation of clones that are capable of becoming resistant to treatment. This is born out by the observations in (Lalonde et al. 2014) that a percent genomic alteration (percentage of a patient’s genome harbouring copy number alterations) (PGA) of ≥7.49 in pre-treatment patient biopsies of low-intermediate risk patients was associated with a hazard risk of 4.5x increase in the chance of biochemical failure. An earlier study identified subpopulations in pre-treatment prostate biopsies that were classified as having an increase in chromatin content slightly over the diploid amount and that the presence of these subpopulations were correlated with a worse outcome for the patient (Pollack et al. 1994). Genomic instability in CTCs is discussed below in sections 7.2.9.) and 7.2.9.1.)

12.3.2.) Lack of Correlation of CTC counts with PSA levels

Goodman et al. (2011)’s comparison CTC enumeration and PSA levels found no correlation between these two, while other studies have found CTC enumeration to be superior to PSA in regard to predicting overall survival (de Bono et al. 2008; Lorente, Mateo, and de Bono 2014) Given that raw levels of PSA themselves have fallen into disrepute as a prognostic tool, focus has shifted to the velocity of change in PSA levels. An increase of > 2 ng/mL per month

after a decrease to their lowest value is considered indicative of poor prognosis. Unfortunately, it is unknown if my patients reached PSA nadir (lowest point) at the +6m time point so I have no way to compare any of my results with this method for treatment evaluation. With this in mind the PSA levels cannot be used in my study as an indication of treatment effectiveness at this time.

12.3.3.) Lack of CTC count correlation with TNM staging or Gleason score

Perhaps the most surprising result of the CTC enumeration was its lack of correlation with tissue biopsy grading, especially the Gleason score. Finding no direct correlation between CTC counts and Gleason score was in agreement with the literature (Kolostova et al. 2014), however given that the degree of tissue differentiation, of which Gleason is a measure, is a strong indicator of disease aggressiveness some relatedness would be expected. It is possible that even though the tissue has increased dedifferentiation there is sufficient diversity in E-cadherin expression to allow for proliferative tumours to have not yet developed the ability to dissociate from the main tumour mass. More likely though is that with only three possible Gleason scores (6, 7, 8, 9) (see **Table 1**, page 42) there is simply not enough variation to make a proper comparison between the Gleason score and CTC enumeration.

Likewise, the lack of correlation between TNM staging is most likely a product of a lack of variation. There are a total of three T values used (1, 2, 3) with most of our samples being T2. Since our study was limited to locally advanced PCa only, none of our samples have an M value over 0 and similarly none have an N value over 0 (see **Table 1**, page 42). Having so few unique values for one of our variables; we will be unable to extract any meaningful data for correlation.

With a larger sample size, it may be possible to determine patient groups which have a relationship between TNM, Gleason score and CTC counts.

12.3.4.) Correlation of CTC counts with mean telomere intensity at +0m

There is a strong negative correlation of our +0m CTC counts and the +0m average telomere length (as measured by signal intensity) (see section 10.4.) .

Table 4: Summary of Spearman Correlation Coefficients with accompanying p values comparing average telomere intensity inter-quartile range at each time point to automated CTC counts. Significant correlation was found at +0m only.

Spearman Correlation Coefficients, N = 20 Prob > |r| under H0: Rho=0			
	+0m	+2m	+6m
avint25	-0.74135	0.18045	0.09023
p value	0.0002	0.4465	0.7052
avint50	-0.67519	0.17444	0.03759
p value	0.0011	0.4620	0.8750
avint75	-0.70075	0.15038	0.18496
p value	0.0006	0.5269	0.4350

Lower telomere intensity has been associated with increased genomic instability and increased tumour aggressiveness (Gadji et al. 2012; Gadji, Fortin, and Tsanaclis 2010; Knecht et al. 2012; Wark et al. 2014; Meeker, Hicks, Gabrielson, et al. 2004). Therefore I conclude that this study indicates that an increase in the initial CTC counts is reflective of the degree of genomic instability in pre-treatment high-risk prostate cancer.

That this correlation does not continue into treatment is an indication that while CTC enumeration is not predictive of patient outcome post-treatment in non-metastatic patients we

still may be able to determine levels of genomic instability (and tumour aggressiveness) in the cells which survive treatment.

12.4.) Telomere profiles in patient CTCs

12.4.1.) Changes in telomere profiles

As reported by Heaphy et al. (2015) the shortening of the telomeres in cells of the prostate stroma is associated with an increase in the incidence of prostate cancer. (Meeker et al. 2002; Meeker et al. 2004) have reported that such telomere shortening is an early event in the development of PCa. We do see a higher number of short telomeres in the +0m CTCs of patients in Group 1, which conforms to these results. However, in Groups 2 and 3 the number of short telomeres is much lower. This indicates that there is heterogeneity in the amount of genomic instability across patients before treatment. This concurs with the heterogeneous nature of prostate cancer. Interestingly, although high-risk prostate cancer has been called a disease of genomic instability (Tapia-Laliena et al. 2014) only half of the patients analyzed showed a large number of short telomeres (**Figure 14**, page 60). This could point to another method of tumourigenesis through activation of specific tumour promoter genes rather than broad genomic changes such as the activation of the *TMPRSS/ERG* fusion gene (see section 7.1.6.2.) . Activation of this fusion gene triggers dedifferentiation and EMT which can lead to prostate cancer without necessarily inducing genomic instability. It may also point to the maintenance of telomere length through the activation of telomerase or the ALT pathway which may mask shortened telomeres from our analysis. A third option is that some CTCs are derived from tumours which have an origin relating to basal cells (see Section 7.1.2.) . (Meeker et al. 2002) showed that telomere shortening is an early event in the formation of PCa, but only in PCa of

luminal epithelial origin. Since PCa may originate from either basal or luminal cells, CTCs with longer telomeres at +0m may be of basal origin.

12.4.1.1.) Degree of change in number of short telomeres $\geq 1x10^{-3}$ (Group 1)

We see CTCs with a higher number of short telomeres before treatment in Group 1 of our high-risk patients. Since short telomeres are associated with an increase in genomic instability (Heaphy et al. 2015; Vukovic et al. 2007) it is reasonable to assume that these cells show a higher degree of GI than those showing a smaller number of short telomeres. Androgens have been shown to play a role in regulating the repair genes of the prostate cells (Polkinghorn et al. 2013) and to have direct interaction with the telomeres (Zhou et al. 2013; Kim et al. 2010). Although increased GI has been associated with a poor prognosis, when paired with deprivation of androgens these prostate cells may be pushed beyond a tumourigenic but stable phenotype, go through cycles of ever-increasing GI and suffer cell death. In Group 1 this would account for the drop seen between +0m and +2m. The much smaller change in the number of short telomeres seen at +2m to +6m could mean these cells are replaced by a smaller population with smaller numbers of short telomeres.

12.4.1.2.) Degree of change in number of short telomeres $\leq -1x10^{-3}$ (Group 3)

CTCs with a smaller number of short telomeres at the baseline time point are seen in groups 2 & 3. Of these two groups 3 shows an increase in the number of short telomeres from +0m to +2m. Applying the same reasoning as with Group 1, this means that Group 3 before treatment has a lower level of GI (and is perhaps the product of a small number of gene mutations) and that the removal of androgens compromises the DNA repair mechanisms allowing the cells to accumulate further large scale genomic changes (Zhou et al. 2013; Kim et al. 2010). If treatment were to be stopped at this point there would be consequences to the

survival of the patient, but since additional damage is induced via radiation the increase in GI in fact radiosensitizes the cells. In fact, (Mirjolet et al. 2015) has stated that tumours showing smaller telomeres may be a possible marker for increased radiosensitivity and possible recommendation for radiation dosage.

This is in line with the results from studies which show a synergistic effect between ADT and RT, and provides a potential possibility of a link between androgen receptor activity and radiosensitivity, but indicates that the effect is limited to a subpopulation of patients.

This evidence from the literature explains the decrease in the number of short telomeres between +2m and +6m, as the unstable cells are destroyed by unrepairable damage to their DNA and replaced by subpopulations more resistant to DNA damage. As one population which may be flourishing, but is sensitive to treatment is decreased it allows for a smaller population which is treatment resistant, but resource deprived to thrive once the competing subpopulation has been removed.

12.4.1.3.) Degree change in number of short telomeres > $1x10^{-3}$, < -$1x10^{-}3$ (Group 2)

As with group 3, group 2 shows few short telomeres at +0m, the difference being that there is little change in the number of short telomeres between +0m and +2m and also between +2m and +6m. Taken with the results reported by (Zhou et al. 2013; Kim et al. 2010) that telomere disruption was not seen in cell lines that had become castrate-resistant, patients in Group 2 may have already progressed to a point where their tumours do not require androgens in the same way that those in Groups 1 and 2 do. If this is the case, more aggressive treatment such as radical prostatectomy might be indicated (though RP performed after RT is more complicated (Mouraviev, Evans, and Polascik 2006)).

Or it could be an indication that Group2 is actually a subgroup of Group 3 which saw a collapse of its genomically unstable cells before the addition of radiation. Unfortunately, this project does not have the temporal resolution to determine the answer to this question. Sampling more often would be a beneficial modification to this project (although inconvenient to the patients).

12.4.2.) Lack of correlation with PSA, TMN & Gleason

The lack of a correlation between telomere profiles and clinical indicators have the same problems as seen with the lack of correlation between the number of CTCs and the same clinical indicators, namely that there is a lack of any variation (see sections 1.2.2., 1.2.3) in said indicators when compared to the telomeric profiles. Again, with a larger sample size it may be possible to determine such a relationship.

12.5.) Genomic Instability

12.5.1.) Potential impact of telomere profiles on genomic instability.

While genomic instability is associated with increase tumourigenic potential as has been reported in the literature (Hanahan and Weinberg 2011), there exists a threshold above which the cancer cells cannot function and experience cell death. This is the basic idea behind radiation therapy. Cells may display a range of responses to the DNA damaging effects of RT (Mirjolet et al. 2015). Inhibition of certain components of a cell's DNA repair machinery has been shown to 'sensitize' these cells to the effects of ionizing radiation (Karanika et al. 2014; Lio et al. 2004).

Because the active androgen receptor is necessary for the stability of telomeres (Zhou et al. 2013; Kim et al. 2010) and the stability of telomeres is necessary for the stability of the genome (Mai 2010), the reduction of androgens would lead to increased levels of genomic instability on top of those induced by ionizing radiation. In addition, a decrease in the AR's

transcription factor functionality would lead to a decrease in its target proteins, many of which are involved in DNA repair (Polkinghorn et al. 2013).

The presence of a subpopulation of patients who show an increase in the number of short telomeres - which is indicative of genomic instability (Mai 2010) – during ADT points to CTCs (and by extension prostate tumours) which are still dependent on the normal binding of androgens to the AR in order to maintain proper telomere functioning and DNA repair.

Conversely, the presence of a subpopulation of patients who show little chance in the number of short telomeres points to CTCs (and by extension prostate tumours) have developed and androgen receptor variant which is able to maintain its activity despite having reduced access to androgens.

12.5.2.) Summary of Results Interpretation

Figure 15: Schematic of possible explanation of results.

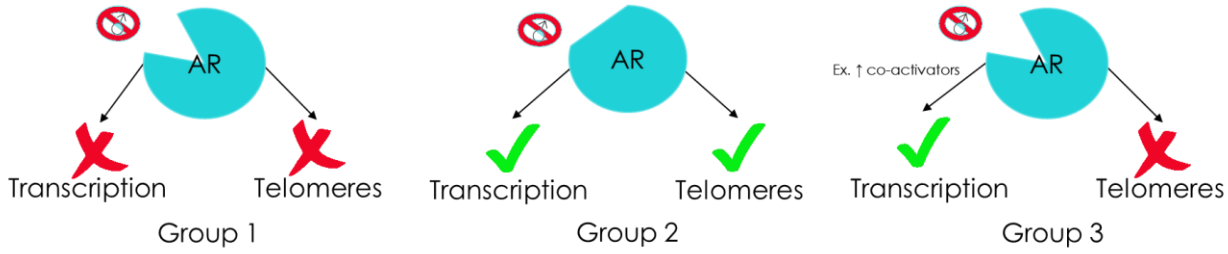

My interpretation of the results of this experiment, as summarized above in Figure 15 are as follows: Group 1 is dominated by androgen dependent cells. Group 2 is dominated by androgen independent cells which don't require androgens for AR mediated transcription or AR mediated transcription genome stability. For example: A change in ligand binding domain has led to constitutive activation. Group 3 is dominated by androgen independent cells which still require androgens for AR mediated genome stability but not for AR mediated gene transcription.

For example: and increase in AR co-activators can increase AR mediated transcription in androgen depleted PCa (Shi, 2008).

12.5.3.) Potential impact on assignment of prostate cancer treatment.

Using the knowledge gained from this project it may be possible to assign patients to radiotherapy based on their response to ADT.

Those patients in Group 1 may be able to avoid radiotherapy, holding it in reserve until they show a relapse, or perhaps be assigned to brachytherapy which is utilized in less severe cases of localized PCa instead of EBRT.

Patients in Group 3 could be moved on to RT more quickly as a way to limit tumour cells showing an increase in GI from possibly creating additional subpopulations.

If indeed patients in Group 2 do develop androgen resistance even before the administration of ADT it would be best for them to could be moved on to more aggressive therapies such as radical prostatectomy or alternative therapies as soon as it is determined there is no reaction of CTC telomeres to ADT.

12.6.) Limitations of Study

As noted above, this project looks at a small sample of high-risk prostate cancer patients which hinders our ability to determine statistical correlations between clinical indicators such as Gleason score and TNM staging since there are a limited number of values these parameters can have. We also have a limited follow up of +6m which means we cannot compare with PSA doubling time since it is unknown whether PSA levels have only reached nadir even at the +6m time point.

While the ScreenCell^{tm} device captures more CTCs than the CellSearch immuno-magnetic procedure it still has limitations. It will not capture any CTCs which might happen to

be smaller than the pore size, although even small cell prostate cancer cells are larger than the pore size (Nadal et al. 2014). It can not natively differentiate between CTCs and lymphocytes or other circulating cells (i.e. it does not rely on features exclusive to CTCs), results must be interpreted by a user.

12.7.) Conclusion and Further Directions

With the limitations of current techniques of isolating cellular material from prostate tumours the filtration-based ScreenCell technique has considerable value for research and diagnostic purposes although the telomeric analysis is a general test for genomic instability which may be found early on in prostate cancer. There is ample evidence in the literature that this is an important feature of prostate tumours and that a knowledge of the amount of genomic instability within the patient prostate may aid in the recommendation of treatment for the patient.

This project has already expanded into collecting patient samples from a larger cohort of patients and increasing the follow-up time in order to track the effectiveness of treatment. We are currently awaiting clinical results from the outcome of treatment including time to biochemical failure as well as the length of disease free survival. There was also a problem with the measuring of testosterone levels of the patients. Sampling in this respect was only done at the baseline time point and even then very sporadically among patients. This may have been because of patient preference, as testosterone levels are potentially a personal matter for some males.

In order to get around the matter of patient preference existing mouse models of prostate cancer could be used (Ko et al. 2014; Hubbard et al. 2015). This would also have the advantage of speeding up the accumulation of survival data and allow us to study the natural tumourigenesis without treatment intervention. The cellular origin (luminal epithelium or basal cell) of CTCs could be determined using a method similar to (Z. A. Wang et al. 2014), limiting

possible phenotypic variations. Also, mouse blood samples could be taken at any time and processed using a method identical to the one used in this project. Given that androgens are necessary for telomere stability in the prostate, hormone manipulations in the mice may be sufficient to produce early genomic instability in the mouse prostate. In their study (Hubbard et al. 2015) acquired a conditional *PTEN* knockout mouse from Jackson labs. Given that *PTEN* loss is one of the most common genetic changes in prostate cancer and necessary for maintenance of genomic stability, this would be the mouse I would be most interested in. Parallel research done in our lab has shown that the concentration of CTCs within mouse blood is much higher than in humans (Macoura Gadji, unpublished), meaning this would be a viable avenue of study. Larger animals such as canines have been shown to develop prostate cancer, however lack of a specific model such as *PTEN* knockouts makes them an unattractive alternative.

In order to increase the temporal resolution of this study patients would have to be sampled more often.

It would be interesting to apply protein assay approaches to the study of prostatic CTCs. Primarily I would be interested in whether we could differentiate cells of basal or luminal epithelial origin. Park et al., (2016) has postulated that basally derived cell have lowered PSA/AR. It would be interesting to continue immunocytochemistry to determine if large CTC populations with low AR levels could be isolated. Similarly assaying for e-cadherin could yield some information about whether lower cadherin levels correlate with an increased number of CTCs. In addition, FISH assays could be performed on CTCs to determine if any duplications of the AR gene are present.

Currently others in our lab are looking at performing single cell sequencing on captured circulating tumour cells in order to get an idea of common genetic changes seen in intermediate

risk PCa. Using next generation sequencing I would like to see a more thorough sequencing of the androgen receptor and its co-activators in the circulating tumour cells, specifically for single nucleotide polymorphisms that may affect the AR protein. These changes could be tracked over the course of treatment in high risk PCa in order to determine how long the average progression is from castrate sensitive to castrate resistant PCa and what changes in the genome are most often seen. Møller et al. 2013 describe utilizing next-gen sequencing to chart the changes they found in disseminated tumour cells when compared to the primary tumour in breast cancer patients. Beltran et al. 2013 identifies common rearrangements in the 182 cancer genes from among 45 biopsy specimens in a broad array of prostate cancer patients showing all types of disease. Plotting the common pathways in the evolution of prostate cancer seems appealing. Ideally I would like to see the (Beltran et al. 2013) study expanded over a larger patient cohort. Given that the biopsy problem mentioned in section 7.1.2.) with regards to the difficulty in biopsying a multifocal tumor still exists in regard to (Beltran et al. 2013), performing sequencing on CTCs would be an interesting undertaking. However, many CTCs would have to be analyzed due to the highly heterogeneous nature of PCa in order to return a representative sampling. This would be a highly expensive undertaking.

I think there is room for improvement in the isolation of circulating tumour cells. With much effort being put into microfluidics this field has produced technology that, while more expensive, can isolate CTCs based on many more characteristics than simple size, allowing for more precise extraction. Given the opportunity (i.e. money) I would like to evaluate some these technologies for use on a future incarnation of this project. Of particular interest would be methods based on atomic force microscopy (AFM), as this method is able to measure the elasticity of the CTCs as described in Osmulski et al. (2014). In addition to using ScreenCell

filters, this group used micromanipulation to isolate immunostained CTCs. Because of its slow speed AFM would have to be paired with a scanning method that could quickly identify CTCs and mark them for isolation. Not only would it be possible to isolate CTCs as cancer cells are shown to be more elastic than normal cells (Cross et al. 2007), but elasticity has a direct impact on the formation of metastases in the patient (Mehlen and Puisieux 2006). In addition, (Osmulski et al. 2014), investigated the properties of deformation and adhesion of CTCs, finding CTCs in metastatic castrate resistant prostate cancer patients three times more elastic and deformable and up to seven times more adhesive than those of metastatic castrate sensitive prostate cancer patients.

CTCs offer the opportunity for advanced molecular analysis of tumour derived cells without invasive measures. This represents a potential boon to the emerging field of personalize medicine.

13.) References

Aarthy, Raghu, Samson Mani, Sridevi Velusami, Shirley Sundarsingh, and Thangarajan Rajkumar. 2015. “Role of Circulating Cell-Free DNA in Cancers.” *Molecular Diagnosis & Therapy* 19 (6): 339–50. doi:10.1007/s40291-015-0167-y.

Adams, Daniel L., Steingrimur Stefansson, Christian Haudenschild, Stuart S. Martin, Monica Charpentier, Saranya Chumsri, Massimo Cristofanilli, Cha Mei Tang, and R. Katherine Alpaugh. 2015. “Cytometric Characterization of Circulating Tumor Cells Captured by Microfiltration and Their Correlation to the Cellsearch CTC Test.” *Cytometry Part A* 87 (2): 137–44. doi:10.1002/cyto.a.22613.

Adebayo Awe, Julius, Mark Chu Xu, Janine Wechsler, Naoual Benali-Furet, Yvon E. Cayre, Jeff Saranchuk, Darrel Drachenberg, and Sabine Mai. 2013. “Three-Dimensional Telomeric Analysis of Isolated Circulating Tumor Cells (CTCs) Defines CTC Subpopulations.” *Translational Oncology* 6 (1): 51–IN4. doi:10.1593/tlo.12361.

Agoulnik, Irina U., Ajula Vaid, William E. Bingman, Halime Erdeme, Anna Frolov, Carolyn L. Smith, Gustavo Ayala, Michael M. Ittmann, and Nancy L. Weigel. 2005. “Role of SRC-1 in the Promotion of Prostate Cancer Cell Growth and Tumor Progression.” *Cancer Research* 65 (17): 7959–67. doi:10.1158/0008-5472.CAN-04-3541.

American Cancer Society. 2012. “Cancer Facts & Figures 2012.”

Amin, N, D Sher, and A Konski. 2014. “Systematic Review of the Cost Effectiveness of Radiation Therapy for Prostate Cancer from 2003 to 2013.” *Appl Health Econ Health Policy* 12 (4): 391–408.

Ashworth, T. R. 1869. “A Case of Cancer in Which Cells Similar to Those in the Tumors Were Seen in the Blood after Death.” *The Australian Medical Journal* 14: 146–49.

Attard, Gerhardt, Joost F Swennenhuis, David Olmos, Alison H M Reid, Elaine Vickers, Roger A’Hern, Rianne Levink, et al. 2009. “Characterization of ERG, AR and PTEN Gene Status in Circulating Tumor Cells from Patients with Castration-Resistant Prostate Cancer.” *Cancer Research* 69 (7): 2912–18. doi:10.1158/0008-5472.CAN-08-3667.

Baade, Peter D, Danny R Youlden, and Lauren J Krnjacki. 2009. “International Epidemiology of Prostate Cancer: Geographical Distribution and Secular Trends.” *Molecular Nutrition & Food Research* 53 (2): 171–84. doi:10.1002/mnfr.200700511.

Bahn, Duke K., Fred Lee, Robert Badalament, Anil Kumar, Jeffrey Greski, and Michael Chernick. 2002. “Targeted Cryoablation of the Prostate: 7-Year Outcomes in the Primary Treatment of Prostate Cancer.” *Urology* 60 (2 SUPPL. 1): 3–11. doi:10.1016/S0090-4295(02)01678-3.

Balk, Steven P, Yoo-Joung Ko, and Glenn J Bubley. 2003. “Biology of Prostate-Specific Antigen.” *Journal of Clinical Oncology : Official Journal of the American Society of Clinical Oncology* 21 (2): 383–91.

Bazinet, M, S M Hamdy, L R Bégin, R A Stephenson, and W R Fair. 1992. “Prognostic Significance of Antigenic Heterogeneity, Gleason Grade, and Ploidy of Lymph Node Metastases in Patients with Prostate Cancer.” *The Prostate* 20 (4): 311–26.

Beheshti, B, P C Park, J M Sweet, J Trachtenberg, M A Jewett, and J A Squire. 2001. “Evidence of Chromosomal Instability in Prostate Cancer Determined by Spectral Karyotyping (SKY) and Interphase Fish Analysis.” *Neoplasia (New York, N.Y.)* 3 (1): 62–69. doi:10.1038/sj/neo/7900125.

Beltran, Himisha, Roman Yelensky, Garrett M. Frampton, Kyung Park, Sean R. Downing, Theresa Y. MacDonald, Mirna Jarosz, et al. 2013. “Targeted next-Generation Sequencing of Advanced Prostate Cancer Identifies Potential Therapeutic Targets and Disease Heterogeneity.” *European Urology* 63 (5): 920–26. doi:10.1016/j.eururo.2012.08.053.

Bettegowda, Chetan, Mark Sausen, Rebecca J. Leary, Isaac Kinde, Yuxuan Wang, Nishant Agrawal, Bjarne R. Bartlett, et al. 2014. “Detection of Circulating Tumor DNA in Early- and Late-Stage Human Malignancies.” *Sci Transl Med* 6 (224): 224ra24. doi:10.1126/scitranslmed.3007094.Detection.

Bolton, Eric C, Alex Y So, Christina Chaivorapol, Christopher M Haqq, Hao Li, and Keith R Yamamoto. 2007. “Cell- and Gene-Specific Regulation of Primary Target Genes by the Androgen Receptor.” *Genes & Development* 21 (16): 2005–17. doi:10.1101/gad.1564207.

Bonner, W. A. 1972. “Fluorescence Activated Cell Sorting.” *Review of Scientific Instruments* 43 (3). AIP Publishing: 404. doi:10.1063/1.1685647.

Bostrom, Peter J., Anders S. Bjartell, James W F Catto, Scott E. Eggener, Hans Lilja, Stacy Loeb, Jack Schalken, Thorsten Schlomm, and Matthew R. Cooperberg. 2015. “Genomic Predictors of Outcome in Prostate Cancer.” *European Urology* 68 (6): 1033–44. doi:10.1016/j.eururo.2015.04.008.

Boveri, Theodor. 2008. “Concerning the Origin of Malignant Tumours by Theodor Boveri. Translated and Annotated by Henry Harris.” *Journal of Cell Science* 121 Suppl (Supplement_1): 1–84. doi:10.1242/jcs.025742.

Bowen, Cai, Jeong-Ho Ju, Ji-Hoon Lee, Tanya T. Paull, and Edward P. Gelmann. 2013. “Functional Activation of ATM by the Prostate Cancer Suppressor NKX3.1.” *Cell Reports* 4 (3): 516–29. doi:10.1016/j.surg.2006.10.010.Use.

Boyd, Lara K, Xueying Mao, Liyan Xue, Dongmei Lin, Tracy Chaplin, Sakunthala C Kudahetti, Elzbieta Stankiewicz, et al. 2012. “High-Resolution Genome-Wide Copy-Number Analysis Suggests a Monoclonal Origin of Multifocal Prostate Cancer.” *Genes, Chromosomes & Cancer* 51 (6): 579–89. doi:10.1002/gcc.21944.

Brenner, J. Chad, Bushra Ateeq, Yong Li, Anastasia K. Yocum, Qi Cao, Irfan A. Asangani, Sonam Patel, et al. 2011. “Mechanistic Rationale for Inhibition of Poly(ADP-Ribose) Polymerase in ETS Gene Fusion-Positive Prostate Cancer.” *Cancer Cell* 19 (5). Elsevier Inc.: 664–78. doi:10.1016/j.ccr.2011.04.010.

Cabot, AT. 1896. “The Question of Castration for Enlarged Prostate.” *Annals of Surgery* 24 (3): 265–309.

Canadian Cancer Society’s Advisory Committee on Cancer Statistics. 2015. “Canadian Cancer Statistics Special Topic : Predictions of the Future Burden of Cancer in Canada.” *Canadian Cancer Statistics*, 1–151.

Capo-chichi, Callinice D, Kathy Q Cai, Fiona Simpkins, Parvin Ganjei-Azar, Andrew K

Godwin, and Xiang-Xi Xu. 2011. “Nuclear Envelope Structural Defects Cause Chromosomal Numerical Instability and Aneuploidy in Ovarian Cancer.” *BMC Medicine* 9 (January): 28. doi:10.1186/1741-7015-9-28.

Caporali, A, L Wark, B J Vermolen, Y Garini, and S Mai. 2007. “Telomeric Aggregates and End-to-End Chromosomal Fusions Require Myc Box II.” *Oncogene* 26 (10): 1398–1406. doi:10.1038/sj.onc.1209928.

Capper, Rebecca, Bethan Britt-Compton, Maira Tankimanova, Jan Rowson, Boitelo Letsolo, Stephen Man, Michele Haughton, and Duncan M Baird. 2007. “The Nature of Telomere Fusion and a Definition of the Critical Telomere Length in Human Cells.” *Genes & Development* 21 (19): 2495–2508. doi:10.1101/gad.439107.

Carozzi, Francesca, Lara Tamburrino, Simonetta Bisanzi, Sara Marchiani, Milena Paglierani, Simonetta Di Lollo, Emanuele Crocetti, et al. 2015. “Are Biomarkers Evaluated in Biopsy Specimens Predictive of Prostate Cancer Aggressiveness?” *Journal of Cancer Research and Clinical Oncology*. Springer Berlin Heidelberg. doi:10.1007/s00432-015-2015-1.

Cesare, Anthony J, and Roger R Reddel. 2010. “Alternative Lengthening of Telomeres: Models, Mechanisms and Implications.” *Nature Reviews. Genetics* 11 (5). Nature Publishing Group: 319–30. doi:10.1038/nrg2763.

Chang, Chawnshang. 2002. *Androgens and Androgen Receptor*. *Journal of Chemical Information and Modeling*. Vol. 53. doi:10.1017/CBO9781107415324.004.

Chang, Kai-Hsiung, Rui Li, Mahboubeh Papari-Zareei, Lori Watumull, Yan Daniel Zhao, Richard J Auchus, and Nima Sharifi. 2011. “Dihydrotestosterone Synthesis Bypasses Testosterone to Drive Castration-Resistant Prostate Cancer.” *Proceedings of the National Academy of Sciences of the United States of America* 108 (33): 13728–33. doi:10.1073/pnas.1107898108.

Chen, Charlie D, Derek S Welsbie, Chris Tran, Sung Hee Baek, Randy Chen, Robert Vessella, Michael G Rosenfeld, and Charles L Sawyers. 2004. “Molecular Determinants of Resistance to Antiandrogen Therapy.” *Nature Medicine* 10 (1): 33–39. doi:10.1038/nm972.

Chen, Chun-Liang, Devalingam Mahalingam, Pawel Osmulski, Rohit R Jadhav, Chiou-Miin Wang, Robin J Leach, Tien-Cheng Chang, et al. 2013. “Single-Cell Analysis of Circulating Tumor Cells Identifies Cumulative Expression Patterns of EMT-Related Genes in Metastatic Prostate Cancer.” *The Prostate* 73 (8): 813–26. doi:10.1002/pros.22625.

Chen, Zhenbang, Lloyd C. Trotman, David Shaffer, Hui-Kuan Lin, Zohar A. Dotan, Masaru Niki, Jason A. Koutcher, et al. 2005. “Crucial Role of p53-Dependent Cellular Senescence in Suppression of Pten-Deficient Tumorigenesis.” *Nature* 436 (7051): 725–30. doi:10.3892/ijo.

Chuang, Tony, Sharareh Moshir, Yuval Garini, Alice Ya-, Chun Chuang, Ian T Young, Bart Vermolen, et al. 2004. “The Three-Dimensional Organization of Telomeres in the Nucleus of Mammalian Cells.” *BMC Biology* 2 (12): 1–8.

Chun, Jarin, Erika S Buechelmaier, and Simon N Powell. 2013. “Rad51 Paralog Complexes BCDX2 and CX3 Act at Different Stages in the BRCA1-BRCA2-Dependent Homologous Recombination Pathway.” *Molecular and Cellular Biology* 33 (2): 387–95. doi:10.1128/MCB.00465-12.

Chybowski, F M, E J Bergstralh, and J E Oesterling. 1992. “The Effect of Digital Rectal Examination on the Serum Prostate Specific Antigen Concentration: Results of a Randomized Study.” *The Journal of Urology* 148 (1): 83–86.

Clavell-Hernandez, Jonathan, and Run Wang. 2015. “Penile Rehabilitation Following Prostate Cancer Treatment: Review of Current Literature.” *Asian Journal of Andrology* 17 (6): 916. doi:10.4103/1008-682X.150838.

Compton, Sarah A., Jun Hyuk Choi, Anthony J. Cesare, Sezgin Ozgur, and Jack D. Griffith. 2007. “Xrcc3 and Nbs1 Are Required for the Production of Extrachromosomal Telomeric Circles in Human Alternative Lengthening of Telomere Cells.” *Cancer Research* 67 (4): 1513–19. doi:10.1158/0008-5472.CAN-06-3672.

Coumans, F. A W, C. J M Doggen, G. Attard, J. S. de Bono, and L. W M M Terstappen. 2010. “All Circulating EpCAM+CK+CD45-Objects Predict Overall Survival in Castration-Resistant Prostate Cancer.” *Annals of Oncology* 21 (9): 1851–57. doi:10.1093/annonc/mdq030.

Crawford, E David, Celestia S Higano, Neal D Shore, Maha Hussain, and Daniel P Petrylak. 2015. “Treating Patients with Metastatic Castration Resistant Prostate Cancer: A Comprehensive Review of Available Therapies.” *The Journal of Urology* 194 (6): 1537–47. doi:10.1016/j.juro.2015.06.106.

Cremer, Thomas, and Marion Cremer. 2010. “Chromosome Territories.” *Cold Spring Harbor Perspectives in Biology* 2 (3): a003889. doi:10.1101/cshperspect.a003889.

Cross, Sarah E, Yu-Sheng Jin, Jianyu Rao, and James K Gimzewski. 2007. “Nanomechanical Analysis of Cells from Cancer Patients.” *Nature Nanotechnology* 2 (12): 780–83. doi:10.1038/nnano.2007.388.

Culig, Z, J Hoffmann, M Erdel, I E Eder, a Hobisch, a Hittmair, G Bartsch, et al. 1999. “Switch from Antagonist to Agonist of the Androgen Receptor Bicalutamide Is Associated with Prostate Tumour Progression in a New Model System.” *British Journal of Cancer* 81: 242–51. doi:10.1038/sj.bjc.6690684.

D’Amico, Anthony V., Ming-Hui Chen, Kimberly A. Roehl, and William J. Catalona. 2004. “Preoperative PSA Velocity and the Risk of Death from Prostate Cancer after Radical Prostatectomy.” *New England Journal of Medicine* 351 (2): 1327–35. doi:10.1056/NEJMoa1109400.

D’Amico, Anthony V., April Desjardin, Ming H. Chen, Steve Paik, Delray Schultz, Andrew A. Renshaw, Kevin R. Loughlin, and Jerome P. Richie. 1998. “Analyzing Outcome-Based Staging for Clinically Localized Adenocarcinoma of the Prostate.” *Cancer* 83 (10): 2172–80. doi:10.1002/(SICI)1097-0142(19981115)83:10<2172::AID-CNCR16>3.0.CO;2-K.

Danila, Daniel C., Martin Fleisher, and Howard I. Scher. 2011. “Circulating Tumor Cells as Biomarkers in Prostate Cancer.” *Clinical Cancer Research* 17: 3903–12. doi:10.1158/1078-0432.CCR-10-2650.

de Bono, Johann S, Howard I Scher, R Bruce Montgomery, Christopher Parker, M Craig Miller, Henk Tissing, Gerald V Doyle, Leon W W M Terstappen, Kenneth J Pienta, and Derek Raghavan. 2008. “Circulating Tumor Cells Predict Survival Benefit from Treatment in Metastatic Castration-Resistant Prostate Cancer.” *Clinical Cancer Research : An Official*

Journal of the American Association for Cancer Research 14 (19): 6302–9. doi:10.1158/1078-0432.CCR-08-0872.

De Vos, Winnok H, R a Hoebe, G H Joss, W Haffmans, S Baatout, P Van Oostveldt, and E M M Manders. 2009. "Controlled Light Exposure Microscopy Reveals Dynamic Telomere Microterritories throughout the Cell Cycle." *Cytometry. Part A : The Journal of the International Society for Analytical Cytology* 75 (5): 428–39. doi:10.1002/cyto.a.20699.

Dehm, Scott M., Lucy J. Schmidt, Hannelore V. Heemers, Robert L. Vessella, and Donald J. Tindall. 2008. "Splicing of a Novel Androgen Receptor Exon Generates a Constitutively Active Androgen Receptor That Mediates Prostate Cancer Therapy Resistance." *Cancer Research* 68 (13): 5469–77. doi:10.1158/0008-5472.CAN-08-0594.

Desitter, Isabelle, Bella S Guerrouahen, Naoual Benali-Furet, Janine Wechsler, Pasi a Jänne, Yanan Kuang, Masahiko Yanagita, et al. 2011. "A New Device for Rapid Isolation by Size and Characterization of Rare Circulating Tumor Cells." *Anticancer Research* 31 (2): 427–41.

Dickinson, Louise, Hashim U. Ahmed, Clare Allen, Jelle O. Barentsz, Brendan Carey, Jurgen J. Futterer, Stijn W. Heijmink, et al. 2011. "Magnetic Resonance Imaging for the Detection, Localisation, and Characterisation of Prostate Cancer: Recommendations from a European Consensus Meeting." *European Urology* 59 (4). European Association of Urology: 477–94. doi:10.1016/j.eururo.2010.12.009.

Dillard, Paulette R., Ming Fong Lin, and Shafiq A. Khan. 2008. "Androgen-Independent Prostate Cancer Cells Acquire the Complete Steroidogenic Potential of Synthesizing Testosterone from Cholesterol." *Molecular and Cellular Endocrinology* 295 (1-2): 115–20. doi:10.1016/j.mce.2008.08.013.

Ding, Zhihu, Chang-Jiun Wu, Mariela Jaskelioff, Elena Ivanova, Maria Kost-Alimova, Alexei Protopopov, Gerald C Chu, et al. 2012. "Telomerase Reactivation Following Telomere Dysfunction Yields Murine Prostate Tumors with Bone Metastases." *Cell* 148 (5). Elsevier Inc.: 896–907. doi:10.1016/j.cell.2012.01.039.

Doksani, Ylli, and Titia de Lange. 2014. "The Role of Double-Strand Break Repair Pathways at Functional and Dysfunctional Telomeres." *Cold Spring Harbor Perspectives in Biology* 6 (12): a016576. doi:10.1101/cshperspect.a016576.

Dolfus, Claire, Nicolas Piton, Emmanuel Toure, and Jean-Christophe Sabourin. 2015. "Circulating Tumor Cell Isolation: The Assets of Filtration Methods with Polycarbonate Track-Etched Filters." *Chinese Journal of Cancer Research* 27 (5): 479–87. doi:10.3978/j.issn.1000-9604.2015.09.01.

Drachenberg, D E. 2000. "Treatment of Prostate Cancer: Watchful Waiting, Radical Prostatectomy, and Cryoablation." *Seminars in Surgical Oncology* 18 (1): 37–44.

Fenoglietto, Pascal, Benoit Laliberte, Ali Allaw, Norbert Ailleres, Katia Idri, Meng Huor Hay, Carmen Llacer Moscardo, Sophie Gourgou, Jean Bernard Dubois, and David Azria. 2008. "Persistently Better Treatment Planning Results of Intensity-Modulated (IMRT) over Conformal Radiotherapy (3D-CRT) in Prostate Cancer Patients with Significant Variation of Clinical Target Volume And/or Organs-at-Risk." *Radiotherapy and Oncology* 88 (1): 77–87. doi:10.1016/j.radonc.2007.12.011.

Frankel, Stephen, George Davey Smith, Jenny Donovan, and David Neal. 2003. “Screening for Prostate Cancer.” *Lancet (London, England)* 361 (9363): 1122–28. doi:10.1016/S0140-6736(03)12890-5.

Freeman, Daniel J., Andrew G. Li, Gang Wei, Heng Hong Li, Nathalie Kertesz, Ralf Lesche, Andrew D. Whale, et al. 2003. “PTEN Tumor Suppressor Regulates p53 Protein Levels and Activity through Phosphatase-Dependent and -Independent Mechanisms.” *Cancer Cell* 3 (2): 117–30. doi:10.1016/S1535-6108(03)00021-7.

Gadji, Macoura, Julius Adebayo Awe, Prerana Rodrigues, Rajat Kumar, Donald S Houston, Ludger Klewes, Tandakha Ndiaye Dièye, et al. 2012. “Profiling Three-Dimensional Nuclear Telomeric Architecture of Myelodysplastic Syndromes and Acute Myeloid Leukemia Defines Patient Subgroups.” *Clinical Cancer Research : An Official Journal of the American Association for Cancer Research* 18 (12): 3293–3304. doi:10.1158/1078-0432.CCR-12-0087.

Gadji, Macoura, David Fortin, and Ana-maria Tsanaclis. 2010. “Three-Dimensional Nuclear Telomere Architecture Is Associated with Differential Time to Progression and Overall Survival in Glioblastoma Patients.” *Neoplasia* 12 (2): 183–91. doi:10.1593/neo.91752.

Gadji, Macoura, Rhea Vallente, Ludger Klewes, Christiaan Righolt, Landon Wark, Narisorn Kongruttanachok, Hans Knecht, and Sabine Mai. 2011. *Nuclear Remodeling as a Mechanism for Genomic Instability in Cancer. Advances in Cancer Research*. Vol. 112. Elsevier Inc. doi:10.1016/B978-0-12-387688-1.00004-1.

Gao, Dong, Ian Vela, Andrea Sboner, Phillip J. Iaquinta, Wouter R. Karthaus, Anuradha Gopalan, Catherine Dowling, et al. 2014. “Organoid Cultures Derived from Patients with Advanced Prostate Cancer.” *Cell* 159 (1). Elsevier Inc.: 176–87. doi:10.1016/j.cell.2014.08.016.

Genesca, Anna, Judit Pampalona, Cristina Frias, Daniel Dominguez, and Laura Tusell. 2011. *Role of Telomere Dysfunction in Genetic Intratumor Diversity*. *Advances in Cancer Research*. Vol. 112. doi:10.1016/B978-0-12-387688-1.00002-8.

Goldkorn, Amir, Benjamin Ely, and CM Tangen. 2014. “Circulating Tumor Cell Telomerase Activity as a Prognostic Marker for Overall Survival in SWOG 0421: A Phase 3 Metastatic Castration Resistant Prostate Cancer Trial.” *... Journal of Cancer*.

Gomella, Leonard G. 2009. “Effective Testosterone Suppression for Patients with Prostate Cancer: Is There a Best Castration Therapy?” *Urology* 11 (2): 207–13. doi:10.1016/S0090-4295(03)00331-5.

Gonzalez-Suarez, Ignacio, Abena B Redwood, Stephanie M Perkins, Bart Vermolen, Daniel Lichtensztejin, David A Grotsky, Lucia Morgado-Palacin, et al. 2009. “Novel Roles for A-Type Lamins in Telomere Biology and the DNA Damage Response Pathway.” *The EMBO Journal* 28 (16). Nature Publishing Group: 2414–27. doi:10.1038/emboj.2009.196.

Goodman, Oscar B, James T Symanowski, Aida Loudyi, Louis M Fink, David C Ward, and Nicholas J Vogelzang. 2011. “Circulating Tumor Cells as a Predictive Biomarker in Patients with Hormone-Sensitive Prostate Cancer.” *Clinical Genitourinary Cancer* 9 (1). Elsevier: 31–38. doi:10.1016/j.clgc.2011.04.001.

Goodwin, Jonathan F, Matthew J Schiewer, Jeffry L Dean, Randy S Schrecengost, Renée de

Leeuw, Sumin Han, Teng Ma, et al. 2013. “A Hormone-DNA Repair Circuit Governs the Response to Genotoxic Insult.” *Cancer Discovery* 3 (11). American Association for Cancer Research: 1254–71. doi:10.1158/2159-8290.CD-13-0108.

Grillet, F., Bayet, E., Villeronce, O., Zappia, L., Lagerqvist, E. L., Lunke, S., … Pannequin, J. (2016). Circulating tumour cells from patients with colorectal cancer have cancer stem cell hallmarks in *ex vivo* culture. *Gut*, gutjnl–2016–311447. http://doi.org/10.1136/gutjnl-2016-311447

Guffei, Amanda, Rahul Sarkar, Ludger Klewes, Christiaan Righolt, Hans Knecht, and Sabine Mai. 2010. “Dynamic Chromosomal Rearrangements in Hodgkin’s Lymphoma Are due to Ongoing Three-Dimensional Nuclear Remodeling and Breakage-Bridge-Fusion Cycles.” *Haematologica* 95 (12): 2038–46. doi:10.3324/haematol.2010.030171.

Guo, Zhiyong, Xi Yang, Feng Sun, Richeng Jiang, Douglas E. Linn, Hege Chen, Hegang Chen, et al. 2009. “A Novel Androgen Receptor Splice Variant Is up-Regulated during Prostate Cancer Progression and Promotes Androgen Depletion-Resistant Growth.” *Cancer Research* 69 (6): 2305–13. doi:10.1158/0008-5472.CAN-08-3795.

Haffner, M C, M J Aryee, A Toubaji, D M Esopi, R Albadine, B Gurel, W B Isaacs, et al. 2010. “Androgen-Induced TOP2B-Mediated Double-Strand Breaks and Prostate Cancer Gene Rearrangements.” *Nature Genetics* 42 (8): 668–75. doi:10.1038/ng.613.

Hanahan, Douglas, and Robert A Weinberg. 2000. “Hallmarks of Cancer.” *Cell* 100: 57–70. doi:10.1007/s00262-010-0968-0.

Hanahan, Douglas, and Robert a Weinberg. 2011. “Hallmarks of Cancer: The next Generation.” *Cell* 144 (5). Elsevier Inc.: 646–74. doi:10.1016/j.cell.2011.02.013.

He, Bin, Rainer B Lanz, Warren Fiskus, Chuandong Geng, Ping Yi, Sean M Hartig, Kimal Rajapakshe, et al. 2014. “GATA2 Facilitates Steroid Receptor Coactivator Recruitment to the Androgen Receptor Complex.” *Proceedings of the National Academy of Sciences of the United States of America* 111 (51): 18261–66. doi:10.1073/pnas.1421415111.

Heaphy, Christopher M., Gaurav Gaonkar, Sarah B. Peskoe, Corinne E. Joshu, Angelo M. De Marzo, M. Scott Lucia, Phyllis J. Goodman, et al. 2015. “Prostate Stromal Cell Telomere Shortening Is Associated with Risk of Prostate Cancer in the Placebo Arm of the Prostate Cancer Prevention Trial.” *The Prostate* 1166 (January): n/a – n/a. doi:10.1002/pros.22997.

Helzer, Kimberly T., Helen E. Barnes, Laura Day, Jeanne Harvey, Paul R. Billings, and Allyn Forsyth. 2009. “Circulating Tumor Cells Are Transcriptionally Similar to the Primary Tumor in a Murine Prostate Model.” *Cancer Research* 69 (19): 7860–66. doi:10.1158/0008-5472.CAN-09-0801.

Heselmeyer-Haddad, Kerstin M., Lissa Y Berroa Garcia, Amanda Bradley, Leanora Hernandez, Yue Hu, Jens K. Habermann, Christoph Dumke, et al. 2014. “Single-Cell Genetic Analysis Reveals Insights into Clonal Development of Prostate Cancers and Indicates Loss of PTEN as a Marker of Poor Prognosis.” *American Journal of Pathology* 184 (10). American Society for Investigative Pathology: 2671–86. doi:10.1016/j.ajpath.2014.06.030.

Hlobilkova, A, P Guldberg, M Thullberg, J Zeuthen, J Lukas, and J Bartek. 2000. “Cell Cycle Arrest by the PTEN Tumor Suppressor Is Target Cell Specific and May Require Protein

Phosphatase Activity." *Experimental Cell Research* 256 (2): 571–77. doi:10.1006/excr.2000.4867.

Hofer, Matthias D, Rainer Kuefer, Wei Huang, Haojie Li, Tarek a Bismar, Sven Perner, Richard E Hautmann, Martin G Sanda, Juergen E Gschwend, and Mark a Rubin. 2006. "Prognostic Factors in Lymph Node-Positive Prostate Cancer." *Urology* 67 (5): 1016–21. doi:10.1016/j.urology.2005.10.055.

Hotte, Sebastien J., and F. Saad. 2010. "Current Management of Castrate-Resistant Prostate Cancer." *Current Oncology* 17 (SUPPL. 2): 72–79. doi:10.3747/co.v17i0.718.

"https://www.cellsearchctc.com/." n.d. *CellSearch.com*.

Hu, Rong, Thomas A. Dunn, Shuanzeng Wei, Sumit Isharwal, Robert W. Veltri, Elizabeth Humphreys, Misop Han, et al. 2009. "Ligand-Independent Androgen Receptor Variants Derived from Splicing of Cryptic Exons Signify Hormone-Refractory Prostate Cancer." *Cancer Research* 69 (1): 16–22. doi:10.1158/0008-5472.CAN-08-2764.

Hubbard, G. K., L. N. Mutton, M. Khalili, R. P. McMullin, J. L. Hicks, D. Bianchi-Frias, L. A. Horn, et al. 2015. "Combined MYC Activation and Pten Loss Are Sufficient to Create Genomic Instability and Lethal Metastatic Prostate Cancer." *Cancer Research*, 8–11. doi:10.1158/0008-5472.CAN-14-3280.

Humphrey, Peter A. 2004. "Gleason Grading and Prognostic Factors in Carcinoma of the Prostate." *Modern Pathology* 17 (3): 292–306. doi:10.1038/modpathol.3800054.

Hwang, Sung Ii, and Hak Jong Lee. 2014. "The Future Perspectives in Transrectal Prostate Ultrasound Guided Biopsy." *Prostate International* 2 (4): 153–60. doi:10.12954/PI.14062.

Jager, G J, J O Barentz, E T G Ruijter, M C H De Rosette, and G O N Oostcrhof. 1996. "Primary Staging of Prostate Cancer." *European Radiology* 139: 134–39.

Jiao, Jing, Shunyou Wang, Rong Qiao, Igor Vivanco, Philip A. Watson, Charles L. Sawyers, and Hong Wu. 2007. "Murine Cell Lines Derived from Pten Null Prostate Cancer Show the Critical Role of PTEN in Hormone Refractory Prostate Cancer Development." *Cancer Research* 67 (13): 6083–91. doi:10.1158/0008-5472.CAN-06-4202.

Joshua, A. M., E. Shen, M. Yoshimoto, P. Marrano, M. Zielenska, A. J. Evans, T. Van Der Kwast, and J. A. Squire. 2011. "Topographical Analysis of Telomere Length and Correlation with Genomic Instability in Whole Mount Prostatectomies." *Prostate* 71 (7): 778–90. doi:10.1002/pros.21294.

Ju, Bong-Gun, Victoria V Lunyak, Valentina Perissi, Ivan Garcia-Bassets, David W Rose, Christopher K Glass, and Michael G Rosenfeld. 2006. "A Topoisomerase IIbeta-Mediated dsDNA Break Required for Regulated Transcription." *Science* 312 (5781): 1798–1802.

Karanika, S, T Karantanos, L Li, P G Corn, and T C Thompson. 2014. "DNA Damage Response and Prostate Cancer: Defects, Regulation and Therapeutic Implications." *Oncogene*, no. February (August). Nature Publishing Group: 1–8. doi:10.1038/onc.2014.238.

Karantanos, Theodoros, Christopher P Evans, Bertrand Tombal, Timothy C Thompson, Rodolfo Montironi, and William B Isaacs. 2014. "Understanding the Mechanisms of Androgen Deprivation Resistance in Prostate Cancer at the Molecular Level." *European Urology*, October. European Association of Urology, 1–10. doi:10.1016/j.eururo.2014.09.049.

Katsogiannou, Maria, Hajer Ziouziou, Sara Karaki, Claudia Andrieu, Marie Henry de Villeneuve, and Palma Rocchi. 2015. “The Hallmarks of Castration-Resistant Prostate Cancers.” *Cancer Treatment Reviews*. Elsevier Ltd. doi:10.1016/j.ctrv.2015.05.003.

Kim, Sahn Ho, Michelle Richardson, Kannagi Chinnakannu, V. Uma Bai, Mani Menon, Evelyn R. Barrack, and G. Prem Veer Reddy. 2010. “Androgen Receptor Interacts with Telomeric Proteins in Prostate Cancer Cells.” *Journal of Biological Chemistry* 285 (14): 10472–76. doi:10.1074/jbc.M109.098798.

Kimura, Takahiro, Hiroshi Sasaki, Kouhei Akazawa, and Shin Egawa. 2015. “Gonadotropin-Releasing Hormone Antagonist: A Real Advantage?” *Urologic Oncology* 33 (7): 322–28. doi:10.1016/j.urolonc.2015.04.013.

Kinnear, N J, G Kichenadasse, S Plagakis, M E O’Callaghan, T Kopsaftis, S Walsh, and D Foreman. 2016. “Prostate Cancer in Men Aged Less than 50 Years at Diagnosis.” *World Journal of Urology*, April. doi:10.1007/s00345-016-1824-4.

Klewes, Ludger, Clemens Höbsch, Nir Katzir, David Rourke, Yuval Garini, and Sabine Mai. 2011. “Novel Automated Three-Dimensional Genome Scanning Based on the Nuclear Architecture of Telomeres.” *Cytometry. Part A : The Journal of the International Society for Analytical Cytology* 79 (2): 159–66. doi:10.1002/cyto.a.21012.

Knecht, Hans, Narisorn Kongruttanachok, Bassem Sawan, Eric Turcotte, Zelda Lichtensztejn, Daniel Lichtensztejn, and Sabine Mai. 2012. “Three-Dimensional Telomere Signatures of Hodgkin- and Reed-Sternberg Cells at Diagnosis Identify Patients with Poor Response to Conventional Chemotherapy.” *Translational Oncology* 5 (4): 269–77. doi:10.1593/tlo.12142.

Ko, Hyun-Kyung, Shin Akakura, Jennifer Peresie, David W Goodrich, Barbara a Foster, and Irwin H Gelman. 2014. “A Transgenic Mouse Model for Early Prostate Metastasis to Lymph Nodes.” *Cancer Research* 74 (3): 945–53. doi:10.1158/0008-5472.CAN-13-1157.

Kobayashi, Marina, Soo Hyeon Kim, Hiroko Nakamura, Shohei Kaneda, and Teruo Fujii. 2015. “Cancer Cell Analyses at the Single Cell-Level Using Electroactive Microwell Array Device.” *PloS One* 10 (11). Public Library of Science: e0139980. doi:10.1371/journal.pone.0139980.

Kobayashi, T., Inoue, T., Kamba, T., & Ogawa, O. (2013). Experimental Evidence of Persistent Androgen-Receptor-Dependency in Castration-Resistant Prostate Cancer. International Journal of Molecular Sciences, 14(8), 15615–15635. http://doi.org/10.3390/ijms140815615

Kolostova, Katarina, Marek Broul, Jan Schraml, Martin Cegan, Rafal Matkowski, Marek Fiutowski, and Vladimir Bobek. 2014. “Circulating Tumor Cells in Localized Prostate Cancer: Isolation, Cultivation in Vitro and Relationship to T-Stage and Gleason Score.” *Anticancer Research* 34 (7): 3641–46.

Kovac, Evan, Ahmed ElShafei, Kae Jack Tay, Melissa Mendez, Thomas J Polascik, and J Stephen Jones. 2016. “Five-Year Biochemical Progression-Free Survival Following Salvage Whole-Gland Prostate Cryoablation: Defining Success with Nadir Prostate-Specific Antigen.” *Journal of Endourology / Endourological Society*, April. doi:10.1089/end.2015.0719.

Kupelian, Patrick A., Louis Potters, Deepak Khuntia, Jay P. Ciezki, Chandana A. Reddy, Alwyn

M. Reuther, Thomas P. Carlson, and Eric A. Klein. 2004. “Radical Prostatectomy, External Beam Radiotherapy 72 Gy, External Beam Radiotherapy 72 Gy, Permanent Seed Implantation, or Combined Seeds/external Beam Radiotherapy for Stage T1-T2 Prostate Cancer.” *International Journal of Radiation Oncology Biology Physics* 58 (1): 25–33. doi:10.1016/S0360-3016(03)00784-3.

Kuzyk, Alexandra, and Sabine Mai. 2012. “Selected Telomere Length Changes and Aberrant Three-Dimensional Nuclear Telomere Organization during Fast-Onset Mouse Plasmacytomas.” *Neoplasia* 14 (4): 344–51. doi:10.1593/neo.12446.

Lalonde, Emilie, Adrian S Ishkanian, Jenna Sykes, Michael Fraser, Helen Ross-Adams, Nicholas Erho, Mark J Dunning, et al. 2014. “Tumour Genomic and Microenvironmental Heterogeneity for Integrated Prediction of 5-Year Biochemical Recurrence of Prostate Cancer: A Retrospective Cohort Study.” *The Lancet Oncology* 15 (13). Lalonde et al. Open Access article distributed under the terms of CC BY: 1521–32. doi:10.1016/S1470-2045(14)71021-6.

Legrier, M E, C Guyader, J Ceraline, B Dutrillaux, S Oudard, M F Poupon, and N Auger. 2009. “Hormone Escape Is Associated with Genomic Instability in a Human Prostate Cancer Model.” *Int J Cancer* 124 (April 2008): 1103–11. doi:10.1002/ijc.24073.

Leze, Eduardo, Clarice F E Maciel-Osorio, and Carlos a Mandarim-de-Lacerda. 2014. “Advantages of Evaluating Mean Nuclear Volume as an Adjunct Parameter in Prostate Cancer.” *PloS One* 9 (7): e102156. doi:10.1371/journal.pone.0102156.

Li, Peng, Zhangming Mao, Zhangli Peng, Lanlan Zhou, Yuchao Chen, Po-hsun Huang, and Cristina I Truica. 2015. “Acoustic Separation of Circulating Tumor Cells.” *Proceedings of the National Academy of Sciences of the United States of America*. doi:10.1073/pnas.1504484112.

Li, Xuan, and Wolf-Dietrich Heyer. 2008. “Homologous Recombination in DNA Repair and DNA Damage Tolerance.” *Cell Research* 18 (1): 99–113. doi:10.1038/cr.2008.1.

Lieber, Michael R., Jiafeng Gu, Haihui Lu, Noriko Shimazaki, and Albert G. Tsai. 2010. “Nonhomologous DNA End Joining (NHEJ) and Chromosomal Translocations in Humans.” *Subcellular Biochemistry* 50: 279–96. doi:10.1007/978-90-481-3471-7.

Lin, Biaoyang, Camari Ferguson, James T White, Shunyou Wang, Robert Vessella, Lawrence D True, Leroy Hood, and Peter S Nelson. 1999. “Prostate-Localized and Androgen-Regulated Expression of the Membrane-Bound Serine Protease TMPRSS2.” *Pharmacia*, 4180–84.

Lindberg, Johan, Daniel Klevebring, Wennuan Liu, M??rten Neiman, Jianfeng Xu, Peter Wiklund, Fredrik Wiklund, Ian G. Mills, Lars Egevad, and Henrik Gr??nberg. 2013. “Exome Sequencing of Prostate Cancer Supports the Hypothesis of Independent Tumour Origins.” *European Urology* 63 (2): 347–53. doi:10.1016/j.eururo.2012.03.050.

Lindberg, Johan, Anna Kristiansen, Peter Wiklund, Henrik Grönberg, and Lars Egevad. 2014. “Tracking the Origin of Metastatic Prostate Cancer.” *European Urology*, September. doi:10.1016/j.eururo.2014.09.006.

Lio, Yi-Ching, David Schild, Mark A Brenneman, J Leslie Redpath, and David J Chen. 2004. “Human Rad51C Deficiency Destabilizes XRCC3, Impairs Recombination, and Radiosensitizes S/G2-Phase Cells.” *The Journal of Biological Chemistry* 279 (40): 42313–

20. doi:10.1074/jbc.M405212200.

Loh, Jasmin, Lidija Jovanovic, Margot Lehman, Anne Capp, David Pryor, Monica Harris, Colleen Nelson, and Jarad Martin. 2014. “Circulating Tumor Cell Detection in High-Risk Non-Metastatic Prostate Cancer.” *Journal of Cancer Research and Clinical Oncology*, July. doi:10.1007/s00432-014-1775-3.

Lorente, David, Joaquin Mateo, and Johann S de Bono. 2014. “Molecular Characterization and Clinical Utility of Circulating Tumor Cells in the Treatment of Prostate Cancer.” *American Society of Clinical Oncology Educational Book / ASCO. American Society of Clinical Oncology. Meeting*, January. American Society of Clinical Oncology, e197–203. doi:10.14694/EdBook_AM.2014.34.e197.

Lotan, Tamara L, Filipe Lf Carvalho, Sarah B Peskoe, Jessica L Hicks, Jennifer Good, Helen L Fedor, Elizabeth Humphreys, et al. 2014. “PTEN Loss Is Associated with Upgrading of Prostate Cancer from Biopsy to Radical Prostatectomy.” *Modern Pathology : An Official Journal of the United States and Canadian Academy of Pathology, Inc*, July. Nature Publishing Group, 1–10. doi:10.1038/modpathol.2014.85.

Louis, Sherif F, Bart J Vermolen, Yuval Garini, Ian T Young, Amanda Guffei, Zelda Lichtensztejn, Fabien Kuttler, et al. 2005. “C-Myc Induces Chromosomal Rearrangements through Telomere and Chromosome Remodeling in the Interphase Nucleus.” *Proceedings of the National Academy of Sciences of the United States of America* 102 (27): 9613–18. doi:10.1073/pnas.0407512102.

Lowes, L E, M Lock, G Rodrigues, D D’Souza, G Bauman, B Ahmad, V Venkatesan, a L Allan, and T Sexton. 2015. “The Significance of Circulating Tumor Cells in Prostate Cancer Patients Undergoing Adjuvant or Salvage Radiation Therapy.” *Prostate Cancer and Prostatic Disease*, no. January: 1–7. doi:10.1038/pcan.2015.36.

Lu-Yao, Grace L, Peter C Albertsen, Dirk F Moore, Weichung Shih, Yong Lin, Robert S DiPaola, and Siu-Long Yao. 2014. “Fifteen-Year Survival Outcomes Following Primary Androgen-Deprivation Therapy for Localized Prostate Cancer.” *JAMA Internal Medicine* 174 (9). American Medical Association: 1460–67. doi:10.1001/jamainternmed.2014.3028.

Mai, Sabine. 2010. “Initiation of Telomere-Mediated Chromosomal Rearrangements in Cancer.” *Journal of Cellular Biochemistry* 109 (6): 1095–1102. doi:10.1002/jcb.22501.

Mai, Sabine, and Yuval Garini. 2005. “Oncogenic Remodeling of the Three-Dimensional Organization of the Interphase Nucleus: C-Myc Induces Telomeric Aggregates Whose Formation Precedes Chromosomal Rearrangements.” *Cell Cycle* 4 (October): 1327–31.

Mai, Sabine, and Yuval Garini. 2006. “The Significance of Telomeric Aggregates in the Interphase Nuclei of Tumor Cells.” *Journal of Cellular Biochemistry* 97 (5): 904–15. doi:10.1002/jcb.20760.

Maloisel, L, F Fabre, and S Gangloff. 2008. “DNA Polymerase Delta Is Preferentially Recruited during Homologous Recombination to Promote Heteroduplex DNA Extension.” *Molecular and Cellular Biology* 28 (4): 1373–82. doi:10.1128/MCB.01651-07.

Manolov, G., & Manolova, Y. (1972). Marker band in one chromosome 14 from Burkitt lymphomas. Nature, 237(5349), 33–34. http://doi.org/10.1038/237033a0

Marcomini, Isabella, and Susan M. Gasser. 2015. “Nuclear Organization in DNA End Processing: Telomeres vs Double-Strand Breaks.” *DNA Repair* 1. Elsevier B.V.: 1–7. doi:10.1016/j.dnarep.2015.04.024.

Mathers, Michael J, Stephan Roth, Monika Klinkhammer-Schalke, Michael Gerken, Ferdinand Hofstaedter, Stefan Wilm, and Theodor Klotz. 2011. “Patients with Localised Prostate Cancer (t1 - t2) Show Improved Overall Long-Term Survival Compared to the Normal Population.” *Journal of Cancer* 2 (1): 76–80.

Matias, Pedro M., Maria Arm??nia Carrondo, Ricardo Coelho, Monica Thomaz, Xiao Yan Zhao, Anja Wegg, Kerstin Crusius, Ursula Egner, and Peter Donner. 2002. “Structural Basis for the Glucocorticoid Response in a Mutant Human Androgen Receptor (ARccr) Derived from an Androgen-Independent Prostate Cancer.” *Journal of Medicinal Chemistry* 45 (7): 1439–46. doi:10.1021/jm011072j.

Meeker, Alan K, Jessica L Hicks, Edward Gabrielson, William M Strauss, Angelo M De Marzo, and Pedram Argani. 2004. “Telomere Shortening Occurs in Subsets of Normal Breast Epithelium as Well as in Situ and Invasive Carcinoma.” *The American Journal of Pathology* 164 (3): 925–35. doi:10.1016/S0002-9440(10)63180-X.

Meeker, Alan K, Jessica L Hicks, Christine a Iacobuzio-Donahue, Elizabeth a Montgomery, William H Westra, Theresa Y Chan, Brigitte M Ronnett, and Angelo M De Marzo. 2004. “Telomere Length Abnormalities Occur Early in the Initiation of Epithelial Carcinogenesis.” *Clinical Cancer Research : An Official Journal of the American Association for Cancer Research* 10 (10): 3317–26. doi:10.1158/1078-0432.CCR-0984-03.

Meeker, Alan K, Jessica L Hicks, Elizabeth A Platz, Gerrun E March, Christina J Bennett, Michael J Delannoy, and Angelo M De Marzo. 2002. “Telomere Shortening Is an Early Somatic DNA Alteration in Human Prostate Tumorigenesis.” *Cancer Research* 62 (22): 6405–9.

Mehlen, Patrick, and Alain Puisieux. 2006. “Metastasis: A Question of Life or Death.” *Nature Reviews. Cancer* 6 (6). Nature Publishing Group: 449–58. doi:10.1038/nrc1886.

Meyer, Christian P, Klaus Pantel, Pierre Tennstedt, Petra Stroelin, Thorsten Schlomm, Hans Heinzer, Sabine Riethdorf, and Thomas Steuber. 2016. “Limited Prognostic Value of Preoperative Circulating Tumor Cells for Early Biochemical Recurrence in Patients with Localized Prostate Cancer.” *Urologic Oncology*, January. doi:10.1016/j.urolonc.2015.12.003.

Mirjolet, Céline, Romain Boidot, Sébastien Saliques, François Ghiringhelli, Philippe Maingon, and Gilles Créhange. 2015. “The Role of Telomeres in Predicting Individual Radiosensitivity of Patients with Cancer in the Era of Personalized Radiotherapy.” *Cancer Treatment Reviews* 41 (4). Elsevier: 354–60. doi:10.1016/j.ctrv.2015.02.005.

Mladenov, Emil, Simon Magin, Aashish Soni, and George Iliakis. 2016. “DNA Double-Strand-Break Repair in Higher Eukaryotes and Its Role in Genomic Instability and Cancer: Cell Cycle and Proliferation-Dependent Regulation.” *Seminars in Cancer Biology* 37-38. Elsevier Ltd: 51–64. doi:10.1016/j.semcancer.2016.03.003.

Mohiuddin, Jahan J., Brock R. Baker, and Ronald C. Chen. 2015. “Radiotherapy for High-Risk

Prostate Cancer." *Nature Reviews Urology* 12 (3). Nature Publishing Group: 145–54. doi:10.1038/nrurol.2015.25.

Møller, Elen K, Parveen Kumar, Thierry Voet, April Peterson, Peter Van Loo, Randi R Mathiesen, Renathe Fjelldal, et al. 2013. "Next-Generation Sequencing of Disseminated Tumor Cells." *Frontiers in Oncology* 3 (December): 320. doi:10.3389/fonc.2013.00320.

Morton, G.C., and P.J. Hoskin. 2013. "Brachytherapy: Current Status and Future Strategies -- Can High Dose Rate Replace Low Dose Rate and External Beam Radiotherapy?" *Clinical Oncology* 25 (8). Elsevier: 474–82. doi:10.1016/j.clon.2013.04.009.

Moss, T J, and D G Sanders. 1990. "Detection of Neuroblastoma Cells in Blood." *Journal of Clinical Oncology : Official Journal of the American Society of Clinical Oncology* 8 (4): 736–40.

Moul, Judd W. 2014. "Utility of LHRH Antagonists for Advanced Prostate Cancer." *The Canadian Journal of Urology* 21: 22–27. doi:10.1056/NEJMra021562.

Mouraviev, V, B Evans, and T J Polascik. 2006. "Salvage Prostate Cryoablation after Primary Interstitial Brachytherapy Failure: A Feasible Approach." *Prostate Cancer and Prostatic Diseases* 9 (1): 99–101. doi:10.1038/sj.pcan.4500853.

Nabetani, Akira, and Fuyuki Ishikawa. 2011. "Alternative Lengthening of Telomeres Pathway: Recombination-Mediated Telomere Maintenance Mechanism in Human Cells." *Journal of Biochemistry* 149 (1): 5–14. doi:10.1093/jb/mvq119.

Nadal, R., Schweizer, M., Kryvenko, O. N., Epstein, J. I., & Eisenberger, M. A. (2014). Small cell carcinoma of the prostate. *Nat Rev Urol*, 1121(4), 213–219. http://doi.org/10.1038/nrurol.2014.21

Nakajima, Toshihiro, Chiharu Uchida, Stephen F. Anderson, Lee Chee-Gun, Jerard Hurwitz, Jeffrey D. Parvin, and Marc Montminy. 1997. "RNA Helicase A Mediates Association of CBP with RNA Polymerase II." *Cell* 90 (6): 1107–12. doi:10.1016/S0092-8674(00)80376-1.

Nguyen, Paul L, Shabbir M H Alibhai, Shehzad Basaria, Anthony V D'Amico, Philip W Kantoff, Nancy L Keating, David F Penson, Derek J Rosario, Bertrand Tombal, and Matthew R Smith. 2014. "Adverse Effects of Androgen Deprivation Therapy and Strategies to Mitigate Them." *European Urology*, August. European Association of Urology, 1–12. doi:10.1016/j.eururo.2014.07.010.

Osguthorpe, DJ, and AT Hagler. 2011. "Mechanism of Androgen Receptor Antagonism by Bicalutamide in the Treatment of Prostate Cancer." *Biochemistry* 50 (19): 4105–13. doi:10.1021/bi102059z.Mechanism.

Osmulski, Pawel, Devalingam Mahalingam, Maria E. Gaczynska, Joseph Liu, Susan Huang, Aaron M. Horning, Chiou-Miin Wang, Ian M. Thompson, Tim H.-M. Huang, and Chun-Liang Chen. 2014. "Nanomechanical Biomarkers of Single Circulating Tumor Cells for Detection of Castration Resistant Prostate Cancer." *The Prostate* 1307 (13): n/a – n/a. doi:10.1002/pros.22846.

Pandini, Giuseppe, Rossana Mineo, Francesco Frasca, Charles T Roberts, Marco Marcelli, Riccardo Vigneri, and Antonino Belfiore. 2005. "Androgens Up-Regulate the Insulin-like

Growth Factor-I Receptor in Prostate Cancer Cells," no. 14: 1849–58.

Paris, Pamela L, Yasuko Kobayashi, Qiang Zhao, Wei Zeng, Shivaranjani Sridharan, Tina Fan, Howard L Adler, et al. 2009. "Functional Phenotyping and Genotyping of Circulating Tumor Cells from Patients with Castration Resistant Prostate Cancer." *Cancer Letters* 277 (2). Elsevier Ireland Ltd: 164–73. doi:10.1016/j.canlet.2008.12.007.

Peters, CA, and PC Walsh. 1987. "The Effect of Nafarelin Acetate, a Luteinizing-Hormone-Releasing Hormone Agonist, on Benign Prostatic Hyperplasia." *New England Journal of Medicine* 317 (10): 599–604.

Ploussard, G, and N Nicolaiew. 2014. "Left Lobe of the Prostate during Clinical Prostate Cancer Screening: The Dark Side of the Gland for Right-Handed Examiners." *Prostate Cancer and Prostatic Disease*, February. doi:10.1038/pcan.2014.2.

Pokorny, Morgan R., Maarten De Rooij, Earl Duncan, Fritz H. Schr??der, Robert Parkinson, Jelle O. Barentsz, and Leslie C. Thompson. 2014. "Prospective Study of Diagnostic Accuracy Comparing Prostate Cancer Detection by Transrectal Ultrasound-Guided Biopsy versus Magnetic Resonance (MR) Imaging with Subsequent Mr-Guided Biopsy in Men without Previous Prostate Biopsies." *European Urology* 66 (1): 22–29. doi:10.1016/j.eururo.2014.03.002.

Polkinghorn, William R., Joel S. Parker, Man X. Lee, Elizabeth M. Kass, Daniel E. Spratt, Phillip J. Iaquinta, Vivek K. Arora, et al. 2013. "Androgen Receptor Signaling Regulates DNA Repair in Prostate Cancers." *Cancer Discovery* 3 (11): 1245–53.

Pollack, A, G K Zagars, A K el-Naggar, M D Gauwitz, and N H Terry. 1994. "Near-Diploidy: A New Prognostic Factor for Clinically Localized Prostate Cancer Treated with External Beam Radiation Therapy." *Cancer* 73 (7): 1895–1903.

Potosky, Arnold L., William W. Davis, Richard M. Hoffman, Janet L. Stanford, Robert A. Stephenson, David F. Penson, and Linda C. Harlan. 2004. "Five-Year Outcomes after Prostatectomy or Radiotherapy for Prostate Cancer: The Prostate Cancer Outcomes Study." *Journal of the National Cancer Institute* 96 (18): 1358–67. doi:10.1093/jnci/djh259.

Powell, S. M., V. Christiaens, D. Voulgaraki, J. Waxman, F. Claessens, and C. L. Bevan. 2004. "Mechanisms of Androgen Receptor Signalling via Steroid Receptor Coactivator-1 in Prostate." *Endocrine-Related Cancer* 11 (1): 117–30. doi:10.1677/erc.0.0110117.

Prostate Cancer Foundation. 2016. "LIVING WITH PROSTATE CANCER: HORMONE THERAPY." Accessed May 17. http://www.pcf.org/site/c.leJRIROrEpH/b.5814015/k.91CD/Hormone_Therapy.htm.

Punnoose, Elizabeth A, Roberta Ferraldeschi, Edith Szafer-Glusman, Eric K Tucker, Sankar Mohan, Penelope Flohr, Ruth Riisnaes, et al. 2015. "PTEN Loss in Circulating Tumour Cells Correlates with PTEN Loss in Fresh Tumour Tissue from Castration-Resistant Prostate Cancer Patients." *British Journal of Cancer* 113 (8). Nature Publishing Group: 1225–33. doi:10.1038/bjc.2015.332.

Qi, Robert, and Judd Moul. 2015. "High-Risk Prostate Cancer: Role of Radical Prostatectomy and Radiation Therapy." *Oncology Research and Treatment* 38 (12): 639–44. doi:10.1159/000441736.

Racila, E, D Euhus, a J Weiss, C Rao, J McConnell, L W Terstappen, and J W Uhr. 1998. "Detection and Characterization of Carcinoma Cells in the Blood." *Proceedings of the National Academy of Sciences of the United States of America* 95 (April): 4589–94. doi:10.1073/pnas.95.8.4589.

Ramalingam, Suresh S, and Paul W Doetsch. 2012. "C-Myc Suppression of DNA Double-Strand Break Repair." Neoplasia 14 (12): 1190–1202. doi:10.1593/neo.121258.

Roach, M., Hanks, G., Thames, H., Schellhammer, P., Shipley, W. U., Sokol, G. H., & Sandler, H. (2006). Defining biochemical failure following radiotherapy with or without hormonal therapy in men with clinically localized prostate cancer: Recommendations of the RTOG-ASTRO Phoenix Consensus Conference. International Journal of Radiation Oncology Biology Physics, 65(4), 965–974. http://doi.org/10.1016/j.ijrobp.2006.04.029

Rodriguez-Lee, Mariam, Peter Kuhn, and David R Webb. 2014. "Advancing Cancer Patient Care by Integrating Circulating Tumor Cell Technology to Understand the Spatial and Temporal Dynamics of Cancer." *Drug Development Research* 75 (6): 384–92. doi:10.1002/ddr.21225.

Rodriguez-Vida, Alejo, Myria Galazi, Sarah Rudman, Simon Chowdhury, and Cora N. Sternberg. 2015. "Enzalutamide for the Treatment of Metastatic Castration-Resistant Prostate Cancer." *Drug Design, Development and Therapy* 9: 3325–39. doi:10.2147/DDDT.S69433.

Rönnau, C G H, G W Verhaegh, M V Luna-Velez, and J a Schalken. 2014. "Noncoding RNAs as Novel Biomarkers in Prostate Cancer." *BioMed Research International* 2014 (January): 591703. doi:10.1155/2014/591703.

Rosenberg, R, R Gertler, J Friederichs, K Fuehrer, M Dahm, R Phelps, S Thorban, H Nekarda, and J R Siewert. 2002. "Comparison of Two Density Gradient Centrifugation Systems for the Enrichment of Disseminated Tumor Cells in Blood." *Cytometry* 49 (4): 150–58. doi:10.1002/cyto.10161.

Rye, Morten Beck, Helena Bertilsson, Finn Drabløs, Anders Angelsen, Tone F Bathen, and May-Britt Tessem. 2014. "Gene Signatures ESC, MYC and ERG-Fusion Are Early Markers of a Potentially Dangerous Subtype of Prostate Cancer." *BMC Medical Genomics* 7 (1): 50. doi:10.1186/1755-8794-7-50.

Saal, Lao H, Peter Johansson, Karolina Holm, Sofia K Gruvberger-Saal, Qing-Bai She, Matthew Maurer, Susan Koujak, et al. 2007. "Poor Prognosis in Carcinoma Is Associated with a Gene Expression Signature of Aberrant PTEN Tumor Suppressor Pathway Activity." *Proceedings of the National Academy of Sciences of the United States of America* 104 (18): 7564–69. doi:10.1073/pnas.0702507104.

Schaefer, L H, D Schuster, and H Herz. 2001. "Generalized Approach for Accelerated Maximum Likelihood Based Image Restoration Applied to Three-Dimensional Fluorescence Microscopy." *Journal of Microscopy* 204 (Pt 2): 99–107.

Schally, Andrew V. 1999. "Luteinizing Hormone-Releasing Hormone Analogs: Their Impact on the Control of Tumorigenesis." *Peptides* 20 (10): 1247–62. doi:10.1016/S0196-9781(99)00130-8.

Schmitz, B., A. Radbruch, T. Kümmel, C. Wickenhauser, H. Korb, M.L. Hansmann, J. Thiele, and R. Fischer. 1994. "Magnetic Activated Cell Sorting (MACS) - a New Immunomagnetic

Method for Megakaryocytic Cell Isolation: Comparison of Different Separation Techniques." *European Journal of Haematology* 52 (5): 267–75. doi:10.1111/j.1600-0609.1994.tb00095.x.

Schoenborn, Jamie R, Pete Nelson, and Min Fang. 2013. "Genomic Profiling Defines Subtypes of Prostate Cancer with the Potential for Therapeutic Stratification." *Clinical Cancer Research : An Official Journal of the American Association for Cancer Research* 19 (15): 4058–66. doi:10.1158/1078-0432.CCR-12-3606.

Schweizer, Michael T, and Evan Y Yu. 2015. "Persistent Androgen Receptor Addiction in Castration-Resistant Prostate Cancer." *Journal of Hematology & Oncology* 8 (1). Journal of Hematology & Oncology: 128. doi:10.1186/s13045-015-0225-2.

Shafi, A A, A E Yen, and N L Weigel. 2013. "Androgen Receptors in Hormone-Dependent and Castration-Resistant Prostate Cancer." *Pharmacology and Therapeutics* 140 (3): 223–38. doi:10.1016/j.pharmthera.2013.07.003.

Shariat, Shahrokh F, and Claus G Roehrborn. 2008. "Using Biopsy to Detect Prostate Cancer." *Reviews in Urology* 10 (4): 262–80.

Sharova, Evgeniya, Angela Grassi, Anna Marcer, Katia Ruggero, Francesco Pinto, Pierfrancesco Bassi, Paola Zanovello, et al. 2016. "A Circulating miRNA Assay as a First-Line Test for Prostate Cancer Screening." *British Journal of Cancer*, no. April: 1–5. doi:10.1038/bjc.2016.151.

Shay, Jerry W, and Woodring E Wright. 2011. "Role of Telomeres and Telomerase in Cancer." *Semin Cancer Biol.* 21 (6): 349–53. doi:10.1016/j.semcancer.2011.10.001.Role.

Silva, Amanda Goncalves Dos Santos, Rahul Sarkar, Jana Harizanova, Amanda Guffei, Michael Mowat, Yuval Garini, and Sabine Mai. 2008. "Centromeres in Cell Division, Evolution, Nuclear Organization and Disease." *Journal of Cellular Biochemistry* 104 (6): 2040–58. doi:10.1002/jcb.21766.

Snyder, Peter J., Shalender Bhasin, Glenn R. Cunningham, Alvin M. Matsumoto, Alisa J. Stephens-Shields, Jane A. Cauley, Thomas M. Gill, et al. 2016. "Effects of Testosterone Treatment in Older Men." *New England Journal of Medicine* 374 (7): 611–24. doi:10.1056/NEJMoa1506119.

Solovei, Irina, Moritz Kreysing, Christian Lanctôt, Süleyman Kösem, Leo Peichl, Thomas Cremer, Jochen Guck, and Boris Joffe. 2009. "Nuclear Architecture of Rod Photoreceptor Cells Adapts to Vision in Mammalian Evolution." *Cell* 137 (2): 356–68. doi:10.1016/j.cell.2009.01.052.

Stamey, T A, N Yang, A R Hay, J E McNeal, F S Freiha, and E Redwine. 1987. "Prostate-Specific Antigen as a Serum Marker for Adenocarcinoma of the Prostate." *The New England Journal of Medicine* 317 (15). Massachusetts Medical Society: 909–16. doi:10.1056/NEJM198710083171501.

Stroun, M, J Lyautey, C Lederrey, A Olson-Sand, and P Anker. 2001. "About the Possible Origin and Mechanism of Circulating DNA Apoptosis and Active DNA Release." *Clinica Chimica Acta; International Journal of Clinical Chemistry* 313 (1-2): 139–42.

Sun, Maxine, Toni K Choueiri, Ole-Petter R Hamnvik, Mark A Preston, Guillermo De Velasco,

Wei Jiang, Stacy Loeb, Paul L Nguyen, and Quoc-Dien Trinh. 2016. “Comparison of Gonadotropin-Releasing Hormone Agonists and Orchiectomy: Effects of Androgen-Deprivation Therapy.” *JAMA Oncology* 2 (4): 500–507. doi:10.1001/jamaoncol.2015.4917.

Sun, Shihua, Cynthia C T Sprenger, Robert L Vessella, Kathleen Haugk, Kathryn Soriano, Elahe A Mostaghel, Stephanie T Page, et al. 2010. “Castration Resistance in Human Prostate Cancer Is Conferred by a Frequently Occurring Androgen Receptor Splice Variant.” *Journal of Clinical Investigation* 120 (8). doi:10.1172/JCI41824DS1.

Sun, Yuting, Bu Er Wang, Kevin G. Leong, Peng Yue, Li Li, Suchit Jhunjhunwala, Darrell Chen, et al. 2012. “Androgen Deprivation Causes Epithelial-Mesenchymal Transition in the Prostate: Implications for Androgen- Deprivation Therapy.” *Cancer Research* 72 (2): 527–36. doi:10.1158/0008-5472.CAN-11-3004.

Sun, Zhuo, Chuanxin Huang, Jinxue He, Kristy L. Lamb, Xi Kang, Tingting Gu, Wen Hong Shen, and Yuxin Yin. 2014. “PTEN C-Terminal Deletion Causes Genomic Instability and Tumor Development.” *Cell Reports* 6 (5). Elsevier: 844–54. doi:10.1016/j.celrep.2014.01.030.

Suzuki, A, J L de la Pompa, V Stambolic, A J Elia, T Sasaki, I del Barco Barrantes, A Ho, et al. 1998. “High Cancer Susceptibility and Embryonic Lethality Associated with Mutation of the PTEN Tumor Suppressor Gene in Mice.” *Current Biology : CB* 8 (21): 1169–78. doi:10.1016/S0960-9822(07)00488-5.

Ta, Huy Q., and Daniel Gioeli. 2014. “The Convergence of DNA Damage Checkpoint Pathways and Androgen Receptor Signaling in Prostate Cancer.” *Endocrine-Related Cancer* 2 (2): 1–21. doi:10.14440/jbm.2015.54.A.

Taimen, Pekka, Katrin Pfleghaar, Takeshi Shimi, Dorothee Möller, Kfir Ben-Harush, Michael R Erdos, Stephen A Adam, et al. 2009. “A Progeria Mutation Reveals Functions for Lamin A in Nuclear Assembly, Architecture, and Chromosome Organization.” *Proceedings of the National Academy of Sciences of the United States of America* 106 (49): 20788–93. doi:10.1073/pnas.0911895106.

Taneja, Samir S., Marc A. Bjurlin, H. Ballentine Carter, Michael S. Cookson, Lenonard G. Gomella, David F. Penson, Paul Schellhammer, Steven Schlossberg, Dean Troyer, and Thomas Wheeler. 2013. “Optimal Techniques of Prostate Biopsy and Specimen Handling.” *American Urological Association*, no. 3: 1–29.

Tapia-Laliena, María a, Nina Korzeniewski, Markus Hohenfellner, and Stefan Duensing. 2014. “High-Risk Prostate Cancer: A Disease of Genomic Instability.” *Urologic Oncology*, June. Elsevier, 1–7. doi:10.1016/j.urolonc.2014.02.005.

Taylor, Barry S, Nikolaus Schultz, Haley Hieronymus, Anuradha Gopalan, Yonghong Xiao, Brett S Carver, Vivek K Arora, et al. 2010. “Integrative Genomic Profiling of Human Prostate Cancer.” *Cancer Cell* 18 (1): 11–22. doi:10.1016/j.ccr.2010.05.026.

Taylor, Renea A., Roxanne Toivanen, Mark Frydenberg, John Pedersen, Laurence Harewood, Anne T. Collins, Norman J. Maitland, and Gail P. Risbridger. 2012. “Human Epithelial Basal Cells Are Cells of Origin of Prostate Cancer, Independent of CD133 Status.” *Stem Cells* 30 (6): 1087–96. doi:10.1002/stem.1094.

Thalgott, Mark, Brigitte Rack, Tobias Maurer, Michael Souvatzoglou, Matthias Eiber, Veronika

Kreß, Matthias M. Heck, et al. 2013. “Detection of Circulating Tumor Cells in Different Stages of Prostate Cancer.” *Journal of Cancer Research and Clinical Oncology* 139 (5): 755–63. doi:10.1007/s00432-013-1377-5.

Trock, Bruce J. 2014. “Circulating Biomarkers for Discriminating Indolent from Aggressive Disease in Prostate Cancer Active Surveillance.” *Current Opinion in Urology* 24 (3): 293–302. doi:10.1097/MOU.0000000000000050.

Ueda, Takeshi, Nasrin R. Mawji, Nicholas Bruchovsky, and Marianne D. Sadar. 2002. “Ligand-Independent Activation of the Androgen Receptor by Interleukin-6 and the Role of Steroid Receptor Coactivator-1 in Prostate Cancer Cells.” *Journal of Biological Chemistry* 277 (41): 38087–94. doi:10.1074/jbc.M203313200.

van de Stolpe, Anja, and Jaap M J den Toonder. 2014. “Circulating Tumor Cells: What Is in It for the Patient? A Vision towards the Future.” *Cancers* 6 (2): 1195–1207. doi:10.3390/cancers6021195.

van der Steen, T., Tindall, D., & Huang, H. (2013). Posttranslational Modification of the Androgen Receptor in Prostate Cancer. *International Journal of Molecular Sciences,* 14(7), 14833–14859. http://doi.org/10.3390/ijms140714833

Veldscholte, J., C. Ris-Stalpers, G.G.J.M. Kuiper, G. Jenster, C. Berrevoets, E. Claassen, H.C.J. van Rooij, J. Trapman, A.O. Brinkmann, and E. Mulder. 1990. “A Mutation in the Ligand Binding Domain of the Androgen Receptor of Human LNCaP Cells Affects Steroid Binding Characteristics and Response to Anti-Androgens.” *Biochemical and Biophysical Research Communications* 173 (2): 534–40. doi:10.1016/S0006-291X(05)80067-1.

Vermolen, B J, Y Garini, S Mai, V Mougey, T Fest, T C Chuang, A Y Chuang, L Wark, and I T Young. 2005. “Characterizing the Three-Dimensional Organization of Telomeres.” *Cytometry* 6 (2): 144–50. doi:10.1002/cyto.a.20159.CHARACTERIZING.

Vona, G, a Sabile, M Louha, V Sitruk, S Romana, K Schütze, F Capron, et al. 2000. “Isolation by Size of Epithelial Tumor Cells : A New Method for the Immunomorphological and Molecular Characterization of Circulatingtumor Cells.” *The American Journal of Pathology* 156 (1): 57–63. doi:10.1016/S0002-9440(10)64706-2.

Vukovic, B., B. Beheshti, P. Park, G. Lim, J. Bayani, M. Zielenska, and J. A. Squire. 2007. “Correlating Breakage-Fusion-Bridge Events with the Overall Chromosomal Instability and in Vitro Karyotype Evolution in Prostate Cancer.” *Cytogenetic and Genome Research* 116 (1-2): 1–11. doi:10.1159/000097411.

Walsh, Claire A., Li Qin, Jean Ching Yi Tien, Leonie S. Young, and Jianming Xu. 2012. “The Function of Steroid Receptor Coactivator-1 in Normal Tissues and Cancer.” *International Journal of Biological Sciences* 8 (4): 470–85. doi:10.7150/ijbs.4125.

Wang, Elyn H., Sarah S. Mougalian, Pamela R. Soulos, Benjamin D. Smith, Bruce G. Haffty, Cary P. Gross, and James B. Yu. 2015. “Adoption of Intensity Modulated Radiation Therapy for Early-Stage Breast Cancer from 2004 through 2011.” *International Journal of Radiation Oncology Biology Physics* 91 (2). Elsevier Inc.: 303–11. doi:10.1016/j.ijrobp.2014.09.011.

Wang, Qianben, Jason S. Carroll, and Myles Brown. 2005. “Spatial and Temporal Recruitment of Androgen Receptor and Its Coactivators Involves Chromosomal Looping and

Polymerase Tracking." *Molecular Cell* 19 (5): 631–42. doi:10.1016/j.molcel.2005.07.018.

Wang, Qianben, Wei Li, X. Shirley Liu, Jason S. Carroll, Olli A. Jänne, Erika Krasnickas Keeton, Arul M. Chinnaiyan, Kenneth J. Pienta, and Myles Brown. 2007. "A Hierarchical Network of Transcription Factors Governs Androgen Receptor-Dependent Prostate Cancer Growth." *Molecular Cell* 27 (3): 380–92. doi:10.1016/j.molcel.2007.05.041.

Wang, Zhu A, Roxanne Toivanen, Sarah K Bergren, Pierre Chambon, and Michael M Shen. 2014. "Luminal Cells Are Favored as the Cell of Origin for Prostate Cancer." *Cell Reports*, August. doi:10.1016/j.celrep.2014.08.002.

Wark, Landon, Adrian Danescu, Suchitra Natarajan, Xuguang Zhu, Sheue-yann Cheng, Sabine Hombach-Klonisch, Sabine Mai, and Thomas Klonisch. 2014. "Three-Dimensional Telomere Dynamics in Follicular Thyroid Cancer." *Thyroid : Official Journal of the American Thyroid Association* 24 (2): 296–304. doi:10.1089/thy.2013.0118.

Wark, Landon, David Novak, Nelly Sabbaghian, Lilian Amrein, Jaganmohan R Jangamreddy, Mary Cheang, Carly Pouchet, et al. 2013. "Heterozygous Mutations in the PALB2 Hereditary Breast Cancer Predisposition Gene Impact on the Three-Dimensional Nuclear Organization of Patient-Derived Cell Lines." *Genes, Chromosomes & Cancer* 52 (5): 480–94. doi:10.1002/gcc.22045.

Washington, Samuel L., Michael Bonham, Jared M. Whitson, Janet E. Cowan, and Peter R. Carroll. 2012. "Transrectal Ultrasonography-Guided Biopsy Does Not Reliably Identify Dominant Cancer Location in Men with Low-Risk Prostate Cancer." *BJU International* 110 (1): 50–55. doi:10.1111/j.1464-410X.2011.10704.x.

Weierich, Claudia, Alessandro Brero, Stefan Stein, Johann von Hase, Christoph Cremer, Thomas Cremer, and Irina Solovei. 2003. "Three-Dimensional Arrangements of Centromeres and Telomeres in Nuclei of Human and Murine Lymphocytes." *Chromosome Research : An International Journal on the Molecular, Supramolecular and Evolutionary Aspects of Chromosome Biology* 11 (5): 485–502.

Wilson, Jean D. 2011. "The Critical Role of Androgens in Prostate Development." *Endocrinology and Metabolism Clinics of North America* 40 (3): 577–90. doi:10.1016/j.ecl.2011.05.003.

World Health Organization. 2016. "WHO Histological Classification of Tumours of the Prostate." In *Pathology and Genetics of Tumours of the Urinary System and Male Genital Organs*, 160–215.

Wu, Dayong, Chunpeng Zhang, Yanping Shen, Kenneth P. Nephew, and Qianben Wang. 2011. "Androgen Receptor-Driven Chromatin Looping in Prostate Cancer." *Trends in Endocrinology and Metabolism* 22 (12). Elsevier Ltd: 474–80. doi:10.1016/j.tem.2011.07.006.

Yu, Jindan, Jianjun Yu, Ram-shankar Mani, Qi Cao, Chad J Brenner, Xuhong Cao, George X Wang, et al. 2010. "An Integrated Network of Androgen Receptor, Polycomb, and TMPRSS2-ERG Gene Fusions in Prostate Cancer Progression." *Cancer Cell* 17 (5): 443–54. doi:10.1016/j.ccr.2010.03.018.An.

Zabaglo, Lila, Michael G Ormerod, Marina Parton, Alistair Ring, Ian E Smith, and Mitch Dowsett. 2003. "Cell Filtration-Laser Scanning Cytometry for the Characterisation of

Circulating Breast Cancer Cells." *Cytometry. Part A : The Journal of the International* Society for Analytical Cytology 55 (2): 102–8. doi:10.1002/cyto.a.10071.

Zech, L., Haglund, U., Nilsson, K., & Klein, G. (1976). Characteristic chromosomal abnormalities in biopsies and lymphoid-cell lines from patients with Burkitt and non-Burkitt lymphomas. International Journal of Cancer, 17(1), 47–56. http://doi.org/10.1002/ijc.2910170108

Zeng, Wen, Hanying Sun, Fankai Meng, Zeming Liu, Jing Xiong, Sheng Zhou, Fan Li, Jia Hu, Zhiquan Hu, and Zheng Liu. 2015. "Nuclear C-MYC Expression Level Is Associated with Disease Progression and Potentially Predictive of Two Year Overall Survival in Prostate Cancer." *International Journal of Clinical and Experimental Pathology* 8 (2): 1878–88.

Zhe, Xiaoning, Michael L Cher, and R Daniel Bonfil. 2011. "Circulating Tumor Cells: Finding the Needle in the Haystack." *American Journal of Cancer Research* 1 (6): 740–51.

Zheng, Siyang, Henry Lin, Jing-Quan Liu, Marija Balic, Ram Datar, Richard J. Cote, and Yu-Chong Tai. 2007. "Membrane Microfilter Device for Selective Capture, Electrolysis and Genomic Analysis of Human Circulating Tumor Cells." *Journal of Chromatography A* 1162 (2): 154–61. doi:10.1016/j.chroma.2007.05.064.

Zhou, Junying, Michelle Richardson, Vidyavathi Reddy, Mani Menon, Evelyn R. Barrack, G. Prem-Veer Reddy, and Sahn Ho Kim. 2013. "Structural and Functional Association of Androgen Receptor with Telomeres in Prostate Cancer Cells." *Aging* 5 (1): 3–17.

14.) Appendices

14.1.) Code for line slope of bin count comparisons.

This code is written in the python 3.4 programming language.

```
# -*- coding: utf-8 -*-
"""
Created on Mon Mar 9 12:18:07 2015

This is the script I created to perform the telomere bin count
    difference between patient samples and return a curve used to
    compare change between time points.

@author: Landon Wark
"""
#imports
import scipy as sp
import numpy as np
import pandas as pd
import matplotlib.pyplot as plt
import file_grabber as fg #my custom file retrieval module
from scipy.stats import ks_2samp #Kolmogrov-Smirnov module

def ctc_parser(data):
#skips over any lymphocyte data if present
    start_list = list(data.columns.values)
    for item in start_list:
        if 'lymp' in item:
            start_list.remove(item)
    return(start_list)

def data_gen(samples, data):
#pulls out intensity bin data
    df = pd.DataFrame(data['Intensity Bins'])
    for item in samples[1:]:
        df[item] = data[item]
    return(df)

def comper(x, y, z):
#gets the maximum count in a bin and creates an array of differences iterating until both histograms reach 0
    may = np.argmax(y)
    maz = np.argmax(z)
    dif_array = []
    if min(may, maz) == may:
```

```
41          sub = y
42      else:
43          sub = z
44      for jjj in range(min(may, maz), len(x)):
45          diff = z[jjj] - y[jjj]
46          dif_array.append(diff)
47          if sub[jjj] == 0:
48              break
49      return(dif_array)
50
51 def graph(bins, dif_array, series1, series2):
52 #format data
53      series1 = series1[0:-10]
54      series2 = series2[0:-10]
55      dif_array = np.array(dif_array).astype(float)
56      dif_array = dif_array[~np.isnan(dif_array)]
57      bins = bins[0:len(dif_array)]
58      print(dif_array)
59 #find line formula
60      fp1, residuals, rank, sv, rcond = sp.polyfit(bins, dif_array, 2, full=True)
61      print("Line equation: %.3e(x^2) + %.3e(x)" % (fp1[0], fp1[1]))
                    # This is the relevant number for this project.
62      f1 = sp.poly1d(fp1)
63      fx = sp.linspace(min(bins), max(bins)) # generate X-values for plotting
64 #make plot
65      plt.scatter(bins, dif_array)
66      plt.title((series2 + " vs. " + series1))
67      plt.xlabel("Signal Intensity")
68      plt.ylabel("Change in count")
69      plt.autoscale(tight=True)
70      plt.grid(True)
71      plt.plot(fx, f1(fx), linewidth=4)
72      plt.legend(["m = %.3e(x^2) + %.3e(x)" % (fp1[0], fp1[1])], loc="lower center")
73      plt.savefig(("C:\\Users\\Landon\\" + series2 + " vs " + series1))
74      plt.show()
75      s_name = series2 + " vs " + series1
76      return(float(fp1[1]), s_name, fp1, bins)
77
78 def kstest(x, y):
79 #perform ks_test
80      result = ks_2samp(x,y)
81      print('KS result: KS = %.3f, p = %.3e' % result)
82      return(result[1])
83
84 def csv_writer(big_list, pat_name):
85 #write results to file
```

```
86    headers = ("Series", "Slope", "KS-p")
87    pat_name = pat_name + '.xlsx'
88    datas = pd.DataFrame(big_list, columns=headers)
89    writer = pd.ExcelWriter("C:\\Users\\Landon\\" + pat_name,
90                            engine='xlsxwriter')
91    datas.to_excel(writer, 'Data')
92    writer.save()
93
94 if __name__ == '__main__':
95    in_path = fg.get_file()
96    try:
97       pat_name = in_path[in_path.rfind("/")+1:-24]
98       data = pd.read_excel(in_path, sheetname = 'IntBins')
99       bins = data['Intensity Bins']
100        slope_list = []
101        ks_list = []
102        name_list = []
103        samples = ctc_parser(data)
104        data = data_gen(samples, data)
105         for iii in range(1, len(samples)-1):
106            AA = data[samples[iii]]
107            BB = data[samples[iii+1]]
108            ks_result = kstest(AA, BB)
109            dif_array = comper(bins,AA,BB)
110            slope, nam, func, bins = graph(bins, dif_array,
          samples[iii], samples[iii+1])
111            slope_list.append(slope)
112            ks_list.append(ks_result)
113            name_list.append(nam)
114       slope_list = np.array(slope_list, dtype=float)
115       big_list = np.dstack((name_list, slope_list, ks_list))
116       csv_writer(np.squeeze(big_list, axis=0), pat_name)
117    except FileNotFoundError:
118        print("Operation cancelled: No file available.")
```

14.2.) Code for CTC segmentation and enumeration

This code is written in the python 3.4 programming language.

```
1  # -*- coding: utf-8 -*-
2  """
3  Created on Wed Jan 20 14:41:00 2016
4
5  @author: Landon
6  """
7
8  import cv2
9  import numpy as np
10 import matplotlib.pyplot as plt
11 import matplotlib.cm as cm
12 from skimage.morphology import watershed
13 #from collections import OrderedDict
14 from contourizer import Contour
15
16 def process(image, show=False):
17     img1 = cv2.imread(image, 0)
18     _, img = cv2.threshold(img1,np.mean(img1),np.max(img1),cv2.THRESH_TOZERO)
19
20     blur = cv2.blur(img,(50,50))
21     final = cv2.subtract(img, blur)
22
23     maxIntensity = np.max(final)
24
25     x = np.arange(maxIntensity)
26
27     # Parameters for manipulating image data
28     phi = 1
29     theta = 0.01
30
31     # Increase intensity such that
32     # dark pixels become much brighter,
33     # bright pixels become slightly bright
34     newImage0 = (maxIntensity/phi)*(final/(maxIntensity/theta))**0.5
35     newImage0 = np.array(newImage0,dtype='uint8')
36     # look at me, random comment in the code no one will notice
37
ret,thresh=cv2.threshold(newImage0,0,255,cv2.THRESH_BINARY+cv2.THRESH_OTSU)
38
39     # noise removal
40     kernel = np.ones((3,3),np.uint8)
```

```
41    opening = cv2.morphologyEx(thresh,cv2.MORPH_OPEN,kernel, iterations = 3)
42
43    #close holes
44    kernel = np.ones((3,3),np.uint8)
45    closed = cv2.morphologyEx(opening, cv2.MORPH_CLOSE, kernel, iterations = 3)
46
47    im_floodfill = closed.copy()
48
49    # Mask used to flood filling.
50    # Notice the size needs to be 2 pixels less than the image.
51    h, w = closed.shape[:2]
52    mask = np.zeros((h+2, w+2), np.uint8)
53
54    # Floodfill from point (0, 0)
55    cv2.floodFill(im_floodfill, mask, (0,0), 255);
56
57    # Invert floodfilled image
58    im_floodfill_inv = cv2.bitwise_not(im_floodfill)
59
60    # Combine the two images to get the foreground.
61    im_out = closed | im_floodfill_inv
62
63    # sure background area
64    sure_bg = cv2.dilate(im_out,kernel,iterations=3)
65    # Finding sure foreground area
66    dist_transform = cv2.distanceTransform(im_out,cv2.DIST_L2,5)
67    ret, sure_fg = cv2.threshold(dist_transform,0.05*dist_transform.max(),255,0)
68    # Finding unknown region
69    sure_fg = np.uint8(sure_fg)
70    unknown = cv2.subtract(sure_bg,sure_fg)
71
72    # Marker labelling
73    ret, markers = cv2.connectedComponents(sure_fg)
74    # Add one to all labels so that sure background is not 0, but 1
75    markers = markers-2
76    # Now, mark the region of unknown with zero
77    markers[unknown==255] = 0
78
79    markers = watershed(final, markers)
80    img[markers == -1] = [255]
81
82    contours, hierarchy =
cv2.findContours(markers.copy(),cv2.RETR_FLOODFILL,cv2.CHAIN_APPROX_SIMPLE)[-
2:]
83    #print(contours)
84    h, w = markers.shape[:2]
```

```
85    mask = np.zeros(markers.shape[:2], dtype="uint8")
86    contours_new = {}
87    iii = 0
88    for obj in contours:
89        res = np.zeros(img.shape, np.uint8)
90        area = cv2.contourArea(obj)
91        perimeter = cv2.arcLength(obj, True)
92        hull = cv2.convexHull(obj)
93        hull_area = cv2.contourArea(hull)
94        cv2.drawContours(res, [obj], -1, 1, -1)
95        mean_int, std_int = cv2.meanStdDev(img, mask=res)
96        covariance = std_int/mean_int
97        leftmost = tuple(obj[obj[:,:,0].argmin()][0])
98        rightmost = tuple(obj[obj[:,:,0].argmax()][0])
99        topmost = tuple(obj[obj[:,:,1].argmin()][0])
100       bottommost = tuple(obj[obj[:,:,1].argmax()][0])
101       if 1 in topmost or 1 in leftmost or w in rightmost or h in bottommost:
102           cv2.drawContours(mask, [obj], 0, 0, 0)
103           continue
104       try:
105           circularity = (4*np.pi*area)/(perimeter**2)
106           solidity = float(area)/hull_area
107           if area >= 2500 and solidity >= 0.90 and circularity >= 0.60 and std_int < 11:
108               #print(topmost, leftmost, rightmost, bottommost)
109               iii += 1
110               contur = Contour(iii)
111               contur.area = area
112               contur.circularity = circularity
113               contur.covariance = covariance[0][0]
114               contur.mean_int = mean_int[0][0]
115               contur.std_int = std_int[0][0]
116               contur.perimeter = perimeter
117               contur.solidity = solidity
118               contours_new[iii] = contur.jsonable()
119               cv2.drawContours(mask, [obj], -1, 1, -1)
120               continue
121           else:
122               cv2.drawContours(mask, [obj], 0, 0, 0)
123               continue
124       except ZeroDivisionError:
125           cv2.drawContours(mask, [obj], 0, 0, 0)
126           continue
127   if show == True:
128       for item in contours_new:
129           print(item, contours_new[item])
130       image = cv2.bitwise_and(markers, markers, mask=mask)
```

```
131         image = np.ma.masked_values(image, 0)
132         hax = plt.subplot(122)
133         hax.imshow(img, cmap=cm.gray )
134         hax.imshow(image, alpha=0.5)
135         plt.title("Processed Image")
136         gax = plt.subplot(121)
137         gax.imshow(img1, cmap=cm.gray)
138         plt.title("Original Image")
139         plt.show()
140     else:
141         return(iii, contours_new)
```

14.3.) Preliminary statistical comparisons of three dimensional nuclear parameters with CTC concentrations and PSA levels.

+0m	Mean Int	Mean % Dist	Mean % Agg	Mean ACRatio	Mean NucVol(um^3)	Mean NucDia(um^2)	Mean # Signals	Peak # Signals	1st Quart	2nd Quart	3rd Quart	4th Quart	Signal/NucVol	Max Telo Int	PSA	Gleason	#CTCs/mL
corr with #CTC																	
r (pearson)	-0.84174	-0.04044	0.46202	0.53001	0.32843	0.03345	0.45144	0.41896	0.13230	-0.12872	-0.13020	-0.09366	0.58202	-0.30903	0.15231	0.10889	na
r^2	0.70852	0.00164	0.21346	0.28091	0.10786	0.00112	0.20380	0.17553	0.01750	0.01657	0.01695	0.00877	0.33875	0.09550	0.02320	0.01186	na
1-(√1-r^2)	0.46011	0.00082	0.11313	0.15201	0.05547	0.00056	0.10770	0.09199	0.00879	0.00832	0.00851	0.00440	0.18683	0.04895	0.01167	0.00595	na
corr with PSA																	
r (pearson)	-0.08547	-0.12260	-0.42046	-0.12855	0.04417	-0.04911	0.09543	0.05132	0.04304	0.00688	-0.21364	-0.15701	0.26897	0.07523	na	0.15314	0.15231
r^2	0.00731	0.01503	0.17679	0.01653	0.00195	0.00241	0.00911	0.00263	0.00185	0.00005	0.04564	0.02465	0.07235	0.00566	na	0.02345	0.02320
1-(√1-r^2)	0.00366	0.00754	0.09269	0.00830	0.00098	0.00121	0.00456	0.00132	0.00093	0.00002	0.02309	0.01240	0.03685	0.00283	na	0.0118	0.01167

+2m	Mean Int	Mean % Dist	Mean % Agg	Mean ACRatio	Mean NucVol(um^3)	Mean NucDia(um^2)	Mean # Signals	Peak # Signals	1st Quart	2nd Quart	3rd Quart	4th Quart	Signal/NucVol	Max Telo Int	PSA	#CTCs
corr with #CTCs																
r	0.10238	-0.15989	0.03189	-0.15696	0.15568	0.24294	-0.08921	0.14790	-0.23561	0.25447	0.13321	0.21212	-0.31466	-0.35546	-0.18674	na
r^2	0.01048	0.02556	0.00102	0.02464	0.02424	0.05902	0.00796	0.02187	0.05551	0.06476	0.01774	0.04499	0.09901	0.12635	0.03487	na
1-(√1-r^2)	0.00525	0.01286	0.00051	0.01240	0.01219	0.02996	0.00399	0.01100	0.02815	0.03292	0.00891	0.02276	0.05080	0.06531	0.01759	na
corr with PSA																
r	-0.21222	0.29702	0.07473	-0.23404	-0.14894	-0.15539	0.29082	0.48692	0.11286	-0.10480	-0.11433	-0.20965	0.34809	-0.01911	na	-0.18674
r^2	0.04504	0.08822	0.00558	0.05478	0.02218	0.02415	0.08458	0.23709	0.01274	0.01098	0.01307	0.04395	0.12117	0.00037	na	0.03487
1-(√1-r^2)	0.02278	0.04513	0.00280	0.02777	0.01115	0.01215	0.04322	0.12655	0.00639	0.00551	0.00656	0.02222	0.06254	0.00018	na	0.01759

+6m	Mean Int	Mean % Dist	Mean % Agg	Mean ACRatio	Mean NucVol(um^3)	Mean NucDia(um^2)	Mean # Signals	Peak # Signals	1st Quart	2nd Quart	3rd Quart	4th Quart	Signal/NucVol	Max Telo Int	PSA	#CTC/mL
corr with #CTCs																
r	-0.08140	-0.34190	0.17392	-0.00826	0.35772	0.09204	0.62324	0.62486	-0.13273	0.12290	0.11784	0.27745	0.18929	-0.26655	0.07319	na
r^2	0.00663	0.11689	0.03025	0.00007	0.12797	0.00847	0.38843	0.39045	0.01762	0.01510	0.01389	0.07698	0.03583	0.07105	0.00536	na
1-(√1-r^2)	0.00332	0.06026	0.01524	0.00003	0.06617	0.00424	0.21797	0.21927	0.00885	0.00758	0.00697	0.03926	0.01808	0.03618	0.00268	na
corr with PSA																
r	-0.02113	-0.31381	0.19193	-0.28988	-0.27908	-0.41784	-0.12290	-0.02981	-0.24860	0.22561	0.29756	0.18824	0.47034	-0.19641	na	0.07319
r^2	0.00045	0.09848	0.03684	0.08403	0.07789	0.17459	0.01510	0.00089	0.06180	0.05090	0.08854	0.03543	0.22122	0.03858	na	0.00536
1-(√1-r^2)	0.00022	0.05051	0.01859	0.04294	0.03973	0.09148	0.00758	0.00044	0.03139	0.02578	0.04530	0.01788	0.11752	0.01948	na	0.00268

14.4.) Maximum, mean, minimum, Q2, median and Q3 nuclear diameter (in µm) for each patient at each time point.

MB0389	+00m	+02m	+06m
Maximum	15.59477	13.37537	20.33546
mean	11.52441	9.320938	13.18591
Minimum	7.432539	6.767585	9.461747
Q1	10.65976	8.414496	11.00518
Median	11.43008	9.121819	12.39706
Q3	12.86609	10.14236	15.41517
MB0393	+00m	+02m	+06m
Maximum	11.7337	17.06789	20.47038
mean	7.942751	12.24554	12.82949
Minimum	5.681581	9.694337	6.325527
Q1	6.70786	10.70384	10.2242
Median	7.811778	12.01397	11.96042
Q3	8.598214	13.70403	16.03518
MB0394	+00m	+02m	+06m
Maximum	14.79138	18.70698	28.01119
mean	8.288818	14.21875	16.27419
Minimum	4.897484	10.3408	8.061055
Q1	6.816144	12.65458	13.75846
Median	7.571486	14.43903	15.48681
Q3	9.130348	15.61645	19.78987
MB0405	+00m	+02m	+06m
Maximum	19.02724	15.19242	23.28041
mean	12.47588	10.19737	12.13245
Minimum	9.405655	6.429111	8.479257
Q1	11.21847	9.07732	10.43492
Median	11.79764	10.17663	11.56744
Q3	13.09543	11.00379	12.62732
MB0408	+00m	+02m	+06m
Maximum	16.16379	20.33355	18.12129
mean	10.31535	14.09542	11.89888
Minimum	8.316412	8.496707	7.932805
Q1	9.880059	11.39807	10.11563
Median	10.1687	14.03036	11.39277
Q3	10.7019	16.3674	13.20771

MB0438	+00m	+02m	+06m
Maximum	40.20238	41.61252	55.65856
mean	18.74151	18.18951	19.56689
Minimum	7.358982	7.27054	7.058213
Q1	10.9975	14.20446	14.15873
Median	17.41536	14.91623	16.60417
Q3	26.46577	19.74524	21.46484
MB0441	+00m	+02m	+06m
Maximum	17.11136	24.6147	20.03879
mean	11.77647	17.56846	12.3587
Minimum	7.265448	7.404688	6.209651
Q1	10.57593	14.40755	10.30136
Median	11.69677	18.06234	11.54635
Q3	12.64634	21.3572	14.12856
MB0444	+00m	+02m	+06m
Maximum	15.84542	24.60133	15.43764
mean	11.28156	13.26793	10.47138
Minimum	8.341925	7.371071	7.786287
Q1	10.29915	10.2707	9.241432
Median	11.04421	12.11797	10.25355
Q3	11.47813	16.08515	11.62137
MB0445	+00m	+02m	+06m
Maximum	18.05441	21.93823	19.44255
mean	12.63639	16.41018	13.25963
Minimum	10.77213	12.57301	9.548989
Q1	11.62951	14.65047	11.68876
Median	12.22742	15.9987	12.68434
Q3	12.91496	18.28453	13.67429
MB0446	+00m	+02m	+06m
Maximum	13.58491	30.12804	19.0081
mean	10.96056	19.01161	13.21684
Minimum	5.665117	10.7701	9.701676
Q1	10.26059	16.26592	11.57433
Median	10.84279	19.0323	12.36613
Q3	12.07415	20.8355	14.45667

MB0410	+00m	+02m	+06m
Maximum	14.04277	16.45161	39.64707
mean	10.84613	11.33404	14.74398
Minimum	6.869285	9.41046	8.561991
Q1	9.726782	10.40957	11.63
Median	11.60117	10.9698	14.01718
Q3	12.33396	11.65139	15.59059
MB0413	+00m	+02m	+06m
Maximum	13.09241	36.9418	29.96286
mean	10.42607	12.32513	19.03068
Minimum	7.345134	7.221082	11.62959
Q1	9.80377	10.45433	15.10499
Median	10.4516	11.29285	18.05229
Q3	10.94113	12.47736	23.39724
MB0418	+00m	+02m	+06m
Maximum	39.47067	41.88004	22.8155
mean	14.79996	15.88052	13.12005
Minimum	10.10127	8.463084	3.5326
Q1	11.51915	9.524474	10.2883
Median	12.66444	13.89395	13.20777
Q3	13.86136	19.46225	15.82276
MB0421	+00m	+02m	+06m
Maximum	19.30963	21.66114	21.19944
mean	12.09083	15.88899	14.98013
Minimum	9.538153	9.139339	10.42624
Q1	10.20038	15.02954	11.91323
Median	10.92628	16.47821	14.02878
Q3	13.99518	17.48847	18.51708
MB0426	+00m	+02m	+06m
Maximum	19.36693	27.80676	16.17402
mean	13.79742	14.38309	10.85514
Minimum	9.204145	9.07125	7.51892
Q1	11.64651	12.99233	10.06973
Median	14.04431	13.676	10.78623
Q3	16.0774	14.55524	11.56886

MB0452	+00m	+02m	+06m
Maximum	19.04346	19.94102	15.45643
mean	12.8196	14.54947	10.9998
Minimum	8.822292	11.52474	7.028114
Q1	11.47525	13.07794	9.49867
Median	12.32881	14.52865	10.70245
Q3	13.4425	15.58399	12.00389
MB0461	+00m	+02m	+06m
Maximum	23.22743	21.76956	16.78354
mean	13.96173	15.89128	12.30767
Minimum	9.548786	4.648348	7.364946
Q1	12.08696	12.99163	11.67555
Median	13.65315	16.12796	12.54771
Q3	15.4808	18.50813	13.19924
MB0466	+00m	+02m	+06m
Maximum	21.98353	18.06243	14.52402
mean	13.55482	11.82683	10.75379
Minimum	6.564418	8.985352	8.204386
Q1	11.41604	10.27311	9.819173
Median	13.20869	10.9246	10.65642
Q3	14.99919	12.56056	11.62486
MB0475	+00m	+02m	+06m
Maximum	18.99242	28.17091	24.41684
mean	12.7096	17.8286	12.80425
Minimum	9.684248	12.60963	9.008528
Q1	11.0936	14.25808	10.77524
Median	12.03188	16.02532	12.48486
Q3	12.93372	21.02236	13.53128
MB0500	+00m	+02m	+06m
Maximum	21.54488	32.08803	18.85024
mean	11.93643	14.84775	13.26467
Minimum	8.315761	4.683158	5.999573
Q1	9.899966	8.464539	11.40642
Median	10.8518	11.23701	13.22882
Q3	12.97833	23.44521	16.29807